Metropolitan Washington Council of Governments

MEMORANDUM

TO:	Metropolitan Washington Air Quality Committee (MWAQC)
FROM:	Julie Kimmel, Air and Climate Public Advisory Committee (ACPAC) Chair
CC:	ACPAC Members
SUBJECT:	Recommendations on Regional Action to Address Air Quality Risks Linked to Climate Change
DATE:	May 20, 2024

As the 18 members of ACPAC, representing a diversity of communities and professions in DC, Maryland, and Virginia, we want to communicate in the strongest terms our concern about the planetary emergency that is climate change. The world has been seeing ever-increasing temperatures in the atmosphere and in the oceans, with worsening impacts on natural ecosystems and human societies and disproportionate harm to low-income and marginalized communities. Here in the metropolitan Washington region, we have been burdened with more frequent and extreme flash flooding, drought, and heat waves; and last year, many of us were stunned to experience Code Red air pollution events resulting from record-shattering wildfires across Canada. The global average temperature increase is now uncomfortably close to the 1.5°C threshold acknowledged in the Paris Climate Agreement that separates us from potentially catastrophic impacts. (Please see the three attachments.)

We acknowledge the important air emissions reductions and resulting air quality improvements that MWAQC has presided over in recent years. At the same time, we believe that nascent, climate-driven, external factors like wildfire smoke and more frequent and intense episodes of hot, humid, and stagnant atmospheric conditions may increasingly reverse air quality gains. The metropolitan Washington region is currently allowed to exclude exceptional events like the 2023 wildfires from air quality monitoring data and thus avoid responsibility for any non-attainment of air quality standards brought about by such events. Furthermore, climate change may exacerbate the unhealthful and unjust impacts of air pollution on over-burdened communities in our region.

ACPAC has sent a parallel memo to CEEPC with climate-specific recommendations. The following are our key recommendations to MWAQC on air quality action:

1. MWAQC should **account for potential impacts of climate change**, including increases in smog-promoting heat waves and exceptional air pollution sources such as wildfires, in its air quality planning and then lead the region's local governments in **reducing pollutant emissions sufficiently to offset the impacts** of those external factors.

2. MWAQC should **work harder to alleviate air pollution hotspots** that harm the health of environmental justice communities. In support of this, MWAQC should do more to **monitor air pollution in these communities**, and **provide more effective alerts and early warning** for them.

3. Any new urban or industrial development will make it even more challenging to meet our region's clean energy demand and air quality standards (as well as our GHG emission reduction targets). Thus, **regional land-use planning and permitting need to consider and firmly address the impacts** of proposed projects on our ability to achieve climate, air quality, and justice and equity goals.

4. MWAQC needs to **continuously track the impacts of wildfires and other external factors on regional air quality**, and make adjustments in its work as necessary in order to better protect public health.

Thank you for hearing our concerns and considering our recommendations. We look forward to hearing back on next steps and would be glad to provide further input.

Attachments (3)

PNAS Nexus, 2024, 3, 1–20
https://doi.org/10.1093/pnasnexus/pgae106
Advance access publication 2 April 2024
Review

Earth at risk: An urgent call to end the age of destruction and forge a just and sustainable future

Charles Fletcher[a,*], William J. Ripple[b], Thomas Newsome[c], Phoebe Barnard[d,e], Kamanamaikalani Beamer[f,g], Aishwarya Behl[a], Jay Bowen[h,i], Michael Cooney[j], Eileen Crist[k], Christopher Field[l], Krista Hiser[m,n], David M. Karl[o,p], David A. King[q], Michael E. Mann[r], Davianna P. McGregor[s], Camilo Mora[t], Naomi Oreskes[u] and Michael Wilson[v]

[a]School of Ocean and Earth Science and Technology, University of Hawai'i at Mānoa, Honolulu, HI 96822, USA
[b]Department of Forest Ecosystems and Society, Oregon State University, Corvallis, OR 97331, USA
[c]School of Life and Environmental Sciences, University of Sydney, Sydney, NSW 2006, Australia
[d]Center for Environmental Politics and School of Interdisciplinary Arts and Sciences, University of Washington, Seattle, WA 98195, USA
[e]African Climate and Development Initiative and FitzPatrick Institute, University of Cape Town, Cape Town 7700, South Africa
[f]Hui 'Āina Momona Program, Richardson School of Law, University of Hawai'i at Mānoa, Honolulu, HI 96822, USA
[g]Hawai'inuiākea School of Hawaiian Knowledge, Kamakakūokalani Center for Hawaiian Studies, University of Hawai'i at Mānoa, Honolulu, HI 96822, USA
[h]Institute of American Indian Arts, Santa Fe, NM 87508, USA
[i]Upper Skagit Tribe, Sedro Woolley, WA 98284, USA
[j]School of Ocean and Earth Science and Technology, Hawai'i Natural Energy Institute, University of Hawai'i at Mānoa, Honolulu, HI 96822, USA
[k]Department of Science Technology and Society, Virginia Tech, Blacksburg, VA 24060, USA
[l]Doerr School for Sustainability, Stanford Woods Institute for the Environment, Stanford University, Stanford, CA 94305, USA
[m]Department of Languages, Linguistics, and Literature, Kapi'olani Community College, Honolulu, HI 96816, USA
[n]Global Council for Science and the Environment, Washington, DC 20006, USA
[o]Department of Oceanography, School of Ocean and Earth Science and Technology, Honolulu, HI 96822, USA
[p]Daniel K. Inouye Center for Microbial Oceanography, Research and Education, University of Hawai'i at Mānoa, Honolulu, HI 96822, USA
[q]Department of Chemistry, University of Cambridge, Cambridge CB2 1DQ, UK
[r]Department of Earth and Environmental Science, University of Pennsylvania, Philadelphia, PA 19104, USA
[s]Department of Ethnic Studies, Center for Oral History, University of Hawai'i at Mānoa, Honolulu, HI 96822, USA
[t]Department of Geography and Environment, University of Hawai'i at Mānoa, Honolulu, HI 96822, USA
[u]Department of the History of Science, Harvard University, Cambridge, MA 02138, USA
[v]Associate Justice, Hawaii Supreme Court (retired), Honolulu, HI 96813, USA
*To whom correspondence should be addressed: Email: fletcher@apps.soest.hawaii.edu
Edited By: Junguo Liu

Abstract

Human development has ushered in an era of converging crises: climate change, ecological destruction, disease, pollution, and socioeconomic inequality. This review synthesizes the breadth of these interwoven emergencies and underscores the urgent need for comprehensive, integrated action. Propelled by imperialism, extractive capitalism, and a surging population, we are speeding past Earth's material limits, destroying critical ecosystems, and triggering irreversible changes in biophysical systems that underpin the Holocene climatic stability which fostered human civilization. The consequences of these actions are disproportionately borne by vulnerable populations, further entrenching global inequities. Marine and terrestrial biomes face critical tipping points, while escalating challenges to food and water access foreshadow a bleak outlook for global security. Against this backdrop of Earth at risk, we call for a global response centered on urgent decarbonization, fostering reciprocity with nature, and implementing regenerative practices in natural resource management. We call for the elimination of detrimental subsidies, promotion of equitable human development, and transformative financial support for lower income nations. A critical paradigm shift must occur that replaces exploitative, wealth-oriented capitalism with an economic model that prioritizes sustainability, resilience, and justice. We advocate a global cultural shift that elevates kinship with nature and communal well-being, underpinned by the recognition of Earth's finite resources and the interconnectedness of its inhabitants. The imperative is clear: to navigate away from this precipice, we must collectively harness political will, economic resources, and societal values to steer toward a future where human progress does not come at the cost of ecological integrity and social equity.

Keywords: environmental policy, global economics, climate change, biodiversity loss, socioeconomic inequality

Climate change and global sustainability

It is unequivocal that human influence has warmed the atmosphere (1) and the climate crisis is now well underway. Global greenhouse gas (GHG) emissions set a new record in 2023 (2), rising an estimated 1.1%, the third annual increase in a row since the COVID-19 recession. With a record 1.45 ± 0.12°C of anthropogenic global heating reached in 2023 (3), we already see nearly one-third of the world population exposed to deadly heat waves (4), a 9-fold

Competing Interest: The authors declare no competing interest.

increase in large North American wildfires (5), record-setting regional-scale megadrought (6), the Antarctic ice sheet losing nearly 75% more ice between 2011 and 2020 than it did for the period 2001 and 2010 (7), animal and plant extinctions projected to increase 2- to 5-fold in coming decades (8), deepening genetic diversity loss (9), and a weakened global ecosystem (10) pushed to its breaking point (11).

Scientists suspect the last several years have been warmer than any point in more than 125,000 years (12). Yet demand for oil climbed to over 100 million barrels per day in 2023, the highest in history (13). Despite decades of global investment in clean energy (14), fossil fuels still provide over 80% of global energy use (15), a figure that has not changed for decades. In the absence of climate action, our world is on course (16) to heat a blistering 3°C, perhaps more (17), potentially displacing one-third of humanity (18).

One study (19) suggests that ~9% of people (>600 million) already live outside the human climate "niche." Another concludes that, compared with people born in 1960, children born today will experience 7.5 times as many heatwaves, 3.6 times as many droughts, 3 times as many crop failures, 2.8 times as many river floods, and 2 times as many wildfires (20). Studies (21) forecast climate-related extinction of 14–32% of macroscopic species in the next ~50 years, including 3–6 million animal and plant species, even under intermediate climate change scenarios. With continued warming, the frequency of wildfires will increase over 74% of the global landmass by the end of this century (22). Such assessments are conservative as they are based on projections from climate models that may not capture some important processes through which human-caused heating amplifies persistent weather extremes (23, 24).

Of the 40 leading economies, all of which agreed in the 2015 Paris Climate Accord to take all necessary actions to stop global heating below 1.5°C, not one nation is on track to do what they promised (25). Globally, current climate policies are incompatible with limiting global heating to 1.5°C (26). The remaining budget for a 50% chance of keeping warming to 1.5°C is approximately 250 $GtCO_2$ as of January 2023, now equal to around 6 years of current emissions (27). The energy plans of countries responsible for the largest GHG emissions would lead to 460% more coal production, 83% more natural gas, and 29% more oil in 2030 than is compatible with limiting global heating to 1.5°C, and 69% more fossil fuels than is compatible with the riskier 2°C target (28).

The market cost of oil, coal, and natural gas is distorted by subsidies and does not include negative externalities related to pollution, climate change, healthcare, and others (29). Worse, the false promise (30) and widespread allure of unregulated quick fixes, such as "net-zero" contracts that lack monitoring, auditing, and verification, threaten to derail even the best-intentioned commercial and governmental plans for climate stabilization (31). Investigations suggest that the great majority of products transacted on carbon offset markets remove very little GHG from the atmosphere (32), and models indicate that even direct removal of atmospheric CO_2 does not recover former environmental conditions crucial to food and water security or ecosystem restoration (33).

We do not promote a "doom and gloom" philosophy regarding the future of human civilization. We are optimistic that humanity can correct the unsustainable pathway that we are on. Later in this review, we describe necessary steps in this direction. However, we do take an objective and realistic stand on the issue of sustainability. The realities described here quantify a severe and immediate threat to human health and well-being. They emphasize the imperative for a rapid, sweeping reduction in GHG emissions, and highlight stubborn barriers that impede progress. Developed nations, emerging economies, and commercial entities must invest in rapid decarbonization; correct market distortions favoring fossil fuels; and avoid the spurious trap of false "net-zero" offsets as an excuse to continue polluting the atmosphere.

Imperialism, overpopulation, and resource extraction

Around the world, a growing number of entities and environmental activists are taking action (34). As of December 2022, there have been 2,180 climate-related legal cases filed in 65 jurisdictions, including international and regional courts, tribunals, quasijudicial bodies, or other adjudicatory bodies. Lawsuits related to climate change have more than doubled over the last 5 years as litigants see courts as a way to enhance (or delay) climate action (35). Children and youth, women's groups, local communities, and Indigenous Peoples, among others, are taking a prominent role in bringing these cases and driving climate change governance reform around the world. This "climate justice movement" seeks to extend the principles of human rights and environmental justice by arguing that future generations have a birthright to a safe climate capable of sustaining genuine human development on a healthy and resilient planet (36).

Yet, for hundreds of years, various manifestations of imperialism, such as slavery, settler colonization, economic and cultural dominance, neocolonialism (37), and the forces of globalization, have promoted a mindset of class privilege and wealth. Motivated by profit, the mechanisms of industrial capitalism have pursued relentless resource depletion achieved by subjugation of local communities, erasure of Indigenous knowledge, and unsustainable plunder of the natural world (38).

Modern imperialism is embodied by industrial capitalism, which prioritizes resource extraction and maximizing profit. This paradigm is deeply embedded in the fabric of global affairs, influencing international trade, political dynamics, and the economic frameworks of nations (39). The persistent reliance on extractive economic practices continues to be a significant obstacle to making critical progress in decarbonization, conserving natural resources, and ensuring social equity. For instance, despite decades of international commitments to end deforestation, around 4.1 M hectares of primary tropical rainforest was lost globally in 2022—an increase of 10% over 2021—producing 2.7 Gt of CO_2 emissions, equivalent to the annual fossil fuel emissions of India (40). Most modern socioeconomic systems still follow extractive rules of exploitation and trade, and ignore natural rates of resource renewal, failing to consider that the end result is catastrophic (41).

Global population growth amplifies the damage wrought by industrial capitalism. On 15 November 2022, the world's population reached 8 billion people. Human population is expected to increase by nearly 2 billion in the next 30 years, and could peak at nearly 10.4 billion in the mid-2080s (42). Cambridge economist Sir Partha Dasgupta developed a rigorous approach to the question "What is optimal human population?" (43). His theory relates population, consumption, and resource capacity, concluding that an optimal global population lies between 0.5 and 5 billion. This theory implies that Earth is already overpopulated relative to ecological carrying capacity. With every additional person added to the planet, wild habitats are disturbed or destroyed by urbanism, agricultural activities, and resource consumption, with humanity demanding more than what the biosphere can sustainably provide.

Dasgupta highlights the critical connection between our economies, livelihoods, and well-being with the Earth's resources. He argues that current global demand for natural resources surpasses its capacity to supply, driven by factors like population growth and consumption patterns. This overuse threatens biodiversity and ecosystem services. To safeguard our prosperity and the environment, we must rethink our approach to economic success. Key recommendations include increasing nature's capacity and ensuring our demands on nature stay within sustainable limits. This involves investing in natural capital, revising economic metrics, transforming institutions (especially finance and education), and empowering citizens. Legitimate sustainability is vital for achieving a long-term balance between population, economic growth, and the environment. Future generations' well-being hinges on how we manage economic, social, and natural resources today. Urgent action is required to address these interconnected challenges.

Given the current state of the ecosphere, a 25% increase in population and projected doubling of economic activity by 2050 (44) may drive major ecological regime shifts (i.e. forest to savannah, savannah to desert, thawing tundra, and others) well before 2080. Nature may impose its own population correction before standard projections are realized (45). Actions to slow and reverse population growth are critical (46). These include empowering women, investing in girls' education, strengthening healthcare systems, and implementing social welfare programs that create job opportunities, reduce poverty, and improve living standards.

Human population growth, increased economic demands, rising heat, and extreme weather events put pressures on ecosystems and landscapes to supply food and maintain services such as clean water. Studies show that ecosystems threatened by sudden regime shifts are at greater risk of collapse than previously thought (47). Researchers warn that more than a fifth of ecosystems worldwide, including the Amazon rainforest, are at risk of a catastrophic breakdown within a human lifetime.

The United Nations' Sustainable Development Goals (SDGs), a suite of 17 objectives with 169 targets established in 2015 for achievement by 2030, face a grim forecast: current trends suggest none of the goals and merely 12% of the targets may be realized (48). This shortfall underscores the urgent need to dismantle the entrenched model of resource extraction and wealth concentration, advocating for a paradigm shift toward genuine sustainability and resource regeneration. Such a transformation is imperative to reverse the tide of biodiversity loss due to overconsumption and to reinstate the security of food and water supplies, which are foundational for the survival of global populations.

Global economics and values

Convergence of worldwide trends threatens safe and sustainable human development: accelerating impacts from climate change (49), biodiversity loss (50) caused by unsustainable consumption (51), extractive agriculture, natural resource exploitation (52) and limitations, emergent disease (53), pervasive pollution (54), and socioeconomic injustice (55). To secure a safe future for humanity, global economics and values must protect the well-being of the natural world. This requires understanding the impacts, intersections and feedbacks of these global emergencies, as well as solutions to ensure a livable planet (56). These emergencies, promulgated by extractive policies (57), human population growth, and modern imperialism (58), overlap in ways that amplify negative outcomes (Fig. 1). If successive governments treat these issues in isolation, hesitate, or formulate shallow responses, the fallout may be catastrophic. Without immediate action, we risk entering a malignant era of global distress and suffering characterized by disease, thirst and hunger, impoverishment, and political instability.

The cocoon of wealth enjoyed by developed nations belies the suffering and misery many low latitude and semiarid communities already endure in tenuous heat and drought conditions. Consider the Northern Hemisphere summer of 2023. Over 80% of the global population experienced climate change-driven heat in the month of July (59) (Fig. 2). It featured 7 consecutive months of record-shattering global temperature driven by a combination of a moderately strong El Niño and a decrease of Earth's albedo (equivalent to an increase of atmospheric CO_2 from 420 to 530 ppm) (60). Extreme heatwaves swept many parts of the world. Sea surface temperatures leapt to record highs. Antarctic sea ice was far below average. Record wildfires burned for months destroying tens of millions of acres and produced continental-scale public health crises in air quality, and tens of thousands of temperature records around the world were broken. Without human-induced climate change these events would have been extremely rare (61).

It is past time to build a new era of reciprocity with nature that redefines natural resource economics. The ecological contributions of Indigenous Peoples through their governance institutions and practices are gaining recognition and interest. Indigenous systems of land management encompass a holistic approach that values sacred, ethical, and reciprocal relationships with nature, integrating traditional knowledge and stewardship principles to sustainably manage land and water resources. Indigenous land management challenges conventional power structures and introduces innovative solutions to environmental issues, especially in the context of climate change.

Indigenous Peoples exercise traditional rights over a quarter of Earth's surface, overlapping with a third of intact forests and intersecting about 40% of all terrestrial protected areas and ecologically intact landscapes. These lands typically have reduced deforestation, degradation, and carbon emissions, compared with nonprotected areas and protected areas (62). Beyond western ideas of quarantining land for conservation, Indigenous land management involves a mix of active land management, biomimicry, and conservation to maximize nutrition, food and water security, carbon sequestration, biodiversity, and ecosystem restoration (63). These qualities offer beneficial feedbacks that increase human health and resiliency, build social equity, and provide for the needs of future generations.

We suggest that an Indigenous worldview, that of kinship with nature, should define sustainable practices. Laws that establish legal rights for nature have reached a critical point at which they may either be normalized or marginalized (64); this progress must be sustained. For instance, Māori in New Zealand have successfully asserted sovereignty to grant legal personhood to the Whanganui River and Te Urewera National Park. This reflects Māori worldviews and recognizes their governance, allowing "nature" to have a legal voice. In the US, the Menominee Forest Management Reserve, recognized as a best practice, is driven by the Menominee vision and worldviews. It operates under the recognition of Menominee sovereignty and decision-making authority.

Nations must build on these regenerative practices by eliminating environmentally harmful subsidies (65), and restricting trade that generates pollution and unsustainable consumption. Studies (66) indicate the global economy must achieve absolute

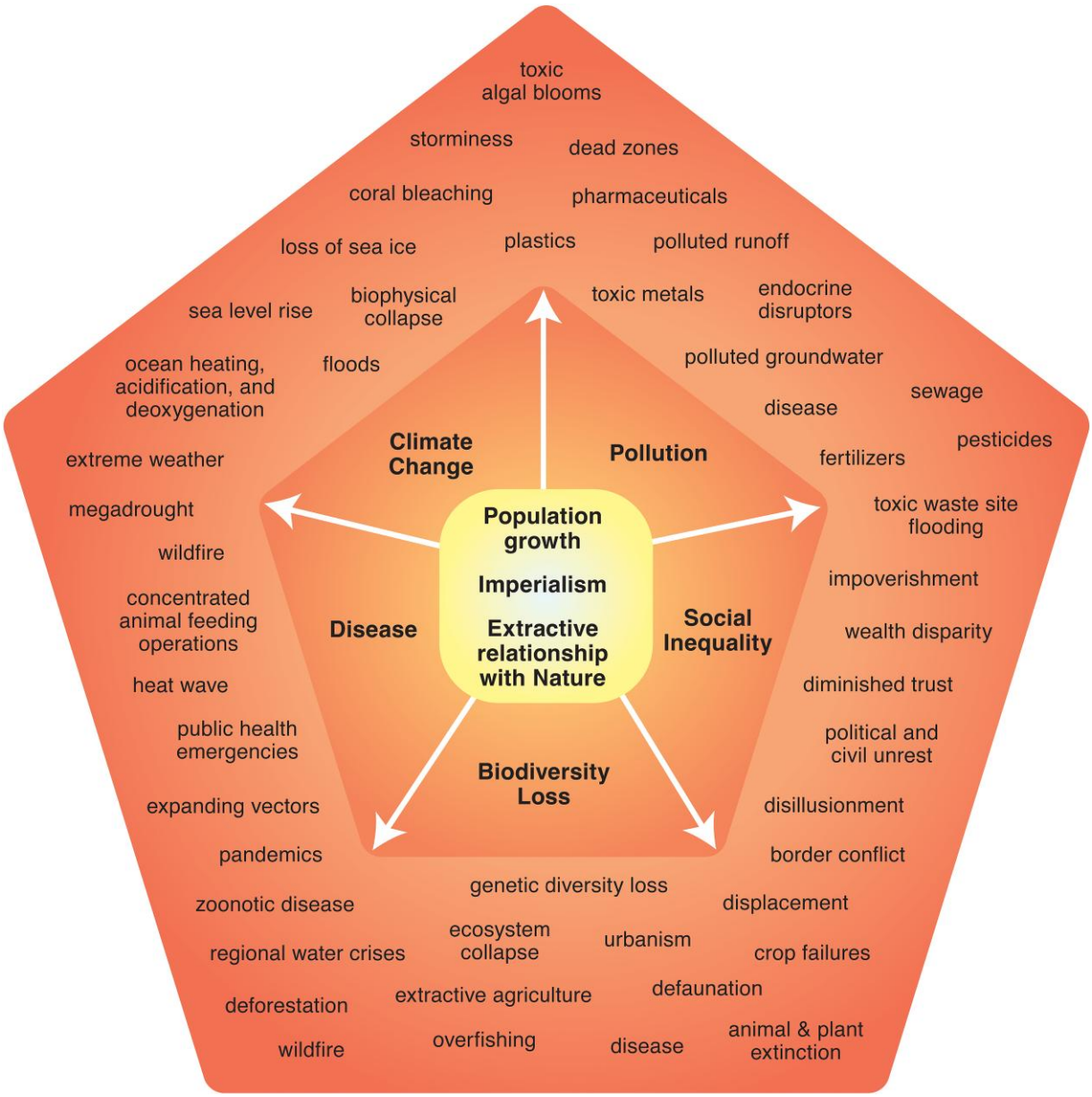

Fig. 1. Global population growth, imperialism, and an economic model based on extractive rules of exploitation and trade that ignores natural rates of resource renewal, set the stage for a convergence of several worldwide trends that threaten safe and sustainable human development: accelerating impacts from climate change, pollution, social inequality, biodiversity loss, and disease.

decoupling (in which resource impacts decline in absolute terms) (67) if we are to eliminate "ecological overshoot"[a] (68).

In the words of coauthor Jay Bowen, Upper Skagit Elder, "We are all Indigenous to this Earth. We are one family." The authors of this review believe that humanity stands at an inflection point in human history that will determine many characteristics of future life on Earth (Fig. 3). Continued failure to integrate these problems in climate resilient development and regenerative practices risks the stability of human communities and natural systems. Heads of state must recognize the existence of a global emergency (56), treat these crises as intertwined issues, and apply the considerable power of the economy toward restoring a livable planet and an equitable and just socioeconomic system before climate instability and ecological regime shift are beyond our control. Later in this paper, we offer specific suggestions for implementing these changes.

Climate realities and the road to action

In April 2023, CO_2 levels measured at Mauna Loa Observatory in Hawai'i reached an annual peak of 424.8 ppm, more than 50% greater than the preindustrial level of 278 ppm. In the first decade of measurement at Mauna Loa (1959–1968), the average annual growth rate was 0.8 ppm per year. The average annual growth rate over the most recent decade (2014–2023) was 3 times that amount, 2.4 ppm per year, the fastest sustained rate of increase in 65 years of monitoring (69).

More than half of all industrial CO_2 emissions have occurred since 1988 and 40% of the CO_2 we emit today will still be in the atmosphere in 100 years, about 20% will still be there in about 1,000 years (70). The last time CO_2 levels were this high was the Pliocene Climatic Optimum, 4.4 milion years ago, when Earth's climate was radically different; global temperature was 2–3°C hotter, beech

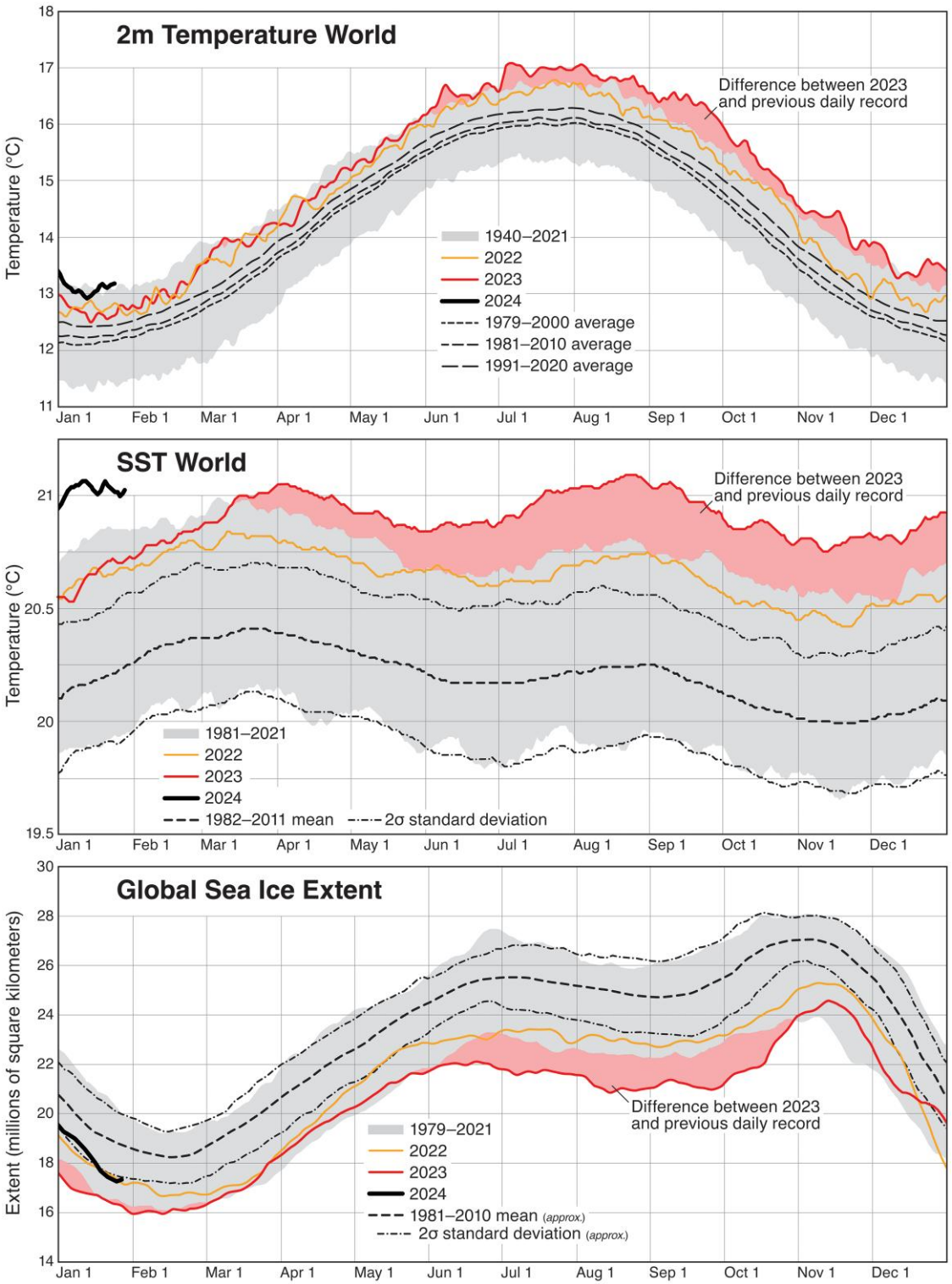

Fig. 2. In 2023, astonishing new records were set in 2 m surface temperature, sea surface temperature (SST), and global sea ice extent (2 m Temperature World, and SST World after Climate Reanalyzer, Climate Change Institute, University of Maine, https://climatereanalyzer.org/; Global Sea Ice Extent after https://zacklabe.com/global-sea-ice-extent-conc/).

trees grew near the South Pole, there was no Greenland ice sheet, no West Antarctic ice sheet, and global sea level was as much as 25 m higher than today (71).

Atmospheric methane (CH_4) growth has surged since 2020. Averaged over 2 decades, the global heating potential of CH_4 is 80 times greater than CO_2. The largest sources of atmospheric CH_4 are wetlands, freshwater areas, agriculture, fossil fuel extraction, landfills, and fires. In 2023, atmospheric CH_4 exceeded 1,919 ppb, on track to triple the preindustrial level of 700 ppb by 2030. Carbon isotopic signatures reveal microbial decomposition of organic matter as the major source of CH_4 emissions, indicating that natural CH_4-producing processes are being amplified by

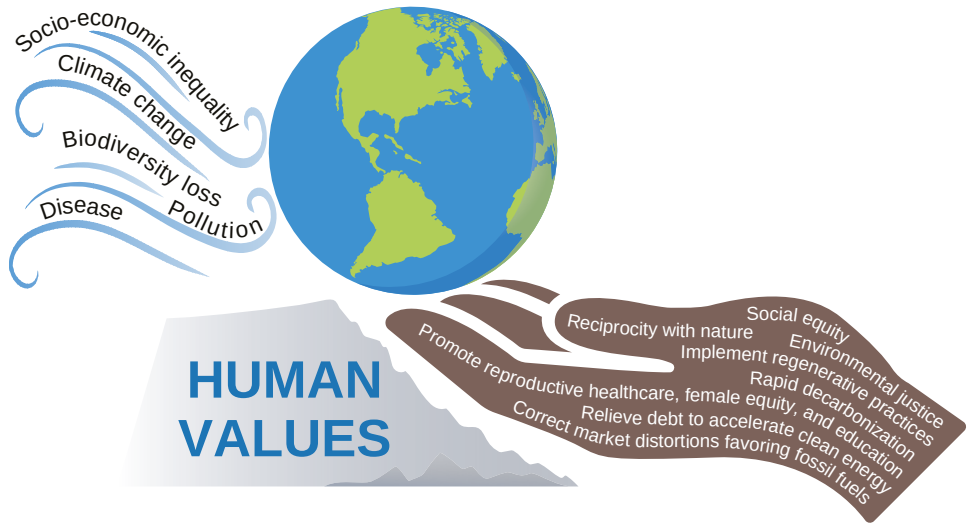

Fig. 3. The stability of human communities and natural ecosystems is at risk under the shocks and stresses of five planetary emergencies: socioeconomic inequality, climate change, biodiversity loss, pollution, and disease. Unless human values shift dramatically and soon, the resulting damage to the natural world will likely be catastrophic, with long-lasting consequences for species and ecosystems, and devastating upheavals for humanity. A systemic change in human values is needed that focuses on Earth-centered governance, and entails a transition in collective values, behaviors, and institutional practices to prioritize long-term ecological health and social well-being over immediate gains.

climate change itself (72). Is this a sign that global heating is shifting beyond our control?

Under an intermediate scenario (SSP2-4.5), GHG emissions are very likely to lead to heating of 1.2–1.8°C in the near term (2021–2040), 1.6–2.5°C in the midterm (2041–2060), and 2.1–3.5°C in the long term (2081–2100) (73). As of November 2023, 145 countries had announced or are considering net-zero targets, covering close to 90% of global emissions (74). Among these are China, EU, USA, and India, who jointly represent more than half of global GHG emissions. However, net-zero evaluations for G20 countries and selected other countries as of November 2023 show that most net-zero targets are formulated vaguely and do not yet conform with good practices.

Even as the vast majority of countries pledged to slash their climate emissions, their own plans and projections put them on track to extract more than twice the level of fossil fuels by 2030 than would be consistent with limiting heating to 1.5°C, and nearly 70% more than would be consistent with 2°C of heating (28). The world has a 67% chance of limiting warming to 2.9°C if countries stick to the nationally determined contributions (NDCs) made under the 2015 Paris agreement (26). Emission cuts of 14 $GtCO_2$ or 28% are needed by 2030 to keep within 2°C of warming. A reduction of more than 40% or 22 $GtCO_2$ is needed for the 1.5°C threshold to be realistic.

The world now only has a 14% chance of limiting warming to the 1.5°C goal, even if countries honor all NDCs. Limiting warming to 1.5°C would require global emission reduction of 8.7% per year. Even with COVID-19 lockdowns limiting manufacturing, ground and air transportation, and other economic activities during 2020, emissions dropped by only 4.7% (26).

Many countries' net-zero pledges "are not currently considered credible" (26). No G20 country is reducing emissions at a pace consistent with their net-zero targets. The lifetime emissions of current and planned oil and gas fields and coal mines is 3 and a half times greater than the carbon budget needed to hold temperature increase to 1.5°C. It would exhaust almost all the budget needed for 2°C.

Under current national climate plans, emissions are expected to rise 9% above 2010 levels by the end of this decade even if NDCs are fully implemented. GHG emissions would fall to 2% below 2019 levels by 2030. Although these numbers suggest the world will see emissions peak this decade, that's still far short of the 43% reduction against 2019 levels that the Intergovernmental Panel on Climate Change (IPCC) says is needed to stay within the 1.5°C target envisioned by the Paris Agreement (26).

Emission reductions of 43% are needed by 2030 to keep 1.5°C in play. But since the 26th Conference of Parties (COP) in 2021, nations have shaved just 1% off their projected emissions for 2030, and COP 28 in 2023 ended with no increase in ambition. Seventy-five percent of nations that have set targets to limit GHG emissions have enshrined them in law or policy documents, but the plans needed to implement those pledges are lacking in almost all cases (74), and policies based on "net-zero" actions no longer have credibility. Current pledges would lead to long-term global heating of 2.4–2.6°C, but on-the-ground policies put the world on track for heating approximately 3°C above preindustrial levels. Avoiding dangerous levels of heating requires systemic transformation to energy, waste, transportation, agriculture, and industry.

Climate indicators show that global heating reached 1.14°C averaged over the past decade, 1.26°C in 2022, and 1.45 ± 0.12°C over the 12-month period of 2023. In 2023, some 7.3 billion people worldwide were exposed, for at least 10 days, to temperatures influenced by global warming, with one-quarter of people facing dangerous levels of extreme heat. Heating is increasing at an unprecedented rate of over 0.2°C per decade (perhaps faster) caused by a combination of annual GHG emissions at an all-time high of 54 ± 5.3 $GtCO_2e$ over the last decade, and reductions in the strength of aerosol cooling (17). The Northern Hemisphere summer of 2023 revealed a shift in climate indicators marking a new level of intensity. "There has never been a summer like this in recorded history: shocking ocean heat, deadly land heat, unprecedented fires and smoke, sea ice melting faster than we've ever seen or thought possible (75)."

Climate outlook

Planned cuts in global emissions are inadequate for protecting human security and Earth's remaining biodiversity. Under

implemented national policies alone, dangerous heating is only avoidable with a massive rollout of GHG removal technologies and large-scale ecosystem restoration that is nowhere in evidence today. For instance, even the planned investment of $3.5B to develop four "direct air capture" hubs under the 2022 US Bipartisan Infrastructure Law will only remove the equivalent of 13 min of global emissions at full annual capacity (30). Planting 8 billion trees, one for every person on Earth, would remove the equivalent of only 43 h of global emissions after the trees reached maturity decades from now, and the change in albedo related to the new ground cover increases the complexity of expected benefits.

The only honest strategy for today is radical, immediate cuts in fossil fuel use. Only after emissions have begun a rapid downward trajectory should investments in carbon removal (the engineering for which has yet to be defined or validated) occur with speed and at scale (76). Even this will be met with ocean outgassing of CO_2 such that climate recovery will see a long delay (33).

This urgency is underscored by the fact that current emissions are underreported, and decreasing natural carbon storage makes limiting global temperatures even more challenging. Global emissions are as much as 3 times higher than reported (77) with 70% underreporting of energy-related CH_4 emissions alone (78). In addition, the terrestrial biome, which sequesters about 31% of anthropogenic CO_2 emissions, has already neared, and in places crossed, a photosynthetic thermal maximum beyond which terrestrial carbon storage will grow increasingly impossible (79). For instance, global carbon loss from tropical forests has doubled in the last 20 years (80), and the Brazilian portion of the Amazon Forest has become a net GHG source (81). Eighty-three percent of tropical forest carbon loss is driven by agriculture, suggesting that strategies to reduce deforestation have failed, and that carbon emissions from forest destruction are undercounted (82).

The United Nations estimates that 1.84 billion people worldwide, or nearly a quarter of humanity, were living under drought in 2022 and 2023, the vast majority in low- and middle-income countries (83). Megadrought projected for the year 2100 could strike up to 50 years earlier according to models (84). Global heating risks food (85) and water (86) availability with human populations in conditions of extreme to exceptional drought (87) doubling by 2100 (88).

Climate change threatens natural ecosystems (89), human security (90), livable conditions for communities (91), and the stability of 1/3 of the human population (18). Under current levels of heating, people are 15 times more likely to die from extreme weather than in years past, and 3.3 billion human lives are "highly vulnerable" to climate change (92). At 2°C heating, up to 3 billion people may suffer chronic water scarcity. Today, 1 in 3 people are exposed to deadly heat stress. This number is projected to increase up to 75% by the end of the century.

By 2050, over 300 million people living on coasts will be exposed to flooding from sea level rise (93). Forced to migrate, the impacts of these displaced communities will ripple through the larger population. Climate change drives the spread of disease in people, crops, domesticated animals, and wildlife. Even if heating is held below 1.6°C, 8% of today's farmland will be unfit to produce food. Declining food production and nutrient losses will result in severe stunting affecting 1 million children in Africa alone and cause 183 million additional people to go hungry by 2050 (92).

Abrupt change

Earth's biophysical systems are shifting toward instability (94), perhaps irreversibly (95). The IPCC has identified 15 Earth system components with potential for abrupt destabilizing change, including ice, ocean, and air circulation; large ecosystems; and precipitation. These systems are the pillars of life that permit stable plant, animal, and microbial communities, food production, clean water and establish the conditions for safe human development. However, these systems may be characterized by threshold behavior. That is, they appear to remain stable as global temperature rises, but at a certain level of heating, they may "tip" into a fundamentally irreversible new state (96).

As Earth retains heat, ice melt accelerates (97), especially in the Arctic which is heating nearly 4 times faster than the global average (98). Arctic sea ice is declining (99), and the transition from a snow- to rain-dominated Arctic in the summer and autumn may occur as early as 2040, with profound climatic, ecosystem, and socioeconomic impacts (100). The Greenland Ice Sheet is vulnerable to ice loss due to melt-elevation feedback (101), and Greenland is losing ice 7 times faster than in the 1990s (102). Antarctic melting has tripled in the past 5 years (103), and ice shelf collapse may lead to amplified sea level rise (104, 105).

According to one study, if temperatures rise by 1.5°C, the loss of four biophysical systems will become "likely" and loss of an additional six will be "possible." Loss of 13 biophysical systems will be either "likely" or "possible" if the planet warms by 2.6°C, as expected under current climate policies (94). Emerging changes such as deep ocean heating (106), marine stratification (107), declining marine vertical circulation (108), and sea level rise (109) will continue for centuries even if net-zero emission targets are reached. The Intergovernmental Panel on Climate Change Assessment Report 6, Working Group I (110) projects possibly abrupt and irreversible change in permafrost carbon, West Antarctic ice sheets and shelves, and ocean acidification and deoxygenation. These changes could unleash feedback loops that place climate impacts beyond our control (111).

Oceans

The world's oceans face irreversible impacts from climate change, with heating, acidification, stratification, and loss of dissolved oxygen posing high costs for marine ecosystems (112). Ocean heating has intensified (113), with the Southern Ocean taking up most of the excess heat generated by anthropogenic activities (114). These changes affect marine species distributions, interactions, abundance, and biomass. Combined with other stressors like pollution, they are putting marine biodiversity and its societal benefits at risk (115).

Amplified by global heating (116), marine biodiversity is being decimated by more than 440,000 industrial fishing vessels around the world that are responsible for 72% of the world's ocean catch. Over 35% of the world's marine fishery stock is overfished and another 57% is sustainably fished at the maximum level (117). One study showed that more than 90% of the world's marine food supplies are at risk from environmental changes such as rising temperatures and pollution, essential to over 3.2 billion people. Top producers like China, Norway and the United States face the biggest threat (118). Marine heatwaves (119) are increasing with negative impacts on marine organisms and ecosystems. Marine coastal biodiversity is at risk, with over 98% of coral reefs projected to experience bleaching-level thermal stress by 2050 (120).

Relative to the period 1995–2014, global mean sea level is conservatively projected to rise 0.15–0.29 m by 2050, and 0.28–1.01 m by 2100 (109). Higher rise would ensue from disintegration of Antarctic ice shelves and faster-than-projected ice melt from Greenland (121). On multiple occasions over the past 3 million

years, when temperatures increased 1–2°C, global sea levels rose at least 6 m above present levels (122). Sea level rise will flood toxic waste sites, cesspools and septic systems, municipal dumps, and polluted groundwater. In many cases, communities of color will be first to experience health impacts (123).

Ocean pollution affects marine species and people who depend on them. Toxic metals, plastics, manufactured chemicals, petroleum, urban and industrial wastes, pesticides, fertilizers, pharmaceutical chemicals, agricultural runoff, and sewage are the most detrimental and persistent pollutants (124). More than 80% of marine pollutants originate from land-based sources, reaching the oceans through rivers, runoff, and atmospheric deposition. Pollution is heaviest in coastal waters, especially in low- and middle-income countries (125).

Toxic metals such as mercury, lead, and cadmium accumulate in marine animals, causing health problems in fish species and disrupting endocrine systems in their human consumers (126). Plastics take hundreds of years to degrade, breaking down into microplastics that are ingested by fish, humans, and other organisms (127). Manufactured chemicals such as polychlorinated biphenyls and dioxins are environmentally persistent toxins that accumulate in the tissues of marine animals, disrupting hormonal systems (128). Urban and agricultural runoff, and sewage contain pathogens (129), heavy metals, and organic compounds that harm marine animals and cause human health problems. Nitrogen pollution also results in toxic algal blooms and oxygen-depleted dead zones (130). The equity and justice implications of this massive problem have been largely overlooked or downplayed (131).

Terrestrial biome

Tropical forests now emit more carbon than they are able to absorb from the atmosphere as a result of the dual effects of deforestation and land degradation (132). Rich-nation demand (133) for lumber, minerals, beef, and animal feed outside their own borders undermine attempts to mitigate climate change (134). Demand for food, feed, fiber, minerals, and energy is resulting in whole forests being clear-cut. CO_2 emissions from boreal forest fires have reached a new high, producing nearly 1/4 of the total global CO_2 emissions from wildfires (135). Only 40% of remaining forests have high ecosystem integrity (136). Forests are degraded (137) by drought, pests, and wildfire related (138) to climate change.

Forest loss sacrifices soil biodiversity and integrity to oxidation, dehydration, and heating, transforming soil into a persistent source of CO_2 emission (139). Only 2.9% of Earth's land remains ecologically intact (140). Essential ecosystems are disappearing, and many species are at risk of extinction (141). Anthropogenic extinction rates are driving Earth's sixth mass extinction (142). Each year, the world consumes more than 92 Gt of materials—biomass (mostly food), metals, fossil fuels, and minerals. This figure is growing at the rate of 3.2% per year. Resources are being extracted from the planet 3 times faster than in 1970, even though the population has only doubled within that time (143). During the 20th century, this boosted the global economy, but since then resources have become more expensive to extract and the environmental costs harder to ignore.

Both plant and soil carbon storage originate with photosynthesis, which withdraws about 31% of annual anthropogenic CO_2 emissions (2). However, studies (144) across a range of forest ecosystems have found that heating leads to thermal stress and reduced carbon assimilation. Many ecosystems (80) are already operating at or beyond thermal thresholds for photosynthesis (145). Widespread terrestrial ecological decline has resulted from the combination of climate change, resource extraction, bushmeat hunting, and agricultural and urban development. Since 1970, vertebrate populations have declined 69% (146), and 1 in 4 species are at risk of extinction (147), in part because 75% of the terrestrial environment has been severely altered by human actions.

Agricultural development has further eroded ecosystem health, with over 15 billion trees per year lost since the emergence of agriculture; the global number of trees has fallen by over 45% (148). An estimated 67,340 km^2 of global forest were lost in 2021 alone, unleashing 3.8 Gt of GHG emissions, roughly 10% of the global average (149). Such losses extend to wetland areas; more than 85% of the wetlands present in 1700 had been lost by 2000, and loss of wetlands is currently 3 times faster than forest loss.

Food and water security

Increasing human population, and the need to expand food production, were the drivers of the Green Revolution over 50 years ago (150). This increased productivity through selective genetic breeding, monocultures, seed improvement, and the use of chemical fertilizers and pesticides. These steps have not solved the problem of food insecurity which has been aggravated in more vulnerable populations (151). Worldwide, it is estimated that 16,000 children are pushed into hunger every day—a 32% increase from 2022 (152).

Agriculture now uses half of the world's ice- and desert-free land, and causes 78% of global ocean and freshwater eutrophication (153). Pesticide and fertilizer runoff, as well as sewage, find their way to aquatic environments (154) and degrade water quality, while spreading infectious diseases. Humans poison the soil annually with microplastics between 4 and 23 times more than we do the oceans. Microplastics reduce beneficial bacteria concentrations, and can be absorbed by plants, and then passed up the food chain (155).

Industrial farming employs deep plowing that depletes and oxidizes soil, turning acreage into a source of GHG (156). Agriculture is responsible for 70% of global freshwater withdrawals (157). By one estimate (158), 94% of nonhuman mammal biomass is now livestock, and 71% of bird biomass is poultry livestock. 50% of all agricultural expansion has come at the expense of forests. In 2022, the rate of global deforestation was the equivalent of 11 soccer/football fields per minute (40), predominantly for cattle ranching and grain animal feed crops (such as soy) for export.

Today, agriculture uses half of all habitable land (159), and either through grazing or growing animal feed, 77% of that is dedicated to livestock (153). Animal agriculture is expanding. From 1998 to 2018 global meat consumption increased 58%. Cattle and the grain they eat use 1/3 of all available land surface, 1/3 of global grain production, and 16% of all available freshwater. Yet cattle agriculture only generates 18% of food calories and 27% of protein (153). The production of fertilizer for feed crops emits 41 $MtCO_2$/yr. The combination of emissions from manufacturing, transporting, and applying synthetic fertilizer on the land (which releases the potent GHG N_2O) today likely outpaces the emissions of the commercial aviation industry. These fertilizer-related GHG emissions are projected to grow. Additionally, livestock feed demands a minimum of 80% of global soybean crop and over 50% of global corn crop. Thirty-five to 40% of yearly anthropogenic CH_4 emissions are a result of domestic livestock production due to enteric fermentation and manure (160).

Under a range of GHG emission pathways, cropland exposure to drought and heat-wave events will increase by a factor of 10 in the midterm and a factor of 20–30 in the long term on all continents, especially Asia and Africa (161). Harvest failures across major crop-producing regions are a threat to global food security. Jet

stream changes are projected to increase synchronous crop failure and lower crop yields in multiple agricultural regions around the world (162). Crop failure due to drought, flood, or extreme weather (163) events increases disproportionately between 1.5 and 2°C of global heating (164). For maize, risks of multiple breadbasket failures increase from 6–40% at 1.5°C to 54% at 2°C. In relative terms, the highest climate risk increases, between 1.5 and 2°C heating, is for wheat (40%), followed by maize (35%) and soybean (23%). Limiting global heating to 1.5°C would reduce the risk of simultaneous crop failure for maize, wheat, and soybean by 26%, 28%, and 19%, respectively (164).

Demand for wheat is projected to increase 60% by 2050. Yet, rising CO_2 depletes the nutrient and protein content of wheat, and with drought, fire, and flood, leads to a 15% decline in projected wheat yield by midcentury (165). Increased levels of CO_2 are decreasing the amount of protein, iron, zinc, and B vitamins in rice with potential adverse health consequences for a global population of approximately 600 million (166). Harvests of staple cereal crops, such as rice and maize, could decrease by 20–40% as a function of heightened surface temperatures in tropical and subtropical regions by 2100 (167). This will exacerbate existing food security issues, as 1 billion people are currently classified as food insecure (168).

Worldwide, fungal infections cause growers to lose 10–23% of their crops each year, and an additional 10–20% is lost following harvest. Global heating is driving a poleward migration of fungal infections, meaning more countries will see fungal infections damaging harvests. Growers have reported wheat stem rust infections, usually tropical, in Ireland and England. Experts (169) also warn that fungi tolerance to higher temperatures could increase the likelihood of soil-dwelling pathogens to infect animals or humans. Across the five most important calorie crops of rice, wheat, maize (corn), soybeans, and potatoes, fungal infections already cause losses equal to provisions for 600 million to 4 billion people. Without major and rapid policy changes, food productivity in 2050 could be reduced to 1980 yield levels because new technologies will be unable to mitigate climate change in major growing regions (170).

Clean water security is a critical issue (171). Research shows that groundwater levels are rapidly declining, especially in dry regions with extensive croplands, and has accelerated over the past four decades in 30% of the world's regional aquifers (172). The Southern Hemisphere has experienced a 20% drop in water availability over the past two decades (173). Approximately 3.6 billion people, or 47% of the global population, suffer water scarcity at least 1 month each year (174). Global water security is an urgent concern due to the increasing imbalance between the finite supply of freshwater and the escalating demand driven by population growth, economic development, and agricultural needs. Climate change compounds the crisis by altering precipitation patterns, causing droughts, and depleting glaciers—key freshwater sources. Contamination from industrial, agricultural, and residential waste further restricts the amount of clean water available. This scarcity threatens human health, food production, and ecosystem stability, leading to conflicts and displacements. Addressing this problem requires global cooperation for sustainable management, technological innovation for conservation and purification, and policies that prioritize equitable access to clean water (174).

Heat

The impact of heat on food production is disproportionately severe in low-income communities. Workers in agriculture, construction, and other outdoor sectors often work in conditions that can lead to heat stress or heatstroke. Food production, too, is critically affected as extreme heat can reduce crop yields, increase irrigation needs, and lead to soil degradation. These communities have less access to heat-protection technologies such as air-conditioned spaces, efficient irrigation systems, or heat-resistant crop varieties. Consequently, their economic stability and food security are more vulnerable to climate-induced temperature increases, exacerbating existing inequalities and pushing these populations further into poverty.

In 2022, global heat stress caused the loss of 490 billion potential labor hours, 143 h per person, a 42% increase from the 1991 to 2000 average (175). The loss of labor due to heat exposure resulted in a $863 billion loss of "potential income" and wiped out the equivalent of 4% of Africa's GDP. The agriculture sector was hardest hit, accounting for 82% of losses in least developed countries. The global land area affected by at least 1 month of extreme drought per year increased from 18% averaged over the decade 1951–1960 to 47% in the decade 2013–2022. Because of heat stress, under a 2°C warming scenario, 525 million additional people will experience food insecurity by midcentury, compared to the period 1995–2014, and the number of heat-related deaths each year will increase by 370%. Older people and infants now are exposed to twice the number of heat-wave days annually as they were averaged over the period 1986–2005.

Heat-related deaths of people older than 65 have increased by 85% since the 1990s (175). Even under moderate warming, heat and drought levels in Europe that were virtually impossible 20 years ago reach 1-in-10 likelihoods as early as the 2030s (84). Averaged over the period 2050–2074, projections for two successive years of single or compound end-of-century extremes, unprecedented to date, exceed 1-in-10 likelihoods; while Europe-wide 5-year megadroughts become plausible. Whole decades of end-of-century heat stress could start by 2040, by 2020 for drought, and with a warm North Atlantic, end-of-century decades starting as early as 2030 become twice as likely.

For thousands of years, fundamental limits on food and water security meant that human communities have concentrated under a narrow range of climate variables characterized by mean annual temperatures (MATs) around 13°C (18). With continued GHG emissions, global heating of 3°C is projected to drive a MAT >29°C across 19% of the planet's land surface and displace one-third of the human population. Today, this MAT accounts for only 0.8% percent of Earth's land surface, mostly concentrated in the deep Sahara.

Model projections indicate that in the Middle East and North Africa, continued emissions will cause the emergence of unprecedented super- and ultraextreme heat-wave conditions (176). These events involve excessively warm temperatures (56°C and higher) and will be of extended duration (several weeks), quickly becoming life-threatening for humans (177). Researchers found that by 2100, under current levels of GHG emissions, 3 of 4 people in the world will be exposed to deadly heat conditions every year, with a higher occurrence of these conditions in intertropical areas (2). Coupled with significant socioeconomic differences within countries, heat waves intensify global disparities in health, especially given the depleted resources for several of these regions to respond to accelerated heating. In the last decade, there has been >2,300% increase in the loss of human life from heat waves as a result of about 1°C heating. On our current pathway, the global health and socioeconomic risks of continued heating are catastrophic.

The distribution of these conditions is unequal, and people and communities subjected to the loss of security are powerless to

respond. The impacts of this inequity may cause regionally existential deterioration and suffering. As temperatures rise, death rates increase most among the poorest populations (178). By 2099, under a scenario of continued high emissions growth, climate change increases death rates in low-income countries by over 106 deaths per 100,000, while high-income countries are projected to see death rates decrease by 25 deaths per 100,000, while spending significantly to prevent more deaths. Overall, today's rich countries pay nearly 3 times more than poor countries to adapt to rising temperatures and prevent additional deaths. When it comes to cutting emissions, the social and economic burden of inaction is predominantly carried by the poorest and most vulnerable in human society, including Indigenous and local communities, concentrated in developing countries.

Illness and disease

As the planet heats up, infectious diseases once confined to tropical regions are expanding their range. The World Health Organization estimates that by the end of this decade the climate impact on health will cost between $2 billion and $4 billion per year (179). Between 2030 and 2050, climate change is expected to cause approximately 250,000 additional deaths per year from, for example, undernutrition, malaria, cholera, diarrhea, and heat stress alone. This does not include massive climate burdens on agriculture, water, and sanitation, which also shape public health.

In July 2023, for the first time in 20 years, the United States experienced locally acquired malaria infections. Six cases were confirmed in Florida and one in Texas, none related to international travel (180). In Seattle, cases of West Nile disease were reported for the first time. Over half of the infectious diseases confronted by humanity have been aggravated by climatic hazards at some point (181). All communities are vulnerable to climate change impacts; however, children, elders, the sick, and the poor face the greatest risks (182). People with cardiovascular and/or respiratory chronic illnesses are particularly vulnerable to high temperatures (183). Air pollution from GHG emissions leads to increased health complications such as asthma and allergies. The impacts of climate change disproportionately affect vulnerable communities, including low-income regions and communities of color which have been disempowered by a history of colonialism, racism, oppression, and injustice. Extreme weather events further exacerbate the situation, driving animals and people together in unsanitary conditions and disrupting essential services like healthcare and clean water supplies.

Approximately 17% of diseases are spread by animal vectors causing over 700,000 deaths annually. Concentrated animal farming operations are breeding grounds for virulent pathogens (184), and over 15,000 new cases of mammals transmitting viruses to other mammals could occur in the next 50 years due to climate change (185). Smaller species like bats, rats, and other rodents are thriving in human-populated areas, contributing to the spread of diseases through their interactions. Biodiversity loss and deforestation are directly linked to the rise of infectious diseases, with 1/3 of zoonotic diseases attributed to these factors. Some 60% of known pathogens, and 3 out of every 4 new or emergent infectious diseases are zoonotic (186), and roughly 1/3 of those are attributed to deforestation and habitat loss (187). A new disease surfaces 5 times a year, and future global heating and precipitation changes will further expand habitats for pathogens and vectors, proliferating dengue fever, cholera, malaria, diarrhea, and other diseases (188).

Climate change intensifies the spread of infectious diseases, particularly in low-income communities, by expanding the habitats of disease vectors such as mosquitoes and ticks. Warmer temperatures and altered rainfall patterns increase the incidence and geographic range of vector-borne diseases like malaria and dengue fever. Flooding and extreme weather events, more common as the climate changes, can lead to waterborne diseases due to the contamination of freshwater supplies. Low-income areas often have insufficient healthcare infrastructure, making them more vulnerable to these outbreaks. Additionally, malnutrition from climate-induced food scarcity can weaken immune systems, further raising the susceptibility to infections. Thus, climate change magnifies health disparities, with low-income communities facing disproportionately high risks of disease.

Economic inequality, ecological destruction, and global security

A grossly unequal distribution of wealth couples with the increasing consumption patterns of a rising global middle class (189) to amplify ecological destruction. The poorest half of the global population owns barely 2% of total global wealth, while the richest 10% owns 76% of all wealth (190). The poorest 50% of the global population contribute just 10% of emissions, while the richest 10% emit more than 50% total carbon emissions (191). Climate change, economic inequality, and rising consumption levels intertwine to amplify ecological destruction.

Climate change, driven by carbon emissions, often stems from industrial activities catering to increased consumption, particularly in wealthier nations. This consumption depletes natural resources and exacerbates pollution and habitat loss. Economic inequality compounds these issues, as poorer communities lack the resources to adapt to environmental changes or invest in sustainable practices. Consequently, low-income communities bear the brunt of ecological degradation, such as soil erosion, water scarcity, and biodiversity loss, while their limited economic means prevent effective response or recovery. This cycle of consumption, inequality, and environmental impact creates a feedback loop, perpetuating and intensifying ecological damage globally.

Fifty years ago, underdevelopment and scarcity were drivers of unsustainable resource use, but today these roots have morphed into overdevelopment, affluence, and privilege driving unsustainable wealth accumulation and aggregate consumption. At present, not a single country delivers what its citizens need without transgressing planetary boundaries of long-term sustainability (192). Modern imperialism amplifies these inequalities through economic exploitation, wealth accumulation, political interference, cultural dominance, and other methods that leverage colonial power structures. Recognizing and addressing neocolonial practices is crucial for promoting equitable and sustainable development and respecting the sovereignty and self-determination of nations (193).

The use of natural materials and their benefits are unevenly distributed across the globe. Overconsumption is closely linked to wealth and income disparities with large amounts of money concentrated in a few rich countries, largely in the Northern Hemisphere (194). For example, environmental stresses and shocks related to natural resource extraction and use are outsourced to countries and regions outside the European Union, while more than 85% of the economic benefits stay within member countries (195).

Global inequality results in fragile regions where intensified conflict over scarce resources allows malevolent actors to thrive

(196). One study (197) found strong causal evidence linking climatic events to human conflict across all major regions of the world: for each 1 SD (1σ) change in climate toward warmer temperatures or more extreme rainfall, data show that the frequency of interpersonal violence rises 4% and the frequency of intergroup conflict rises 14%. Temperatures across the developed world are expected to warm 2σ to 4σ by 2050. Hence, amplified rates of human conflict could represent a large and critical impact of anthropogenic climate change.

Over the next 3 decades, even under best-case scenarios of low heating, national, and global security face severe risks in every region of the world. Higher levels of heating will pose catastrophic, and likely irreversible, global security risks over the course of the 21st century. A world where global mean surface temperature has increased 3°C will be characterized by widespread and intense heat stress, extreme weather events, ruptured and unproductive marine and terrestrial ecosystems, broken food systems, disease and morbidity, intense decadal megadrought, freshwater scarcity, catastrophic sea level rise, and large numbers of migrant populations. By 2050, under these malignant conditions, up to 1.2 billion humans could be displaced by climate change (198). These intensifying crises now threaten the very fabric of our global socioeconomic system. Immediate action is imperative to avert a collapse that endangers societal structures worldwide.

Climate purgatory

Although the global condition is bleak, after 200 years of fossil fuel expansion, we are at a turning point in the energy system. The clean-energy revolution is underway. Global sales of vehicles powered by fossil fuels peaked in 2017 (199), and in 2023 electric vehicle sales grew by 55%, reaching a record high of more than 10 million. For the first time ever, announced manufacturing capacity for electric vehicle batteries is now sufficient to fulfill expected demand requirements by 2030 (200).

Renewable energy installations jumped nearly 50% in 2023, the most rapid growth rate in two decades (200). After remaining flat for several years, global clean energy spending is increasing. Last year, renewables made up about 30% of total electricity generation, up from 25% in 2018. Global investment in the energy transition totaled $1.77 trillion in 2023, an increase of 17% from the prior year. Solar energy is expected to become the cheapest form of energy in many places by 2030 and major global powers are investing in infrastructure for energy transformation.

However, increasing global energy consumption offsets these gains in renewable energy. Because of rising power needs in developing nations due to population growth and industrialization, ongoing electrification of the transport and building sectors, and other areas of energy expansion, the International Energy Agency (IEA) projects increasing growth of energy demand, rising at an annual average rate of 3.4% in 2024–2026. Although the expansion of clean-energy sources is set to meet this demand growth, decoupling energy consumption and CO_2 production, the separation is not nearly wide enough to meet Paris Agreement Goals for stopping global heating.

Countries and companies are taking steps to address climate change while simultaneously making choices that undermine these efforts. This paradox places us in a state of climate purgatory. The IEA predicts (200) a peak in fossil fuel demand by 2030, but reports show governments planning to increase coal, oil, and gas production well beyond climate commitments. This math does not align with the 1.5°C or even the 2°C warming targets. Many experts consider these targets nearly impossible due to the global reluctance to urgently phase out fossil fuels. In this climate purgatory, we are at a critical juncture, where urgent, transformative action is required to reconcile our ambitions with our actions.

The 2023 UN "gap report" (26) tells us that governments plan to produce around 110% more fossil fuels in 2030 than would be consistent with limiting warming to 1.5°C, and 69% more than would be consistent with 2°C. National carbon-cutting policies are so inadequate that 3°C of heating could be reached this century. Based on existing national pledges, global emissions in 2030 will be only 2% below 2019 levels, rather than the 43% cut required to limit global heating to 1.5°C. To get on track, 22 $GtCO_2$ must be cut from currently projected global emissions in 2030. That is 42% of the total and equivalent to the output of the world's five worst polluters: China, US, India, Russia, and Japan.

The world will need to increase climate spending to around $9 trillion annually by 2030 and to nearly $11 trillion by 2035 to roll out clean sources of energy and prepare for the inevitable impacts of a warming climate during coming decades (201). To limit warming to 1.5°C now requires eliminating emissions shortly after 2040. Although technically feasible, few mainstream scientists believe it is still achievable (202). Instead, analysts predict (203) that global fossil fuel emissions will peak at some point in the next decade, followed not by a decline but a long plateau (204), culminating with end-of-century warming potentially reaching 3°C (Fig. 4).

Although global renewable energy capacity is growing, there is a lack of financing for emerging and developing economies. Redirecting financial resources to lower income nations is crucial. More than 90% of clean-energy investment comes from advanced economies and China, risking new dividing lines in global energy. The biggest shortfalls in clean-energy investment are in emerging and developing economies. More needs to be done by the international community to drive investment in lower income economies, where the private sector has been reluctant to venture. There is ample capital available—evidenced by the nearly $12 trillion allocated for COVID-19 economic relief and the over $1 trillion annually in fossil fuel subsidies, which balloons to $7 trillion with indirect incentives. Reallocating these funds is complex, particularly due to potential impacts on the poorest populations, yet it remains a vital reservoir for investment as the world plans for a sustainable future.

A new era of reciprocity with nature and among human societies

The purpose of this review is to draw immediate attention to the careless, foolish way that humanity is gambling with the future. Unless things change dramatically, and soon, damage to the natural world will have long-lasting consequences for species and ecosystems, and devastating upheavals for humanity. Although this will particularly affect vulnerable populations, all of humanity faces an unprecedented catastrophe.

There are signs that humanity is awakening to the need for a new system of values that recognize Earth as an island in space with limitations on resource availability. No one is coming to rescue us. Many of the changes that we call for in this essay are consistent with the work of the Intergovernmental Science-Policy Platform on Biodiversity and Ecosystem Services (141) and the UN SDG framework (205). But carbon assimilation in natural systems is decreasing—potentially with significant effects in only decades; planetary-scale biophysical systems such as the Atlantic Meridional Overturning Circulation, the Southern

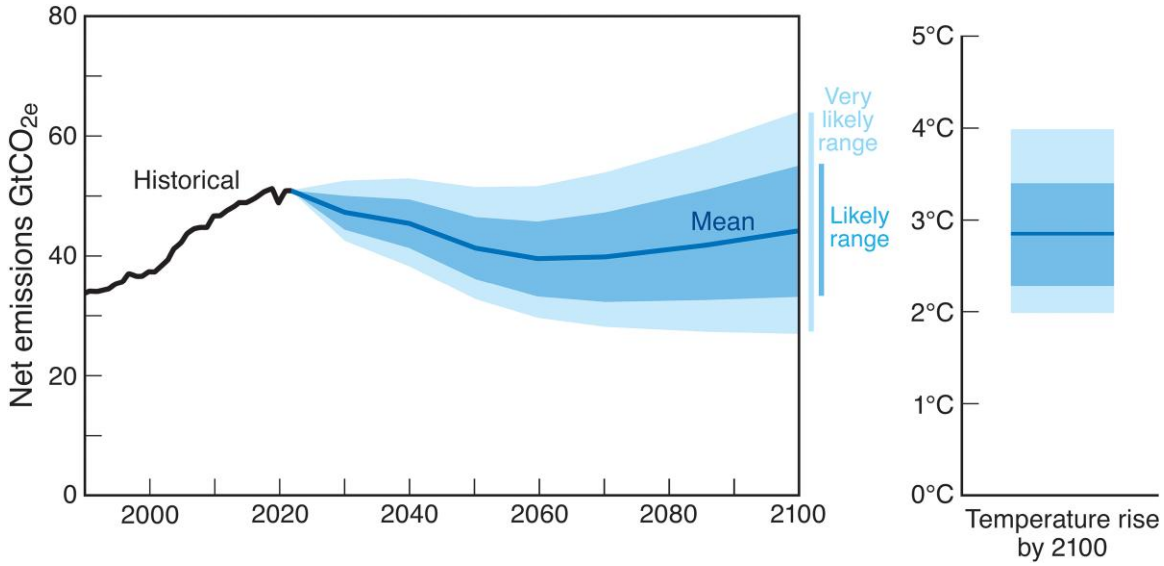

Fig. 4. Global GHG emissions and temperature rise. Net emissions including removals (billion metric tons of CO_2-equivalent). Policy and technological progress over the past 8 years has significantly reduced the global temperature outlook. Models now project very likely temperature increases of 2.0 to 4.0°C by century's end, with a 2.3 to 3.4°C likely range and a mean of 2.8°C. While this is progress from just 8 years ago, it still represents a dire climate future—falling significantly short of the Paris Agreement goal of limiting warming to well below 2°C (204).

Ocean overturning circulation, atmospheric Hadley circulation, summer sea ice, tropical forests, and others have shifted and are projected to falter. And urbanism, deforestation, consumerism, pollution, disease, social stratification, and extractive agriculture are all on accelerating and expanding trends.

This is a human inflection point that will determine future conditions of life on Earth (206). While transitioning to a carbon-free energy system comes with major societal restructuring, the socioeconomic adjustments needed to rapidly decrease emissions also present opportunities for achieving social and ecological justice, reducing disease, promoting the successful achievement of SDGs, and securing food and water availablity for our children.

We *can* end pollution, improve human health, reign in population growth, and reduce further biophysical risks. Indigenous communities have practiced regenerative ways of managing natural resources by understanding the reciprocal relationship between humans and their natural surroundings. Nature is not a commodity for exploitation, but a living system with its own rights, where humans are life-supported and in turn play a regenerative role. This kinship promotes nature and humanity thriving together.

Under current national plans, global GHG emissions are set to increase 9% by 2030, compared to 2010 levels. Yet the science is clear: emissions must fall by 45% by the end of this decade compared to 2010 levels to meet the goal of limiting global temperature rise to 1.5°C (207). As governments invest in renewable energy sources, there are enormous cobenefits to be gained in terms of disease reduction, social equity, and a growing respect for Earth's rhythms. Yet renewable energy will not address the root problem of ecological overshoot, social justice, or pollution. Policies are needed that end the production of superfluous and luxury commodities, conserve energy at household and societal levels, stabilize global population, and replace the extractive model with one that emphasizes true sustainability so that more natural resources per capita become available and wealth is far more equitably distributed (208).

The shift away from an extractive, resource-driven global economy toward one that values human rights and livelihoods could redefine global economics and offer reasons for optimism. Opportunities to prevent catastrophic levels of heating are being missed due to accelerating consumerism, the false seduction of dubious climate quick fixes, unverifiable "carbon offsets", exorbitant pollution levels, and growing economic disparity. Halting global ecological decline and addressing the crises of climate change, biodiversity collapse, pollution, pandemics, and human injustice requires a shift in economic structures, human behavior, and above all, values.

Whether the world is considered overpopulated depends on various factors. It is essential to consider not only population numbers but also consumption patterns, resource distribution, and sustainability when discussing this complex issue. Additionally, strategies for addressing concerns related to population growth often involve a combination of policies related to education, healthcare, resource management, and environmental protection. In developing economies, overpopulation is not just about how many people there are but also about how much each person consumes compared to the availability of resources.

High levels of consumption in developed countries contribute to environmental degradation, raising the issue of unequal distribution of resources. While some regions may be densely populated and face resource constraints, others have much lower population densities and abundant resources. Inequities in resource distribution can lead to perceptions of overpopulation but are in reality more closely related to social inequalities, often with deep historical roots related to imperialism and unjust resource extraction.

Humans must become rejuvenators of natural systems (209). We must shift from wealth as a goal, to sustainaiblity as a goal driving our decisons. This includes developing replacements for plastics, adopting regenerative and restorative cultivation and harvesting methods, investing in cradle to grave research and development focused on material reuse, absolute decoupling of the economy from net resource depletion, and establishing conservation goals to conserve 30–50% of Earth's land, freshwater, and oceans (210).

Addressing social inequities based on gender, ethnicity, and income is crucial, and leaders in political, educational, business, and religious organizations must analyze and redress discriminatory practices, historical racism, and unjust distributions of power that hinder communities from adapting to climate change. It is imperative to promote reproductive healthcare, education, poverty eradication, ecological restoration, environmental justice, and reciprocal relationships with nature. Economic development must not come at the cost of destroying Earth.

As reported in numerous peer-reviewed studies (211), to reverse the many negative impacts generated by our modern socioeconomic system there must be global investment in (Fig. 5):

1. *Rapid and legitimate decarbonization*, correcting market distortions favoring fossil fuels, avoiding the spurious trap of "net zero" as an excuse to continue polluting the atmosphere (212), and proper monitoring, verification, and reporting of carbon offset contracts.
2. *Revising the basis for decision-making under the UNFCCC*. Decision-making under the UNFCCC should be reorganized by transitioning from unanimous voting to qualified majority voting, enabling decisions to be made with agreement from a defined majority of member nations. To encourage compliance and accountability, penalties such as financial sanctions could be introduced for noncompliance with UNFCCC decisions. These changes would enhance efficiency, enabling prompt action and stronger enforcement of climate-related agreements among member nations.
3. *Building a new era of reciprocity and kinship with nature*, and decoupling economic activity from net resource depletion. We must shift Earth-centered governance from an aspirational political issue to a foundational principle through constitutional reforms with policy implications (213).
4. *Implementing sustainable/regenerative practices* in all areas of natural resource economics including, especially, agriculture.
5. *Eliminating environmentally harmful subsidies* and restricting trade that promotes pollution and unsustainable consumption.
6. *Promote gender justice* by supporting women's and girls' education and rights, which reduces fertility rates and raises the standard of living.
7. *Accelerating human development in all SDG sectors*, especially promoting reproductive healthcare, education, and equity for girls and women.
8. *In low- and middle-income nations*, relieving debt, providing low-cost loans, financing loss and damage, funding clean-energy acceleration, arresting the dangerous loss of biodiversity, and restoring natural ecosystems.

A cultural shift in values

How do we achieve these goals? The authors call for a global cultural shift in social and economic values. Creating a cultural shift toward regenerative practices in socioeconomic activities is complex and requires a multifaceted approach involving, critically, the leaders of the G20, and all nations, comprehensively engaging programs in the following:

1. *Education in sustainability and equity concepts*: Increasing awareness and understanding of sustainability and equity issues through education at all levels to empower individuals to make more environmentally conscious decisions. Embedding sustainability and equity into educational curricula at all levels can shape future generations' values and actions. We advocate adoption of the issues discussed in this paper in school curricula, public service announcements, and as a guide to government decision-making.
2. *Policy, legal frameworks, and legislation*: Governments can enact and enforce policies that mandate sustainable practices and ensure social equity, such as progressive environmental regulations, social justice legislation, and economic reforms that prioritize community well-being over individual profit.
3. *Economic incentives*: Shifting the economic focus from growth at any cost to a model that values environmental and social well-being. Aligning economic incentives with sustainable outcomes, such as tax breaks for green businesses, can encourage companies and consumers to adopt better practices.
4. *Cross-sector partnerships*: Facilitating collaboration between the public sector, private sector, civil society, and academia to develop integrated and comprehensive approaches to sustainability and equity.
5. *Community empowerment and inclusion*: Encouraging participatory governance that includes diverse community voices in decision-making processes, particularly those of marginalized and indigenous groups, to ensure that practices are equitable and culturally sensitive.
6. *Corporate responsibility and accountability*: Promoting corporate social responsibility through transparency, fair trade, ethical sourcing, and sustainability reporting.
7. *Incentives for sustainable/equitable behavior*: Channeling investment into the development and deployment of green technologies that enable sustainable production and consumption patterns. Creating economic and social incentives for businesses and individuals to adopt sustainable practices, like subsidies for renewable energy or tax benefits for sustainable/equitable business practices.
8. *Innovation and technology*: Investing in research and development for new technologies can provide more efficient and cleaner alternatives to current practices.
9. *Leadership and commitment*: Encouraging leaders within communities, businesses, and governments to model sustainable and equitable behaviors. Leaders in business, politics, and community groups must commit to sustainability goals and lead by example to inspire others.
10. *Cultural narratives*: Leveraging media, art, and culture to promote stories and images that valorize sustainability and equity, thereby shaping public opinion and cultural values. Changing the cultural narratives around consumption and progress to value sustainability and long-term thinking over immediate gratification or economic growth at any cost.
11. *Global engagement and solidarity*: Participating in international efforts and agreements that aim to address global challenges collectively, ensuring that sustainability and social equity are global priorities.

This systemic transformation requires a shift in collective values, behaviors, and institutional practices to prioritize long-term ecological health and social well-being over immediate gains.

Heads of state must immediately pivot the considerable power of the economy toward restoring a livable planet and an equitable and just socioeconomic system. To achieve a successful future where humanity can thrive, economic values must embrace human equity, health, and welfare, kinship with nature, regenerative resource

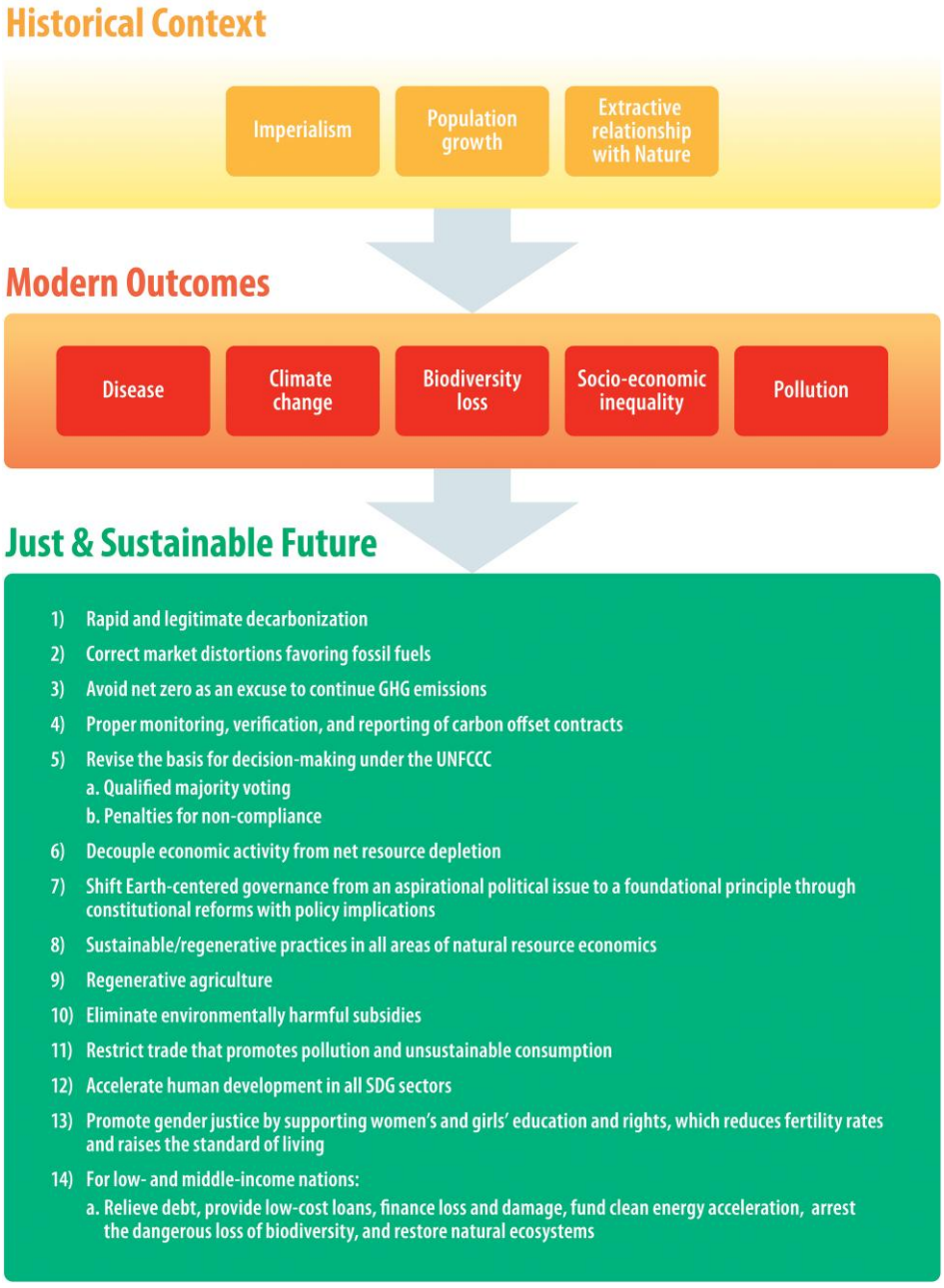

Fig. 5. The historical context of imperialism, population growth, and an extractive relationship with nature has led to a series of modern outcomes that put our planet at risk: disease, climate change, biodiversity loss, socioeconomic inequality, and pollution. These risk the stability of human communities. Humanity may achieve a just and sustainable future through global investment in rapid decarbonization, correcting market distortions favoring fossil fuels, avoiding "net zero" as an excuse to continue GHG emissions, proper monitoring and validation of carbon offsets, revising the basis for decision-making under the UNFCCC, decoupling economic activity from net resource depletion, shifting to Earth-centered governance, sustainable/regenerative practices in all areas of natural resource economics, eliminating environmentally harmful subsidies, restrict trade that promotes pollution and unsustainable consumption, accelerate human development in all SDG sectors, promote gender justice by supporting women's and girls' education and rights which reduces fertility rates and raises the standard of living, and for low- and middle-income nations: relieve debt, provide low-cost loans, finance loss and damage, fund clean-energy acceleration, arrest the dangerous loss of biodiversity, and restore natural ecosystems.

use, sustainability, and resilience. Emphasizing fairness and inclusivity, these values promote social cohesion and reduce disparities.

Recognizing our interconnectedness with the environment, a focus on sustainability and regenerative resource use ensures the preservation of nature for future generations. Prioritizing health and well-being, societies must invest in healthcare systems, fostering a higher quality of life by building resilience against uncertainties. A new economic paradigm is needed to create a prosperous and harmonious future, meeting the challenges of a rapidly deteriorating world.

Earth is our lifeboat in the sea of space

As succinctly stated by Rees (68), "We are consuming and polluting the biophysical basis of our own existence." Climate change, biodiversity loss, pollution, disease, and social injustice risk the stability of human communities on Earth (Fig. 6). We must stop treating these issues as isolated challenges, and establish a systemic response based on kinship with nature that recognizes Earth as our lifeboat in the cosmic sea of space.

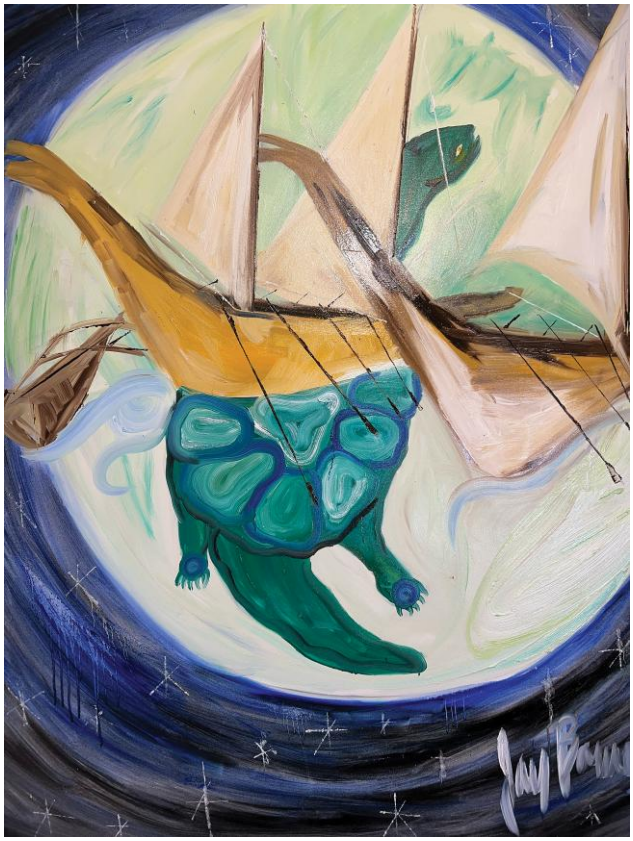

Fig. 6. Turtle Island. Original art commissioned for this paper, Jay Bowen (https://jaybowen-art.com/wordpress/).

Coauthor Jay Bowen, Upper Skagit Elder, explained why North American Indigenous Peoples described their North America as "turtle island" (Fig. 6):

> "It was not understood why the ancestors had referenced it in this way until the pictures of Earth were seen in 1969 from the Apollo Space Mission. The outline of North America resembled a turtle. We had an understanding of the whole Earth even though we lived on only a tiny piece of it. The ancestors understood global society. We understood that Earth was of one family. This family built and strengthened ties through voyaging to engage in trade, cultural exchange, and discovery."

There is no guarantee of a just, nourishing, and healthy future for humanity, and hope will not catalyze the change we need. That work must fall upon us, and it is clear from this review that we are past due for, and critically far away from, an appropriate reaction to the global emergency we have created.

Note

[a] "Ecological overshoot" is defined as depleting essential ecosystems faster than they can regenerate and polluting the ecosphere beyond nature's assimilative capacity.

Acknowledgments

This work was supported in part by the University of Hawai'i at Mānoa, School of Ocean and Earth Science and Technology. Many thanks to artists Brooks Bays, Nancy Hulbirt, and Georgina Casey.

Funding

Costs related to illustration and public access provided by the School of Ocean and Earth Science and Technology, University of Hawai'i at Mānoa, Honolulu, HI, US.

Author Contributions

C.F. conceived this work and wrote the original draft. W.J.R., T.N., P.B., E.C., C.F., D.M.K., A.B., and K.H. provided substantial edits. K.B., J.B., M.C., C.F., D.A.K., M.E.M., D.P.M., C.M., N.O., and M.W. reviewed and edited drafts of the manuscript.

References

1 IPCC. 2023. *Summary for policymakers. In: Climate change 2023: synthesis report. Contribution of Working Groups I, II, and III to the Sixth Assessment Report of the Intergovernmental Panel on Climate Change*. Geneva: IPCC. p. 1–34.
2 Friedlingstein P, *et al.* 2023. Global carbon budget 2023. *Earth Syst Sci Data*. 15:5301–5369.
3 World Meteorological Organization. WMO confirms that 2023 smashes global temperature record. WMO [2024 Jan 12]. https://wmo.int/media/news/wmo-confirms-2023-smashes-global-temperature-record.
4 Mora C, *et al.* 2017. Global risk of deadly heat. *Nat Clim Change*. 7: 501–506.
5 Abatzoglou JT, Williams AP. 2016. Impact of anthropogenic climate change on wildfire across western US forests. *Proc Natl Acad Sci U S A*. 113:11770–11775.
6 Williams AP, Cook BI, Smerdon JE. 2022. Rapid intensification of the emerging Southwestern North American megadrought in 2020–2021. *Nat Clim Change*. 12:232–234.
7 World Meteorological Organization. The global climate 2011–2020: a decade of acceleration. WMO [accessed 2023 Dec 5]. https://wmo.int/resources/publications/global-climate-2011-2020-decade-of-acceleration.
8 Wiens JJ. 2016. Climate-related local extinctions are already widespread among plant and animal species. *PLoS Biol*. 14: e2001104.
9 Exposito-Alonso M, *et al.* 2022. Genetic diversity loss in the Anthropocene. *Science*. 377:1431–1435.
10 Díaz S, *et al.* 2019. Pervasive human-driven decline of life on earth points to the need for transformative change. *Science*. 366:eaax3100.
11 Ripple WJ, *et al.* 2017. World scientists' warning to humanity: a second notice. *BioScience*. 67:1026–1028.
12 IPCC. 2021. *Climate change 2021: the physical science basis. Contribution of Working Group I to the Sixth Assessment Report of the Intergovernmental Panel on Climate Change*. Cambridge (UK) and New York (NY): Cambridge University Press. p. 2391.
13 International Energy Agency. Oil 2023: analysis and forecast to 2028. IEA [accessed 2023 Jun]. https://www.iea.org/reports/oil-2023.
14 UN Framework Convention on Climate Change. Addendum to the synthesis report for the technical assessment component of the first global stocktake. UNCC [accessed 2023 Apr 17]. https://unfccc.int/documents/627853.
15 Perkins R, Edwardes-Evans H. Fossil fuels 'stubbornly' dominating global energy despite surge in renewables: energy institute. S&P Global Commodity Insights [accessed 2023 Jun 26]. https://www.spglobal.com/commodityinsights/en/market-insights/latest-news/oil/062623-fossil-fuels-stubbornly-dominating-global-energy-despite-surge-in-renewables-energy-institute.

16 Samset BH,*et al.* 2023. Steady global surface warming from 1973 to 2022 but increased warming rate after 1990, https://doi.org/10.1038/s43247-023-01061-4. *Commun Earth Environ*. 4:400.
17 Hansen JE, *et al.* 2023. Global warming in the pipeline. *Oxf Open Clim Change*. 3:kgad008.
18 Xu C, Kohler TA, Lenton TM, Svenning J-C, Scheffer M. 2020. Future of the human climate niche. *Proc Natl Acad Sci U S A*. 117:11350–11355.
19 Lenton TM, *et al.* 2023. Quantifying the human cost of global warming. *Nat Sustain*. 6:1237–1247.
20 Thiery W, *et al.* 2021. Intergenerational inequities in exposure to climate extremes. *Science*. 374:158–160.
21 Wiens JJ, Zelinka J. 2024. How many species will earth lose to climate change? *Glob Change Biol*. 30:e17125.
22 Park BY, *et al.* 2021. The association between wildfire exposure in pregnancy and foetal gastroschisis: a population-based cohort study. *Paediatr Perinat Epidemiol*. 36:45–53.
23 Mann ME, *et al.* 2017. Influence of anthropogenic climate change on planetary wave resonance and extreme weather events. *Sci Rep*. 7:45242.
24 Mann ME, *et al.* 2018. Projected changes in persistent extreme summer weather events: the role of quasi-resonant amplification. *Sci Adv*. 4:eaat3272.
25 Climate Action Tracker. The CAT thermometer. Climate Action Tracker [accessed 2023 Dec]. https://climateactiontracker.org/global/cat-thermometer/.
26 United Nations Environment Programme. 2023. *Emissions gap report 2023: broken record—temperatures hit new highs, yet world fails to cut emissions (again)*. Nairobi: United Nations Environment Programme.
27 Lamboll RD, *et al.* 2023. Assessing the size and uncertainty of remaining carbon budgets. *Nat Clim Change*. 13:1360–1367.
28 SEI, Climate Analytics, E3G, IISD, UNEP. 2023. The production gap report 2023: Phasing down or phasing up? Top fossil fuel producers plan even more extraction despite climate promises. SEI. https://doi.org/10.51414/sei2023.050.
29 Barbier EB. 2023. Three climate policies that the G7 must adopt—for itself and the wider world. *Nature*. 617:459–461.
30 Ho DT. 2023. Carbon dioxide removal is not a current climate solution—we need to change the narrative. *Nature*. 616:9.
31 Dyke J, Watson R, Knorr W. Climate scientists: concept of net zero is a dangerous trap. The Conversation [2021 Apr 22]. https://theconversation.com/climate-scientists-concept-of-net-zero-is-a-dangerous-trap-157368.
32 Kapla RS, Ramanna K, Roston M. Accounting for carbon offsets. Harvard Business Review [accessed 2024 Mar 16]. https://hbr.org/2023/07/accountingfor-carbon-offsets.
33 Kim S-Y, *et al.* 2023. Hemispherically asymmetric Hadley cell response to CO_2 removal. *Sci Adv*. 9:eadg1801.
34 Shuen R. 2021. Addressing a constitutional right to a safe climate: using the court system to secure climate justice. *J Gend Race Justice*. 24:377–410.
35 United Nations Environment Programme. 2023. *Global climate litigation report: 2023 status review*. Nairobi: United Nations Environment Programme.
36 Dolšak N, Prakash A. 2022. Three faces of climate justice. *Annu Rev Political Sci*. 25:283–301.
37 Pearson Z, Ellingrod S, Billo E, McSweeney K. 2019. Corporate social responsibility and the reproduction of (neo)colonialism in the Ecuadorian Amazon. *Extr Ind Soc*. 6:881–888.
38 Dunlap A. 2021. The politics of ecocide, genocide and megaprojects: interrogating natural resource extraction, identity and the normalization of erasure. *J Genocide Res*. 23:212–235. https://doi.org/10.1080/14623528.2020.1754051.
39 Lenin VI. 2017. Imperialism, the highest stage of capitalism. In: Betts RK, editor. *Conflict after the Cold War*. 5th ed. New York: Routledge. p. 319–326.
40 Weisse M, Goldman E, Carter S. Tropical primary forest loss worsened in 2022 despite international commitments to end deforestation. Global Forest Review. World Resources Institute [accessed 2024 Mar 16]. https://research.wri.org/gfr/latest-analysis-deforestation-trends?utm_campaign=treecoverloss2022&utm_medium=bitly&utm_source=PressKit.
41 Bradshaw CJ, *et al.* 2021. Underestimating the challenges of avoiding a ghastly future. *Front Conserv Sci*. 1:9.
42 United Nations. Global issues: population. UN [accessed 2024 Mar 16]. https://www.un.org/en/global-issues/population#:%E2%88%BC:text=The%20world's%20population%20is%20expected,billion%20in%20the%20mid%2D2080s.
43 Dasgupta P. 2019. *Time and the generations: population ethics for a diminishing planet*. New York: Columbia University Press.
44 PWC. The long view, how will the global economic order change by 2050? PWC [accessed 2024 Mar 16]. https://www.pwc.com/gx/en/world-2050/assets/pwc-the-world-in-2050-full-report-feb-2017.pdf.
45 Rees WE. 2023. The human ecology of overshoot: why a major 'population correction' is inevitable. *World*. 4:509–527.
46 Speidel JJ, O'Sullivan JN. 2023. Advancing the welfare of people and the planet with a common agenda for reproductive justice, population, and the environment. *World*. 4:259–287.
47 Willcock S, Cooper GS, Addy J, Dearing JA. 2023. Earlier collapse of Anthropocene ecosystems driven by multiple faster and noisier drivers. *Nat Sustain*. 6:1331–1342.
48 United Nations. Global sustainable development report (GSDR) 2023. Advance, unedited version. UN [accessed 2024 Mar 16). https://sdgs.un.org/gsdr/gsdr2023.
49 Wunderling N, *et al.* 2022. Global warming overshoots increase risks of climate tipping cascades in a network model. *Nat Clim Change*. 13:75–82.
50 Dasgupta P, Levin S. 2023. Economic factors underlying biodiversity loss. *Philos Trans R Soc B Biol Sci*. 378:20220197.
51 Garcia AC, Ambrose A, Hawkins A, Parkes S. 2021. High consumption, an unsustainable habit that needs more attention. *Energy Res Soc Sci*. 80:102241.
52 Lampert A. 2019. Over-exploitation of natural resources is followed by inevitable declines in economic growth and discount rate. *Nat Commun*. 10:1419.
53 Brooks DR, Hoberg EP, Boeger WA, Trivellone V. 2022. Emerging infectious disease: an underappreciated area of strategic concern for food security. *Transbound Emerg Dis*. 69:254–267.
54 Hannah DM, *et al.* 2022. Illuminating the 'invisible water crisis' to address global water pollution challenges. *Hydrol Process*. 36:e14525.
55 Rivera A, Darden JT, Dear N, Grady SC. 2023. Environmental injustice among hispanics in Santa Clara, California: a human–environment heat vulnerability assessment. *GeoJournal*. 88:2651–2667.
56 Atwoli L, *et al.* 2021. Call for emergency action to limit global temperature increases, restore biodiversity, and protect health. *Lancet*. 398:939–941.
57 Blattner C. 2020. Just transition for agriculture? A critical step in tackling climate change. *J Agric Food Syst Community Dev*. 9:53–58.

58 Bordner AS, Ferguson CE, Ortolano L. 2020. Colonial dynamics limit climate adaptation in Oceania: perspectives from the Marshall Islands. *Glob Environ Change*. 61:102054.

59 Climate Central. Worldwide daily fingerprints of climate Change during earth's hottest month. Climate Central [accessed 2023 Aug 2]. https://www.climatecentral.org/climate-matters/climate-shift-index-global-july-2023.

60 Hansen J, Sato M, Kharecha P. Groundhog Day. Another Gobsmackingly bananas month. What's up? [accessed 2024 Mar 16]. https://www.columbia.edu/~jeh1/mailings/2024/Groundhog.04January2024.pdf.

61 Zachariah M, *et al.* Extreme heat in North America, Europe and China in July 2023 made much more likely by climate change. Imperial College [accessed 2024 Mar 16]. https://spiral.imperial.ac.uk/handle/10044/1/105549.

62 Sze JS, Childs DZ, Carrasco LR, Edwards DP. 2022. Indigenous lands in protected areas have high forest integrity across the tropics. *Curr Biol*. 32:4949–4956.e3.

63 Gonçalves CD, Schlindwein MM, Martinelli GD. 2021. Agroforestry systems: a systematic review focusing on traditional indigenous practices, food and nutrition security, economic viability, and the role of women. *Sustainability*. 13:11397.

64 Epstein Y, Ellison AM, Echeverría H, Abbott JK. 2023. Science and the legal rights of nature. *Science*. 380:eadf4155.

65 Koplow D, Steenblik R. Protecting nature by reforming environmentally harmful subsidies: the role of business [accessed 2022 Feb]. https://www.earthtrack.net/sites/default/files/documents/EHS_Reform_Background_Report_fin.pdf.

66 Hickel J, Kallis G. 2019. Is green growth possible? *New Political Econ*. 25:469–486.

67 Briel G. Economic growth and the environment–is green growth possible? Tralac [accessed 2022 Apr 21]. https://www.tralac.org/blog/article/15589-economic-growth-and-the-environment-is-green-growth-possible.html#_ftn9.

68 Rees WE. 2023. The human eco-predicament: overshoot and the population conundrum. *Vienna Yearb Popul Res*. 21:1–19.

69 NOAA Global Monitoring Laboratory. Trends in atmospheric carbon dioxide. NOAA [accessed 2024 Mar 16]. https://gml.noaa.gov/ccgg/trends/.

70 Ciais P, *et al.* 2013. Carbon and other biogeochemical cycles. In: Stocker TF, *et al.*, editors. *Climate change 2013: the physical science basis. Contribution of Working Group I to the Fifth Assessment Report of the Intergovernmental Panel on Climate Change*. Cambridge (UK): Cambridge University Press. p. 6SM-1–4.

71 Dumitru OA, *et al.* 2019. Constraints on global mean sea level during Pliocene warmth. *Nature*. 574:233–236.

72 Lan X, *et al.* 2021. Improved constraints on global methane emissions and sinks using δ^{13}C-CH_4. *Glob Biogeochem Cycles*. 35:e2021GB007000.

73 IPCC. 2021. *Summary for policymakers. Climate change 2021: the physical science basis*. Cambridge (UK): Cambridge University Press.

74 Climate Action Tracker. 2030 emissions gap: CAT projections and resulting emissions gap in meeting the 1.5°C Paris agreement goal. Climate Action Tracker [accessed 2023 Dec 5]. https://climateactiontracker.org/global/cat-emissions-gaps/.

75 Kalmus P. 2023 Jul 27. Joe Biden must declare a climate emergency. And he must do so now. The Guardian. https://www.theguardian.com/commentisfree/2023/jul/27/joe-biden-climate-emergency-peter-kalmus.

76 Climate Crisis Advisory Group (CCAG). A critical pathway for a manageable future for humanity. CCAG [accessed 2024 Mar 16]. https://www.ccag.earth/.

77 Harvey F. 2022 Nov 9. Oil and gas greenhouse emissions 'three times higher' than producers claim. The Guardian. https://www.theguardian.com/environment/2022/nov/09/oil-and-gas-greenhouse-emissions-three-times-higher-than-producers-claim.

78 International Energy Agency. Methane emissions from the energy sector are 70% higher than official figures. IEA [accessed 2022 Feb 23]. https://www.iea.org/news/methane-emissions-from-the-energy-sector-are-70-higher-than-official-figures.

79 Duffy KA, *et al.* 2021. How close are we to the temperature tipping point of the terrestrial biosphere? *Sci Adv*. 7:eaay1052.

80 Feng Y, *et al.* 2022. Doubling of annual forest carbon loss over the tropics during the early twenty-first century. *Nat Sustain*. 5:444–451.

81 Gatti LV, *et al.* 2021. Amazonia as a carbon source linked to deforestation and climate change. *Nature*. 595:388–393.

82 Li Y, *et al.* 2022. Deforestation-induced climate change reduces carbon storage in remaining tropical forests. *Nat Commun*. 13:1964.

83 United Nations Convention to Combat Desertification. Global drought snapshot. UNCCD [accessed 2024 Mar 16]. https://www.droughtglobal.org/_files/ugd/184219_4dcb7a4451514f2281981f604c3848cc.pdf?index=true.

84 Suarez-Gutierrez L, Müller WA, Marotzke J. 2023. Extreme heat and drought typical of an end-of-century climate could occur over Europe soon and repeatedly. *Commun Earth Environ*. 4:415.

85 Teressa B. 2021. Impact of climate change on food availability—a review. *Int J Food Sci Agric*. 5:465–470.

86 Vollmer D, Harrison IJ. 2021. $H_2O \neq CO_2$: framing and responding to the global water crisis. *Environ Res Lett*. 16:011005.

87 Chiang F, Mazdiyasni O, AghaKouchak A. 2021. Evidence of anthropogenic impacts on global drought frequency, duration, and intensity. *Nat Commun*. 12:2754.

88 Pokhrel Y, *et al.* 2021. Global terrestrial water storage and drought severity under climate change. *Nat Clim Change*. 11:226–233.

89 Nolan C, *et al.* 2018. Past and future global transformation of terrestrial ecosystems under climate change. *Science*. 361:920–923.

90 Brock S, *et al.* 2021. *The world climate and security report 2021: a product of the expert group of the International Military Council on Climate and Security*. Washington (DC): Center for Climate and Security.

91 Clement V, *et al.* 2021. *Groundswell part 2: acting on internal climate migration*. Washington (DC): World Bank.

92 IPCC. 2022. Climate change 2022: impacts, adaptation and vulnerability. In: Pörtner HO, *et al.*, editors. *Climate change 2022: impacts, adaptation and vulnerability. Contribution of Working Group II to the Sixth Assessment Report of the Intergovernmental Panel on Climate Change*. Cambridge (UK): Cambridge University Press. p. 3–33.

93 Kulp SA, Strauss BH. 2019. New elevation data triple estimates of global vulnerability to sea-level rise and coastal flooding. *Nat Commun*. 10:4844.

94 Lenton TM, *et al.* 2019. Climate tipping points—too risky to bet against. *Nature*. 575:592–595.

95 McKay DIA, *et al.* 2022. Exceeding 1.5°C global warming could trigger multiple climate tipping points. *Science*. 377:eabn7950.

96 Ripple WJ, *et al.* 2023. Many risky feedback loops amplify the need for climate action. *One Earth*. 6:86–91.

97 Slater T, *et al.* 2021. Earth's ice imbalance. *Cryosphere*. 15:233–246.

98 Rantanen M, *et al.* 2022. The Arctic has warmed nearly four times faster than the globe since 1979. *Commun Earth Environ*. 3:168.

99 Perovich D, *et al.* 2019. Sea ice. In: Richter-Menge J, Druckenmiller M, Jeffries M, editors. *Arctic report card 2019*. Silver Spring (MD): NOAA. p. 26–34.

100 McCrystall MR, Stroeve J, Serreze M, Forbes BC, Screen JA. 2021. New climate models reveal faster and larger increases in Arctic precipitation than previously projected. *Nat Commun*. 12:6765.

101 Höning D, *et al.* 2023. Multistability and transient response of the Greenland ice sheet to anthropogenic CO_2 emissions. *Geophys Res Lett*. 50:e2022GL101827.

102 The IMBIE Team. 2020. Mass balance of the Greenland ice sheet from 1992 to 2018. *Nature*. 579:233–239.

103 The IMBIE Team. 2018. Mass balance of the Antarctic ice sheet from 1992 to 2017. *Nature*. 558:219–222.

104 Rignot E, Mouginot J, Morlighem M, Seroussi H, Scheuchl B. 2014. Widespread, rapid grounding line retreat of Pine Island, Thwaites, Smith, and Kohler glaciers, West Antarctica, from 1992 to 2011. *Geophys Res Lett*. 41:3502–3509.

105 Joughin I, Smith BE, Medley B. 2014. Marine ice sheet collapse potentially under way for the Thwaites glacier basin, West Antarctica. *Science*. 344:735–738.

106 Messias M-J, Mercier H. 2022. The redistribution of anthropogenic excess heat is a key driver of warming in the North Atlantic. *Commun Earth Environ*. 3:118.

107 Li G, *et al.* 2020. Increasing ocean stratification over the past half-century. *Nat Clim Change*. 10:1116–1123.

108 Li Q, England MH, Hogg AM, Rintoul SR, Morrison AK. 2023. Abyssal ocean overturning slowdown and warming driven by Antarctic meltwater. *Nature*. 615:841–847.

109 Fox-Kemper B, *et al.* 2021. Ocean, cryosphere and sea level change. In: Masson-Delmotte V, *et al.*, editors. *Climate change 2021: the physical science basis*. Cambridge (UK): Cambridge University Press. p. 1211–1362.

110 Lee JY, *et al.* 2021. Future global climate: scenario-based projections and near-term information. In: Masson-Delmotte V, *et al.*, editors. *Climate change 2021: the physical science Basis*. Cambridge (UK): Cambridge University Press. p. 1–195.

111 Hansen J, *et al.* 2016. Ice melt, sea level rise and superstorms: evidence from paleoclimate data, climate modeling, and modern observations that 2°C global warming could be dangerous. *Atmos Chem Phys*. 16:3761–3812.

112 Heinze C, *et al.* 2020. The quiet crossing of ocean tipping points. *Proc Natl Acad Sci U S A*. 118:e2008478118.

113 Von Schuckmann K, *et al.* 2020. Heat stored in the earth system: where does the energy go? *Earth Syst Sci Data*. 12:2013–2041.

114 Cheng L, *et al.* 2024. New record ocean temperatures and related climate indicators in 2023. *Adv Atmos Sci*. 1–15

115 Penn JL, Deutsch C. 2022. Avoiding ocean mass extinction from climate warming. *Science*. 376:524–526.

116 Pauly D. 2019. *Vanishing fish: shifting baselines and the future of global fisheries*. Vancouver (CA): Greystone Books.

117 FAO. The state of world fisheries and aquaculture 2022. Towards blue transformation. FAO [accessed 2024 Mar 16]. https://doi.org/10.4060/cc0461en.

118 Cao L, *et al.* 2023. Vulnerability of blue foods to human-induced environmental change. *Nat Sustain*. 6:1186–1198.

119 Cheng Y, *et al.* 2023. A quantitative analysis of marine heatwaves in response to rising sea surface temperature. *Sci Total Environ*. 881:163396.

120 Heron SF, Maynard JA, Van Hooidonk R, Eakin CM. 2016. Warming trends and bleaching stress of the world's coral reefs 1985–2012. *Sci Rep*. 6:38402.

121 Ciracì E, *et al.* 2023. Melt rates in the kilometer-size grounding zone of Petermann Glacier, Greenland, before and during a retreat. *Proc Natl Acad Sci U S A*. 120:e2220924120.

122 Dutton A, *et al.* 2015. Sea-level rise due to polar ice-sheet mass loss during past warm periods. *Science*. 349:aaa4019.

123 Cushing LJ, *et al.* 2023. Toxic tides and environmental injustice: social vulnerability to sea level rise and flooding of hazardous sites in coastal California. *Environ Sci Technol*. 57:7370–7381.

124 Landrigan PJ, *et al.* 2020. Human health and ocean pollution. *Ann Glob Health*. 86:151.

125 Bennett NJ, *et al.* 2023. Environmental (in)justice in the Anthropocene ocean. *Mar Policy*. 147:105383.

126 Mahjoub M, Fadlaoui S, El Maadoudi M, Smiri Y. 2021. Mercury, lead, and cadmium in the muscles of five fish species from the Mechraâ-Hammadi Dam in Morocco and health risks for their consumers. *J Toxicol*. 2021:8865869.

127 Thushari GGN, Senevirathna JDM. 2020. Plastic pollution in the marine environment. *Heliyon*. 6:e04709.

128 Hens B, Hens L. 2017. Persistent threats by persistent pollutants: chemical nature, concerns and future policy regarding PCBs—what are we heading for? *Toxics*. 6:1.

129 Sonone SS, Jadhav S, Sankhla MS, Kumar R. 2020. Water contamination by heavy metals and their toxic effect on aquaculture and human health through food chain. *Lett Appl NanoBioScience*. 10:2148–2166.

130 Pitcher GC, Jacinto GS. 2019. Ocean deoxygenation links to harmful algal blooms. In: Laffoley D, Baxter JM, editors. *Ocean deoxygenation: everyone's Problem: causes, impacts, consequences and solutions*. Gland (Switzerland): IUCN. p. 153–170.

131 Bennett NJ. 2018. Navigating a just and inclusive path towards sustainable oceans. *Mar Policy*. 97:139–146.

132 Baccini A, *et al.* 2017. Tropical forests are a net carbon source based on aboveground measurements of gain and loss. *Science*. 358:230–234.

133 Hoang NT, Kanemoto K. 2021. Mapping the deforestation footprint of nations reveals growing threat to tropical forests. *Nat Ecol Evol*. 5:845–853.

134 Overpeck JT, Breshears DD. 2021. The growing challenge of vegetation change. *Science*. 372:786–787.

135 Zheng B, *et al.* 2023. Record-high CO_2 emissions from boreal fires in 2021. *Science*. 379:912–917.

136 Grantham HS, *et al.* 2020. Anthropogenic modification of forests means only 40% of remaining forests have high ecosystem integrity. *Nat Commun*. 11:5978.

137 Lecina-Diaz J, *et al.* 2020. Characterising forest vulnerability and risk to climate-change hazards. *Front Ecol Environ*. 19:126–133.

138 Seidl R, *et al.* 2017. Forest disturbances under climate change. *Nat Clim Change*. 7:395–402.

139 Veldkamp E, Schmidt M, Powers JS, Corre MD. 2020. Deforestation and reforestation impacts on soils in the tropics. *Nat Rev Earth Environ*. 1:590–605.

140 Plumptre AJ, *et al.* 2021. Where might we find ecologically intact communities? *Front For Glob Change*. 4:26.

141 Brondizio ES, Settele J, Díaz S, Ngo HT. 2019. *Global assessment report on biodiversity and ecosystem services of the intergovernmental science-policy platform on biodiversity and ecosystem services*. Bonn (Germany): IPBES Secretariat.

142 Ceballos G, Ehrlich PR, Raven PH. 2020. Vertebrates on the brink as indicators of biological annihilation and the sixth mass extinction. *Proc Natl Acad Sci U S A*. 117:13596–13602.

143 Oberle B, *et al.* 2019. *Global resources outlook 2019: natural resources for the future we want. A report of the International Resource Panel*. Nairobi (Kenya): International Resource Panel (IRP).

144 Still CJ, *et al.* 2022. No evidence of canopy-scale leaf thermoregulation to cool leaves below air temperature across a range of forest ecosystems. *Proc Natl Acad Sci U S A*. 119:e2205682119.

145 Mau AC, Reed SC, Wood TE, Cavaleri MA. 2018. Temperate and tropical forest canopies are already functioning beyond their thermal thresholds for photosynthesis. *Forests*. 9:47.

146 Almond REA, Grooten M, Bignoli DJ, Petersen T. Living Planet Report 2022: building a nature-positive society. WWF-World Wide Fund for Nature [accessed 2024 Mar 16]. https://livingplanet.panda.org/en-US/.

147 National Academies of Sciences, Engineering, and Medicine. 2022. *Biodiversity at risk: today's choices matter*. Washington (DC): The National Academies Press.

148 Armstrong A. 2015. Forest ecology: three trillion trees. *Nat Plants*. 1:15154.

149 Forest Declaration Assessment Partners. Forest declaration assessment: are we on track for 2030? Executive summary. Climate focus (Coordinator and editor). Forest Declaration Assessment [accessed 2024 Mar 16]. www.forestdeclaration.org.

150 Pingali PL. 2012. Green revolution: impacts, limits, and the path ahead. *Proc Natl Acad Sci U S A*. 109:12302–12308.

151 FAO, IFAD, PAHO, WFP, UNICEF. Regional overview of food security and nutrition in Latin America and the Caribbean 2020-Food security and nutrition for lagging territories. FAO, IFAD, PAHO, WFP, UNICEF [accessed 2024 Mar 16]. https://doi.org/10.4060/cb2242en.

152 Save the Children. 2023 in review—nearly 16,000 children a day plunged into hunger in top 10 worsening food crises. Save the Children [accessed 2023 Dec 21]. https://www.savethechildren.net/news/2023-review-nearly-16000-children-day-plunged-hunger-top-10-worsening-food-crises.

153 Poore J, Nemecek T. 2018. Reducing food's environmental impacts through producers and consumers. *Science*. 360:987–992.

154 Bashir I, *et al.* 2020. Concerns and threats of contamination on aquatic ecosystems. In: Hakeem KR, Bhat RA, Qadri H, editors. *Bioremediation and biotechnology: sustainable approaches to pollution degradation*. Geneva (Switzerland): Springer. p. 1–26.

155 Withana PA, *et al.* 2024. Machine learning prediction and interpretation of the impact of microplastics on soil properties. *Environ Pollut*. 341:122833.

156 Paustian K, *et al.* Climate mitigation potential of regenerative agriculture is significant. Princeton University [accessed 2024 Mar 16]. https://searchinger.princeton.edu/sites/g/files/toruqf4701/files/tsearchi/files/paustian_et_al._response_to_wri_soil_carbon_blog_.pdf.

157 FAO. 2021. *The State of the World's Land and Water Resources for Food and Agriculture (SOLAW)–managing systems at risk*. Rome (Italy): Food and Agriculture Organization of the United Nations.

158 Bar-On YM, Phillips R, Milo R. 2018. The biomass distribution on Earth. *Proc Natl Acad Sci U S A* 115:6506–6511.

159 Samset BH, *et al.* 2023. Steady global surface warming from 1973 to 2022 but increased warming rate after 1990. *Commun Earth Environ*. 4:400. https://doi.org/10.1038/s43247-023-01061-4.

160 Koneswaran G, Nierenberg D. 2008. Global farm animal production and global warming: impacting and mitigating climate change. *Environ Health Perspect*. 116:578–582.

161 Wang A, *et al.* 2023. Global cropland exposure to extreme compound drought heatwave events under future climate change. *Weather Clim Extrem*. 40:100559.

162 Kornhuber K, *et al.* 2023. Risks of synchronized low yields are underestimated in climate and crop model projections. *Nat Commun*. 14:3528.

163 Lehmann J, Coumou D, Frieler K. 2015. Increased record-breaking precipitation events under global warming. *Clim Change*. 132:501–515.

164 Gaupp F, Hall J, Mitchell D, Dadson S. 2019. Increasing risks of multiple breadbasket failure under 1.5 and 2°C global warming. *Agric Syst*. 175:34–45.

165 Myers SS, *et al.* 2014. Increasing CO_2 threatens human nutrition. *Nature*. 510:139–142.

166 Zhu C, *et al.* 2018. Carbon dioxide (CO_2) levels this century will alter the protein, micronutrients, and vitamin content of rice grains with potential health consequences for the poorest rice-dependent countries. *Sci Adv*. 4:eaaq1012.

167 Battisti DS, Naylor RL. 2009. Historical warnings of future food insecurity with unprecedented seasonal heat. *Science*. 323:240–244.

168 Barrett CB. 2010. Measuring food insecurity. *Science*. 327:825–828.

169 Stukenbrock E, Gurr S. 2023. Address the growing urgency of fungal disease in crops. *Nature*. 617:31–34.

170 Liang X-Z, *et al.* 2017. Determining climate effects on US total agricultural productivity. *Proc Natl Acad Sci U S A*. 114:E2285–E2292.

171 Boretti A, Rosa L. 2019. Reassessing the projections of the world water development report. *NPJ Clean Water*. 2:15.

172 Jasechko S, *et al.* 2024. Rapid groundwater decline and some cases of recovery in aquifers globally. *Nature*. 625:715–721.

173 Zhang Y, *et al.* 2023. Southern hemisphere dominates recent decline in global water availability. *Science*. 382:579–584.

174 United Nations. 2018. *World water development report 2018: World Water Assessment Programme (United Nations)*. Paris (France): United Nations Educational, Scientific and Cultural Organization.

175 Romanello M, *et al.* 2023. The 2023 report of the Lancet countdown on health and climate change: the imperative for a health-centred response in a world facing irreversible harms. *Lancet*. 402:2346–2394.

176 Zittis G, *et al.* 2021. Business-as-usual will lead to super and ultra-extreme heatwaves in the Middle East and North Africa. *NPJ Clim Atmos Sci*. 4:20.

177 Asseng S, Spänkuch D, Hernandez-Ochoa IM, Laporta J. 2021. The upper temperature thresholds of life. *Lancet Planet Health*. 5:e378–e385.

178 Carleton T, *et al.* 2022. Valuing the global mortality consequences of climate change accounting for adaptation costs and benefits. *Q J Econ*. 137:2037–2105.

179 World Health Organization. Fact sheet on climate change and health. WHO [accessed 2023 Oct 12]. https://www.who.int/news-room/fact-sheets/detail/climate-change-and-health.

180 Cosdon N. For the first time in 20 years, US reports 7 locally acquired malaria cases. ContangionLive [2023 Jul 10]. https://www.contagionlive.com/view/for-the-first-time-in-20-years-us-reports-7-locally-acquired-malaria-cases.

181 Mora C, *et al.* 2022. Over half of known human pathogenic diseases can be aggravated by climate change. *Nat Clim Change*. 12:869–875.

182 U.S. Environmental Protection Agency. Climate change and the health of socially vulnerable people [accessed 2024 Mar 16].

https://www.epa.gov/climateimpacts/climate-change-and-health-socially-vulnerablepeople.
183 Vicedo-Cabrera AM, *et al.* 2021. The burden of heat-related mortality attributable to recent human-induced climate change. *Nat Clim Change*. 11:492–500.
184 Guo Y, Ryan U, Feng Y, Xiao L. 2022. Association of common zoonotic pathogens with concentrated animal feeding operations. *Front Microbiol*. 12:810142.
185 Carlson CJ, *et al.* 2022. Climate change increases cross-species viral transmission risk. *Nature*. 607:555–562.
186 Centers for Disease Control and Prevention. Zoonotic diseases. CDC [accessed 2021 Jul 1]. https://www.cdc.gov/onehealth/basics/zoonotic-diseases.html.
187 Jones KE, *et al.* 2008. Global trends in emerging infectious diseases. *Nature*. 451:990–993.
188 Mora C, *et al.* 2018. Broad threat to humanity from cumulative climate hazards intensified by greenhouse gas emissions. *Nat Clim Change*. 8:1062–1071.
189 Kharas H. 2017. *The unprecedented expansion of the global middle class: an update*. Washington (DC): Brookings Global Economy and Development.
190 United Nations. World social report 2020: inequality in a rapidly changing world. UN [accessed 2024 Mar 16]. https://www.un.org/development/desa/dspd/wp-content/uploads/sites/22/2020/01/World-Social-Report-2020-FullReport.pdf.
191 Chancel L. 2022. Global carbon inequality over 1990–2019. *Nat Sustain*. 5:931–938.
192 SEI and CEEW. 2022. *Stockholm+ 50: unlocking a better future, SEI report*. Stockholm: Stockholm Environment Institute.
193 Kashwan P, Duffy RV, Massé F, Asiyanbi AP, Marijnen E. 2021. From racialized neocolonial global conservation to an inclusive and regenerative conservation. *Environ Sci Policy Sustain Dev*. 63:4–19.
194 Wilting HC, Schipper AM, Bakkenes M, Meijer JR, Huijbregts MAJ. 2017. Quantifying biodiversity losses due to human consumption: a global-scale footprint analysis. *Environ Sci Technol*. 51:3298–3306.
195 Bruckner B, *et al.* 2023. Ecologically unequal exchanges driven by EU consumption. *Nat Sustain*. 6:587–598.
196 Guy K, Femia F, Werrell C. 2020. *A security threat assessment of global climate change: how likely warming scenarios indicate a catastrophic security future*. Washington (DC): The Center for Climate and Security, Institute of the Council on Strategic Risks.
197 Hsiang SM, Burke M, Miguel E. 2013. Quantifying the influence of climate on human conflict. *Science*. 341:1235367.
198 Institute for Economics & Peace. Ecological threat report 2022: analysing ecological threats, resilience & peace. Vision of Humanity [accessed 2022 Oct]. http://visionofhumanity.org/resources.
199 RMI. The EV revolution in 5 charts. Clinotechnica [accessed 2024 Mar 16]. https://cleantechnica.com/2023/09/21/the-ev-revolution-in-5-charts/.
200 International Energy Agency. Renewable Energy Progress Tracker. IEA [accessed 2024 Jan 11]. https://www.iea.org/data-and-statistics/data-tools/renewable-energy-progress-tracker.
201 Tollefson J. 2023. Is it too late to keep global warming below 1.5°C? The challenge in 7 charts. *Nature*. https://www.nature.com/immersive/d41586-023-03601-6/index.html#article.
202 Postdam Institute for Climate Impact Research. Real progress, yet transition away from fossil fuels too vague: PIK assessment on COP28 closing. PIK [accessed 2023 Dec 13]. https://www.pik-potsdam.de/en/news/latest-news/pivotal-land-mark-pik-assessment-on-cop28-closing#:~:text=%22No%2C%20the%20COP28%20agreement%20will,PIK)%20on%20the%20COP28%20outcome.
203 CarbonBrief. Analysis: global CO_2 emissions could peak as soon as 2023. IEA data reveals. CarbonBrief [accessed 2023 Oct 26]. https://www.carbonbrief.org/analysis-global-co2-emissions-could-peak-as-soon-as-2023-iea-data-reveals/.
204 Larsen K, *et al.* AR5 100-year GWP values. Following IPCC conventions, this report uses very likely to indicate a 90% probability of occurring and likely to indicate a 67% probability. Rhodium Group. https://rhg.com/research/rhodium-climate-outlook-2023/#:~:text=Policy%20and%20technological%20progress%20over,mean%20of%202.8%C2%B0C.
205 United Nations. The 17 goals. UN [accessed 2024 Mar 16]. https://sdgs.un.org/goals.
206 Ripple WJ, *et al.* 2023. The 2023 state of the climate report: entering uncharted territory. *BioScience*. 73:841–850.
207 United Nations Secretary General. Secretary-general's message-UNFCCC NDC synthesis report launch. UN [accessed 2024 Mar 16]. https://www.un.org/sg/en/content/sg/statement/2023-11-14/secretary-generalsmessage-unfccc-ndc-synthesis-report-launch%C2%A0.
208 Hickel J. 2021. What does degrowth mean? A few points of clarification. *Globalizations*. 18:1105–1111.
209 Barnard P, *et al.* 2021. World scientists' warnings into action, local to global. *Sci Prog*. 104:00368504211056290.
210 Crist E, *et al.* 2021. Protecting half the planet and transforming human systems are complementary goals. *Front Conserv Sci*. 2:761292.
211 Ripple WJ, Wolf C, van Vuuren DP, Gregg JW, Lenzen M. 2024. An environmental and socially just climate mitigation pathway for a planet in peril. *Environ Res Lett*. 19(2):021001.
212 Zickfeld K, *et al.* 2023. Net-zero approaches must consider earth system impacts to achieve climate goals. *Nat Clim Change*. 13:1298–1305.
213 Doncaster CP, Bullock JM. 2024. Living in harmony with nature is achievable only as a non-ideal vision. *Environ Sci Policy*. 152:103658.

Article

The economic commitment of climate change

https://doi.org/10.1038/s41586-024-07219-0

Received: 25 January 2023

Accepted: 21 February 2024

Published online: 17 April 2024

Open access

Check for updates

Maximilian Kotz[1,2], Anders Levermann[1,2] & Leonie Wenz[1,3]✉

Global projections of macroeconomic climate-change damages typically consider impacts from average annual and national temperatures over long time horizons[1–6]. Here we use recent empirical findings from more than 1,600 regions worldwide over the past 40 years to project sub-national damages from temperature and precipitation, including daily variability and extremes[7,8]. Using an empirical approach that provides a robust lower bound on the persistence of impacts on economic growth, we find that the world economy is committed to an income reduction of 19% within the next 26 years independent of future emission choices (relative to a baseline without climate impacts, likely range of 11–29% accounting for physical climate and empirical uncertainty). These damages already outweigh the mitigation costs required to limit global warming to 2 °C by sixfold over this near-term time frame and thereafter diverge strongly dependent on emission choices. Committed damages arise predominantly through changes in average temperature, but accounting for further climatic components raises estimates by approximately 50% and leads to stronger regional heterogeneity. Committed losses are projected for all regions except those at very high latitudes, at which reductions in temperature variability bring benefits. The largest losses are committed at lower latitudes in regions with lower cumulative historical emissions and lower present-day income.

Projections of the macroeconomic damage caused by future climate change are crucial to informing public and policy debates about adaptation, mitigation and climate justice. On the one hand, adaptation against climate impacts must be justified and planned on the basis of an understanding of their future magnitude and spatial distribution[9]. This is also of importance in the context of climate justice[10], as well as to key societal actors, including governments, central banks and private businesses, which increasingly require the inclusion of climate risks in their macroeconomic forecasts to aid adaptive decision-making[11,12]. On the other hand, climate mitigation policy such as the Paris Climate Agreement is often evaluated by balancing the costs of its implementation against the benefits of avoiding projected physical damages. This evaluation occurs both formally through cost–benefit analyses[1,4–6], as well as informally through public perception of mitigation and damage costs[13].

Projections of future damages meet challenges when informing these debates, in particular the human biases relating to uncertainty and remoteness that are raised by long-term perspectives[14]. Here we aim to overcome such challenges by assessing the extent of economic damages from climate change to which the world is already committed by historical emissions and socio-economic inertia (the range of future emission scenarios that are considered socio-economically plausible[15]). Such a focus on the near term limits the large uncertainties about diverging future emission trajectories, the resulting long-term climate response and the validity of applying historically observed climate–economic relations over long timescales during which socio-technical conditions may change considerably. As such, this focus aims to simplify the communication and maximize the credibility of projected economic damages from future climate change.

In projecting the future economic damages from climate change, we make use of recent advances in climate econometrics that provide evidence for impacts on sub-national economic growth from numerous components of the distribution of daily temperature and precipitation[3,7,8]. Using fixed-effects panel regression models to control for potential confounders, these studies exploit within-region variation in local temperature and precipitation in a panel of more than 1,600 regions worldwide, comprising climate and income data over the past 40 years, to identify the plausibly causal effects of changes in several climate variables on economic productivity[16,17]. Specifically, macroeconomic impacts have been identified from changing daily temperature variability, total annual precipitation, the annual number of wet days and extreme daily rainfall that occur in addition to those already identified from changing average temperature[2,3,18]. Moreover, regional heterogeneity in these effects based on the prevailing local climatic conditions has been found using interactions terms. The selection of these climate variables follows micro-level evidence for mechanisms related to the impacts of average temperatures on labour and agricultural productivity[2], of temperature variability on agricultural productivity and health[7], as well as of precipitation on agricultural productivity, labour outcomes and flood damages[8] (see Extended Data Table 1 for an overview, including more detailed references). References 7,8 contain a more detailed motivation for the use of these particular climate variables and provide extensive empirical tests about the robustness and nature of their effects on economic output, which are summarized in Methods. By accounting for these extra climatic variables at the sub-national level, we aim for a more comprehensive description of climate impacts with greater detail across both time and space.

[1]Research Domain IV, Research Domain IV, Potsdam Institute for Climate Impact Research, Potsdam, Germany. [2]Institute of Physics, Potsdam University, Potsdam, Germany. [3]Mercator Research Institute on Global Commons and Climate Change, Berlin, Germany. ✉e-mail: leonie.wenz@pik-potsdam.de

Constraining the persistence of impacts

A key determinant and source of discrepancy in estimates of the magnitude of future climate damages is the extent to which the impact of a climate variable on economic growth rates persists. The two extreme cases in which these impacts persist indefinitely or only instantaneously are commonly referred to as growth or level effects[19,20] (see Methods section 'Empirical model specification: fixed-effects distributed lag models' for mathematical definitions). Recent work shows that future damages from climate change depend strongly on whether growth or level effects are assumed[20]. Following refs. 2,18, we provide constraints on this persistence by using distributed lag models to test the significance of delayed effects separately for each climate variable. Notably, and in contrast to refs. 2,18, we use climate variables in their first-differenced form following ref. 3, implying a dependence of the growth rate on a change in climate variables. This choice means that a baseline specification without any lags constitutes a model prior of purely level effects, in which a permanent change in the climate has only an instantaneous effect on the growth rate[3,19,21]. By including lags, one can then test whether any effects may persist further. This is in contrast to the specification used by refs. 2,18, in which climate variables are used without taking the first difference, implying a dependence of the growth rate on the level of climate variables. In this alternative case, the baseline specification without any lags constitutes a model prior of pure growth effects, in which a change in climate has an infinitely persistent effect on the growth rate. Consequently, including further lags in this alternative case tests whether the initial growth impact is recovered[18,19,21]. Both of these specifications suffer from the limiting possibility that, if too few lags are included, one might falsely accept the model prior. The limitations of including a very large number of lags, including loss of data and increasing statistical uncertainty with an increasing number of parameters, mean that such a possibility is likely. By choosing a specification in which the model prior is one of level effects, our approach is therefore conservative by design, avoiding assumptions of infinite persistence of climate impacts on growth and instead providing a lower bound on this persistence based on what is observable empirically (see Methods section 'Empirical model specification: fixed-effects distributed lag models' for further exposition of this framework). The conservative nature of such a choice is probably the reason that ref. 19 finds much greater consistency between the impacts projected by models that use the first difference of climate variables, as opposed to their levels.

We begin our empirical analysis of the persistence of climate impacts on growth using ten lags of the first-differenced climate variables in fixed-effects distributed lag models. We detect substantial effects on economic growth at time lags of up to approximately 8–10 years for the temperature terms and up to approximately 4 years for the precipitation terms (Extended Data Fig. 1 and Extended Data Table 2). Furthermore, evaluation by means of information criteria indicates that the inclusion of all five climate variables and the use of these numbers of lags provide a preferable trade-off between best-fitting the data and including further terms that could cause overfitting, in comparison with model specifications excluding climate variables or including more or fewer lags (Extended Data Fig. 3, Supplementary Methods Section 1 and Supplementary Table 1). We therefore remove statistically insignificant terms at later lags (Supplementary Figs. 1–3 and Supplementary Tables 2–4). Further tests using Monte Carlo simulations demonstrate that the empirical models are robust to autocorrelation in the lagged climate variables (Supplementary Methods Section 2 and Supplementary Figs. 4 and 5), that information criteria provide an effective indicator for lag selection (Supplementary Methods Section 2 and Supplementary Fig. 6), that the results are robust to concerns of imperfect multicollinearity between climate variables and that including several climate variables is actually necessary to isolate their separate effects (Supplementary Methods Section 3 and Supplementary Fig. 7). We provide a further robustness check using a restricted distributed lag model to limit oscillations in the lagged parameter estimates that may result from autocorrelation, finding that it provides similar estimates of cumulative marginal effects to the unrestricted model (Supplementary Methods Section 4 and Supplementary Figs. 8 and 9). Finally, to explicitly account for any outstanding uncertainty arising from the precise choice of the number of lags, we include empirical models with marginally different numbers of lags in the error-sampling procedure of our projection of future damages. On the basis of the lag-selection procedure (the significance of lagged terms in Extended Data Fig. 1 and Extended Data Table 2, as well as information criteria in Extended Data Fig. 3), we sample from models with eight to ten lags for temperature and four for precipitation (models shown in Supplementary Figs. 1–3 and Supplementary Tables 2–4). In summary, this empirical approach to constrain the persistence of climate impacts on economic growth rates is conservative by design in avoiding assumptions of infinite persistence, but nevertheless provides a lower bound on the extent of impact persistence that is robust to the numerous tests outlined above.

Committed damages until mid-century

We combine these empirical economic response functions (Supplementary Figs. 1–3 and Supplementary Tables 2–4) with an ensemble of 21 climate models (see Supplementary Table 5) from the Coupled Model Intercomparison Project Phase 6 (CMIP-6)[22] to project the macroeconomic damages from these components of physical climate change (see Methods for further details). Bias-adjusted climate models that provide a highly accurate reproduction of observed climatological patterns with limited uncertainty (Supplementary Table 6) are used to avoid introducing biases in the projections. Following a well-developed literature[2,3,19], these projections do not aim to provide a prediction of future economic growth. Instead, they are a projection of the exogenous impact of future climate conditions on the economy relative to the baselines specified by socio-economic projections, based on the plausibly causal relationships inferred by the empirical models and assuming ceteris paribus. Other exogenous factors relevant for the prediction of economic output are purposefully assumed constant.

A Monte Carlo procedure that samples from climate model projections, empirical models with different numbers of lags and model parameter estimates (obtained by 1,000 block-bootstrap resamples of each of the regressions in Supplementary Figs. 1–3 and Supplementary Tables 2–4) is used to estimate the combined uncertainty from these sources. Given these uncertainty distributions, we find that projected global damages are statistically indistinguishable across the two most extreme emission scenarios until 2049 (at the 5% significance level; Fig. 1). As such, the climate damages occurring before this time constitute those to which the world is already committed owing to the combination of past emissions and the range of future emission scenarios that are considered socio-economically plausible[15]. These committed damages comprise a permanent income reduction of 19% on average globally (population-weighted average) in comparison with a baseline without climate-change impacts (with a likely range of 11–29%, following the likelihood classification adopted by the Intergovernmental Panel on Climate Change (IPCC); see caption of Fig. 1). Even though levels of income per capita generally still increase relative to those of today, this constitutes a permanent income reduction for most regions, including North America and Europe (each with median income reductions of approximately 11%) and with South Asia and Africa being the most strongly affected (each with median income reductions of approximately 22%; Fig. 1). Under a middle-of-the road scenario of future income development (SSP2, in which SSP stands for Shared Socio-economic Pathway), this corresponds to global annual damages in 2049 of 38 trillion in 2005 international dollars (likely range of 19–59 trillion 2005 international dollars). Compared with empirical specifications that assume pure growth or pure level effects,

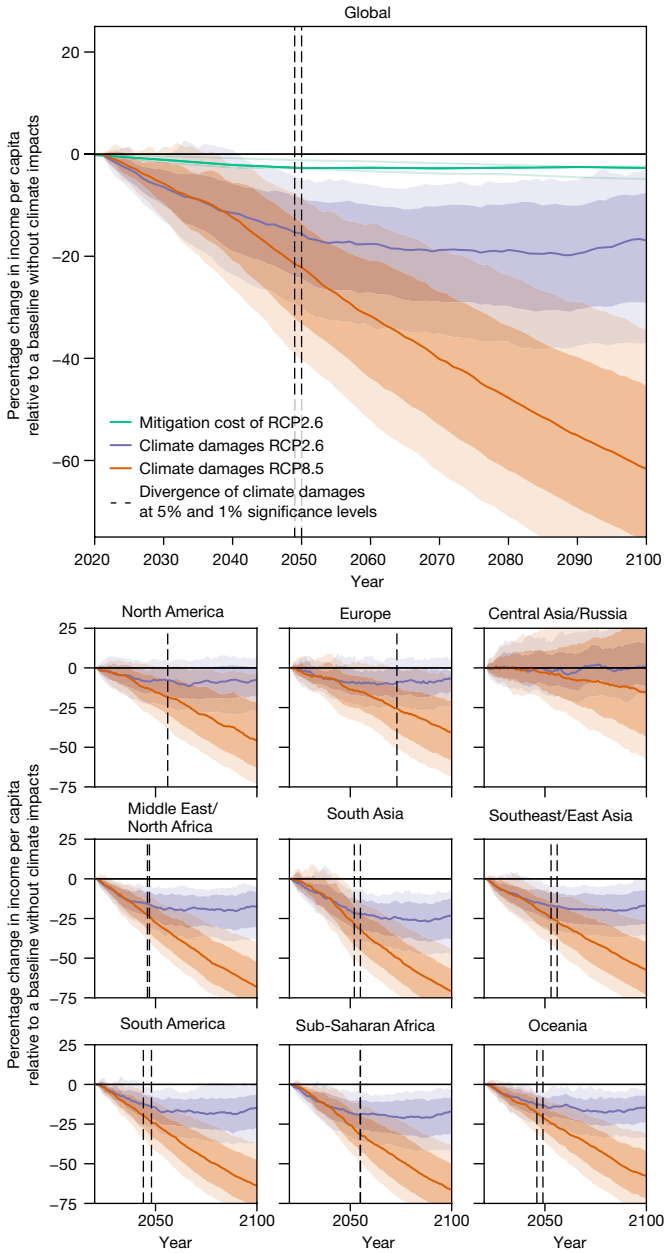

Fig. 1 | The commitment and divergence of economic climate damages versus mitigation costs. Estimates of the projected reduction in income per capita from changes in all climate variables based on empirical models of climate impacts on economic output with a robust lower bound on their persistence (Extended Data Fig. 1) under a low-emission scenario compatible with the 2 °C warming target and a high-emission scenario (SSP2-RCP2.6 and SSP5-RCP8.5, respectively) are shown in purple and orange, respectively. Shading represents the 34% and 10% confidence intervals reflecting the likely and very likely ranges, respectively (following the likelihood classification adopted by the IPCC), having estimated uncertainty from a Monte Carlo procedure, which samples the uncertainty from the choice of physical climate models, empirical models with different numbers of lags and bootstrapped estimates of the regression parameters shown in Supplementary Figs. 1–3. Vertical dashed lines show the time at which the climate damages of the two emission scenarios diverge at the 5% and 1% significance levels based on the distribution of differences between emission scenarios arising from the uncertainty sampling discussed above. Note that uncertainty in the difference of the two scenarios is smaller than the combined uncertainty of the two respective scenarios because samples of the uncertainty (climate model and empirical model choice, as well as model parameter bootstrap) are consistent across the two emission scenarios, hence the divergence of damages occurs while the uncertainty bounds of the two separate damage scenarios still overlap. Estimates of global mitigation costs from the three IAMs that provide results for the SSP2 baseline and SSP2-RCP2.6 scenario are shown in light green in the top panel, with the median of these estimates shown in bold.

our preferred specification that provides a robust lower bound on the extent of climate impact persistence produces damages between these two extreme assumptions (Extended Data Fig. 3).

Damages already outweigh mitigation costs

We compare the damages to which the world is committed over the next 25 years to estimates of the mitigation costs required to achieve the Paris Climate Agreement. Taking estimates of mitigation costs from the three integrated assessment models (IAMs) in the IPCC AR6 database[23] that provide results under comparable scenarios (SSP2 baseline and SSP2-RCP2.6, in which RCP stands for Representative Concentration Pathway), we find that the median committed climate damages are larger than the median mitigation costs in 2050 (six trillion in 2005 international dollars) by a factor of approximately six (note that estimates of mitigation costs are only provided every 10 years by the IAMs and so a comparison in 2049 is not possible). This comparison simply aims to compare the magnitude of future damages against mitigation costs, rather than to conduct a formal cost–benefit analysis of transitioning from one emission path to another. Formal cost–benefit analyses typically find that the net benefits of mitigation only emerge after 2050 (ref. 5), which may lead some to conclude that physical damages from climate change are simply not large enough to outweigh mitigation costs until the second half of the century. Our simple comparison of their magnitudes makes clear that damages are actually already considerably larger than mitigation costs and the delayed emergence of net mitigation benefits results primarily from the fact that damages across different emission paths are indistinguishable until mid-century (Fig. 1).

Although these near-term damages constitute those to which the world is already committed, we note that damage estimates diverge strongly across emission scenarios after 2049, conveying the clear benefits of mitigation from a purely economic point of view that have been emphasized in previous studies[4,24]. As well as the uncertainties assessed in Fig. 1, these conclusions are robust to structural choices, such as the timescale with which changes in the moderating variables of the empirical models are estimated (Supplementary Figs. 10 and 11), as well as the order in which one accounts for the intertemporal and international components of currency comparison (Supplementary Fig. 12; see Methods for further details).

Damages from variability and extremes

Committed damages primarily arise through changes in average temperature (Fig. 2). This reflects the fact that projected changes in average temperature are larger than those in other climate variables when expressed as a function of their historical interannual variability (Extended Data Fig. 4). Because the historical variability is that on which the empirical models are estimated, larger projected changes in comparison with this variability probably lead to larger future impacts in a purely statistical sense. From a mechanistic perspective, one may plausibly interpret this result as implying that future changes in average temperature are the most unprecedented from the perspective of the historical fluctuations to which the economy is accustomed and therefore will cause the most damage. This insight may prove useful in terms of guiding adaptation measures to the sources of greatest damage.

Nevertheless, future damages based on empirical models that consider changes in annual average temperature only and exclude the other climate variables constitute income reductions of only 13% in 2049

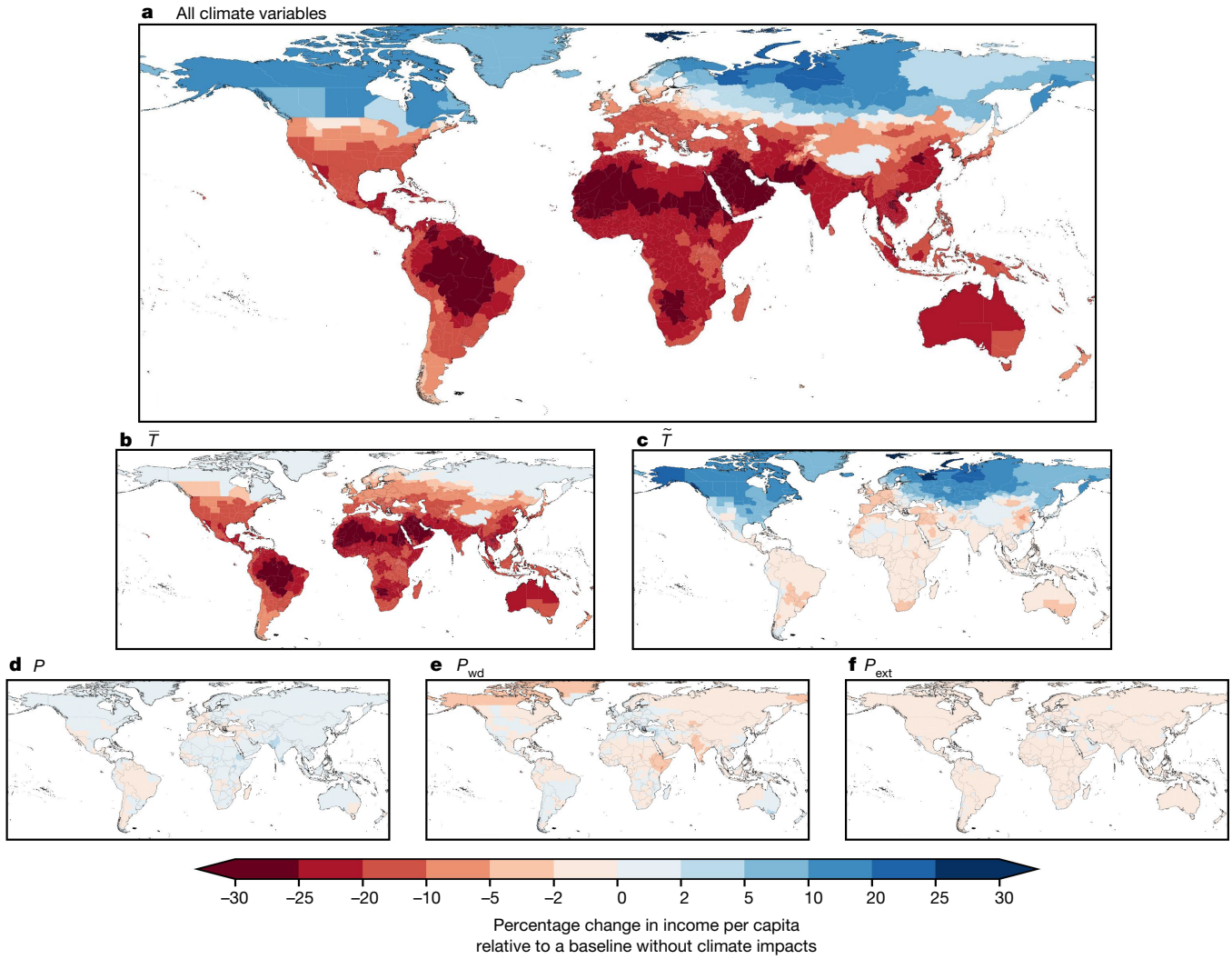

Fig. 2 | The committed economic damages of climate change by sub-national region and climatic component. Estimates of the median projected reduction in sub-national income per capita across emission scenarios (SSP2-RCP2.6 and SSP2-RCP8.5) as well as climate model, empirical model and model parameter uncertainty in the year in which climate damages diverge at the 5% level (2049, as identified in Fig. 1). **a**, Impacts arising from all climate variables. **b**–**f**, Impacts arising separately from changes in annual mean temperature (**b**), daily temperature variability (**c**), total annual precipitation (**d**), the annual number of wet days (>1 mm) (**e**) and extreme daily rainfall (**f**) (see Methods for further definitions). Data on national administrative boundaries are obtained from the GADM database version 3.6 and are freely available for academic use (https://gadm.org/).

(Extended Data Fig. 5a, likely range 5–21%). This suggests that accounting for the other components of the distribution of temperature and precipitation raises net damages by nearly 50%. This increase arises through the further damages that these climatic components cause, but also because their inclusion reveals a stronger negative economic response to average temperatures (Extended Data Fig. 5b). The latter finding is consistent with our Monte Carlo simulations, which suggest that the magnitude of the effect of average temperature on economic growth is underestimated unless accounting for the impacts of other correlated climate variables (Supplementary Fig. 7).

In terms of the relative contributions of the different climatic components to overall damages, we find that accounting for daily temperature variability causes the largest increase in overall damages relative to empirical frameworks that only consider changes in annual average temperature (4.9 percentage points, likely range 2.4–8.7 percentage points, equivalent to approximately 10 trillion international dollars). Accounting for precipitation causes smaller increases in overall damages, which are—nevertheless—equivalent to approximately 1.2 trillion international dollars: 0.01 percentage points (−0.37–0.33 percentage points), 0.34 percentage points (0.07–0.90 percentage points) and 0.36 percentage points (0.13–0.65 percentage points) from total annual precipitation, the number of wet days and extreme daily precipitation, respectively. Moreover, climate models seem to underestimate future changes in temperature variability[25] and extreme precipitation[26,27] in response to anthropogenic forcing as compared with that observed historically, suggesting that the true impacts from these variables may be larger.

The distribution of committed damages

The spatial distribution of committed damages (Fig. 2a) reflects a complex interplay between the patterns of future change in several climatic components and those of historical economic vulnerability to changes in those variables. Damages resulting from increasing annual mean temperature (Fig. 2b) are negative almost everywhere globally, and larger at lower latitudes in regions in which temperatures are already higher and economic vulnerability to temperature increases is greatest (see the response heterogeneity to mean temperature embodied in Extended Data Fig. 1a). This occurs despite the amplified warming projected at higher latitudes[28], suggesting that regional heterogeneity

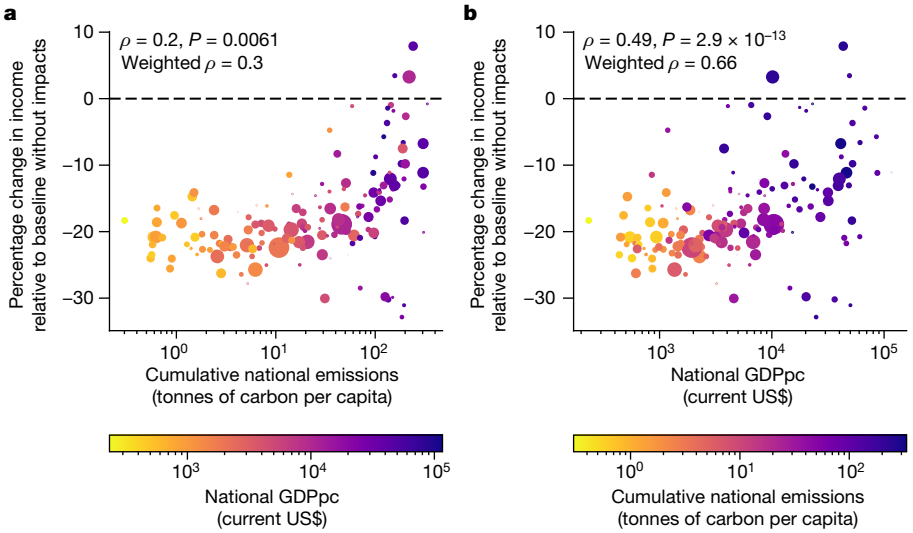

Fig. 3 | The injustice of committed climate damages by cumulative historical emissions and income. Estimates of the median projected change in national income per capita across emission scenarios (RCP2.6 and RCP8.5) as well as climate model, empirical model and model parameter uncertainty in the year in which climate damages diverge at the 5% level (2049, as identified in Fig. 1) are plotted against cumulative national emissions per capita in 2020 (from the Global Carbon Project) and coloured by national income per capita in 2020 (from the World Bank) in **a** and vice versa in **b**. In each panel, the size of each scatter point is weighted by the national population in 2020 (from the World Bank). Inset numbers indicate the Spearman's rank correlation ρ and P-values for a hypothesis test whose null hypothesis is of no correlation, as well as the Spearman's rank correlation weighted by national population.

in economic vulnerability to temperature changes outweighs heterogeneity in the magnitude of future warming (Supplementary Fig. 13a). Economic damages owing to daily temperature variability (Fig. 2c) exhibit a strong latitudinal polarisation, primarily reflecting the physical response of daily variability to greenhouse forcing in which increases in variability across lower latitudes (and Europe) contrast decreases at high latitudes[25] (Supplementary Fig. 13b). These two temperature terms are the dominant determinants of the pattern of overall damages (Fig. 2a), which exhibits a strong polarity with damages across most of the globe except at the highest northern latitudes. Future changes in total annual precipitation mainly bring economic benefits except in regions of drying, such as the Mediterranean and central South America (Fig. 2d and Supplementary Fig. 13c), but these benefits are opposed by changes in the number of wet days, which produce damages with a similar pattern of opposite sign (Fig. 2e and Supplementary Fig. 13d). By contrast, changes in extreme daily rainfall produce damages in all regions, reflecting the intensification of daily rainfall extremes over global land areas[29,30] (Fig. 2f and Supplementary Fig. 13e).

The spatial distribution of committed damages implies considerable injustice along two dimensions: culpability for the historical emissions that have caused climate change and pre-existing levels of socio-economic welfare. Spearman's rank correlations indicate that committed damages are significantly larger in countries with smaller historical cumulative emissions, as well as in regions with lower current income per capita (Fig. 3). This implies that those countries that will suffer the most from the damages already committed are those that are least responsible for climate change and which also have the least resources to adapt to it.

To further quantify this heterogeneity, we assess the difference in committed damages between the upper and lower quartiles of regions when ranked by present income levels and historical cumulative emissions (using a population weighting to both define the quartiles and estimate the group averages). On average, the quartile of countries with lower income are committed to an income loss that is 8.9 percentage points (or 61%) greater than the upper quartile (Extended Data Fig. 6), with a likely range of 3.8–14.7 percentage points across the uncertainty sampling of our damage projections (following the likelihood classification adopted by the IPCC). Similarly, the quartile of countries with lower historical cumulative emissions are committed to an income loss that is 6.9 percentage points (or 40%) greater than the upper quartile, with a likely range of 0.27–12 percentage points. These patterns reemphasize the prevalence of injustice in climate impacts[31–33] in the context of the damages to which the world is already committed by historical emissions and socio-economic inertia.

Contextualizing the magnitude of damages

The magnitude of projected economic damages exceeds previous literature estimates[2,3], arising from several developments made on previous approaches. Our estimates are larger than those of ref. 2 (see first row of Extended Data Table 3), primarily because of the facts that sub-national estimates typically show a steeper temperature response (see also refs. 3,34) and that accounting for other climatic components raises damage estimates (Extended Data Fig. 5). However, we note that our empirical approach using first-differenced climate variables is conservative compared with that of ref. 2 in regard to the persistence of climate impacts on growth (see introduction and Methods section 'Empirical model specification: fixed-effects distributed lag models'), an important determinant of the magnitude of long-term damages[19,21]. Using a similar empirical specification to ref. 2, which assumes infinite persistence while maintaining the rest of our approach (sub-national data and further climate variables), produces considerably larger damages (purple curve of Extended Data Fig. 3). Compared with studies that do take the first difference of climate variables[3,35], our estimates are also larger (see second and third rows of Extended Data Table 3). The inclusion of further climate variables (Extended Data Fig. 5) and a sufficient number of lags to more adequately capture the extent of impact persistence (Extended Data Figs. 1 and 2) are the main sources of this difference, as is the use of specifications that capture nonlinearities in the temperature response when compared with ref. 35. In summary, our estimates develop on previous studies by incorporating the latest data and empirical insights[7,8], as well as in providing a robust empirical lower bound on the persistence of impacts on economic growth, which constitutes a middle ground between the extremes of the growth-versus-levels debate[19,21] (Extended Data Fig. 3).

Compared with the fraction of variance explained by the empirical models historically (<5%), the projection of reductions in income of 19% may seem large. This arises owing to the fact that projected changes in climatic conditions are much larger than those that were experienced historically, particularly for changes in average temperature (Extended Data Fig. 4). As such, any assessment of future climate-change impacts necessarily requires an extrapolation outside the range of the historical data on which the empirical impact models were evaluated. Nevertheless, these models constitute the most state-of-the-art methods for inference of plausibly causal climate impacts based on observed data. Moreover, we take explicit steps to limit out-of-sample extrapolation by capping the moderating variables of the interaction terms at the 95th percentile of the historical distribution (see Methods). This avoids extrapolating the marginal effects outside what was observed historically. Given the nonlinear response of economic output to annual mean temperature (Extended Data Fig. 1 and Extended Data Table 2), this is a conservative choice that limits the magnitude of damages that we project. Furthermore, back-of-the-envelope calculations indicate that the projected damages are consistent with the magnitude and patterns of historical economic development (see Supplementary Discussion Section 5).

Missing impacts and spatial spillovers

Despite assessing several climatic components from which economic impacts have recently been identified[3,7,8], this assessment of aggregate climate damages should not be considered comprehensive. Important channels such as impacts from heatwaves[31], sea-level rise[36], tropical cyclones[37] and tipping points[38,39], as well as non-market damages such as those to ecosystems[40] and human health[41], are not considered in these estimates. Sea-level rise is unlikely to be feasibly incorporated into empirical assessments such as this because historical sea-level variability is mostly small. Non-market damages are inherently intractable within our estimates of impacts on aggregate monetary output and estimates of these impacts could arguably be considered as extra to those identified here. Recent empirical work suggests that accounting for these channels would probably raise estimates of these committed damages, with larger damages continuing to arise in the global south[31,36–42].

Moreover, our main empirical analysis does not explicitly evaluate the potential for impacts in local regions to produce effects that 'spill over' into other regions. Such effects may further mitigate or amplify the impacts we estimate, for example, if companies relocate production from one affected region to another or if impacts propagate along supply chains. The current literature indicates that trade plays a substantial role in propagating spillover effects[43,44], making their assessment at the sub-national level challenging without available data on sub-national trade dependencies. Studies accounting for only spatially adjacent neighbours indicate that negative impacts in one region induce further negative impacts in neighbouring regions[45–48], suggesting that our projected damages are probably conservative by excluding these effects. In Supplementary Fig. 14, we assess spillovers from neighbouring regions using a spatial-lag model. For simplicity, this analysis excludes temporal lags, focusing only on contemporaneous effects. The results show that accounting for spatial spillovers can amplify the overall magnitude, and also the heterogeneity, of impacts. Consistent with previous literature, this indicates that the overall magnitude (Fig. 1) and heterogeneity (Fig. 3) of damages that we project in our main specification may be conservative without explicitly accounting for spillovers. We note that further analysis that addresses both spatially and trade-connected spillovers, while also accounting for delayed impacts using temporal lags, would be necessary to adequately address this question fully. These approaches offer fruitful avenues for further research but are beyond the scope of this manuscript, which primarily aims to explore the impacts of different climate conditions and their persistence.

Policy implications

We find that the economic damages resulting from climate change until 2049 are those to which the world economy is already committed and that these greatly outweigh the costs required to mitigate emissions in line with the 2 °C target of the Paris Climate Agreement (Fig. 1). This assessment is complementary to formal analyses of the net costs and benefits associated with moving from one emission path to another, which typically find that net benefits of mitigation only emerge in the second half of the century[5]. Our simple comparison of the magnitude of damages and mitigation costs makes clear that this is primarily because damages are indistinguishable across emissions scenarios—that is, committed—until mid-century (Fig. 1) and that they are actually already much larger than mitigation costs. For simplicity, and owing to the availability of data, we compare damages to mitigation costs at the global level. Regional estimates of mitigation costs may shed further light on the national incentives for mitigation to which our results already hint, of relevance for international climate policy. Although these damages are committed from a mitigation perspective, adaptation may provide an opportunity to reduce them. Moreover, the strong divergence of damages after mid-century reemphasizes the clear benefits of mitigation from a purely economic perspective, as highlighted in previous studies[1,4,6,24].

Online content

Any methods, additional references, Nature Portfolio reporting summaries, source data, extended data, supplementary information, acknowledgements, peer review information; details of author contributions and competing interests; and statements of data and code availability are available at https://doi.org/10.1038/s41586-024-07219-0.

1. Glanemann, N., Willner, S. N. & Levermann, A. Paris Climate Agreement passes the cost-benefit test. *Nat. Commun.* **11**, 110 (2020).
2. Burke, M., Hsiang, S. M. & Miguel, E. Global non-linear effect of temperature on economic production. *Nature* **527**, 235–239 (2015).
3. Kalkuhl, M. & Wenz, L. The impact of climate conditions on economic production. Evidence from a global panel of regions. *J. Environ. Econ. Manag.* **103**, 102360 (2020).
4. Moore, F. C. & Diaz, D. B. Temperature impacts on economic growth warrant stringent mitigation policy. *Nat. Clim. Change* **5**, 127–131 (2015).
5. Drouet, L., Bosetti, V. & Tavoni, M. Net economic benefits of well-below 2°C scenarios and associated uncertainties. *Oxf. Open Clim. Change* **2**, kgac003 (2022).
6. Ueckerdt, F. et al. The economically optimal warming limit of the planet. *Earth Syst. Dyn.* **10**, 741–763 (2019).
7. Kotz, M., Wenz, L., Stechemesser, A., Kalkuhl, M. & Levermann, A. Day-to-day temperature variability reduces economic growth. *Nat. Clim. Change* **11**, 319–325 (2021).
8. Kotz, M., Levermann, A. & Wenz, L. The effect of rainfall changes on economic production. *Nature* **601**, 223–227 (2022).
9. Kousky, C. Informing climate adaptation: a review of the economic costs of natural disasters. *Energy Econ.* **46**, 576–592 (2014).
10. Harlan, S. L. et al. in *Climate Change and Society: Sociological Perspectives* (eds Dunlap, R. E. & Brulle, R. J.) 127–163 (Oxford Univ. Press, 2015).
11. Bolton, P. et al. *The Green Swan* (BIS Books, 2020).
12. Alogoskoufis, S. et al. *ECB Economy-wide Climate Stress Test: Methodology and Results* European Central Bank, 2021).
13. Weber, E. U. What shapes perceptions of climate change? *Wiley Interdiscip. Rev. Clim. Change* **1**, 332–342 (2010).
14. Markowitz, E. M. & Shariff, A. F. Climate change and moral judgement. *Nat. Clim. Change* **2**, 243–247 (2012).
15. Riahi, K. et al. The shared socioeconomic pathways and their energy, land use, and greenhouse gas emissions implications: an overview. *Glob. Environ. Change* **42**, 153–168 (2017).
16. Auffhammer, M., Hsiang, S. M., Schlenker, W. & Sobel, A. Using weather data and climate model output in economic analyses of climate change. *Rev. Environ. Econ. Policy* **7**, 181–198 (2013).
17. Kolstad, C. D. & Moore, F. C. Estimating the economic impacts of climate change using weather observations. *Rev. Environ. Econ. Policy* **14**, 1–24 (2020).
18. Dell, M., Jones, B. F. & Olken, B. A. Temperature shocks and economic growth: evidence from the last half century. *Am. Econ. J. Macroecon.* **4**, 66–95 (2012).
19. Newell, R. G., Prest, B. C. & Sexton, S. E. The GDP-temperature relationship: implications for climate change damages. *J. Environ. Econ. Manag.* **108**, 102445 (2021).
20. Kikstra, J. S. et al. The social cost of carbon dioxide under climate-economy feedbacks and temperature variability. *Environ. Res. Lett.* **16**, 094037 (2021).
21. Bastien-Olvera, B. & Moore, F. Persistent effect of temperature on GDP identified from lower frequency temperature variability. *Environ. Res. Lett.* **17**, 084038 (2022).

22. Eyring, V. et al. Overview of the Coupled Model Intercomparison Project Phase 6 (CMIP6) experimental design and organization. *Geosci. Model Dev.* **9**, 1937–1958 (2016).
23. Byers, E. et al. AR6 scenarios database. *Zenodo* https://zenodo.org/records/7197970 (2022).
24. Burke, M., Davis, W. M. & Diffenbaugh, N. S. Large potential reduction in economic damages under UN mitigation targets. *Nature* **557**, 549–553 (2018).
25. Kotz, M., Wenz, L. & Levermann, A. Footprint of greenhouse forcing in daily temperature variability. *Proc. Natl Acad. Sci.* **118**, e2103294118 (2021).
26. Myhre, G. et al. Frequency of extreme precipitation increases extensively with event rareness under global warming. *Sci. Rep.* **9**, 16063 (2019).
27. Min, S.-K., Zhang, X., Zwiers, F. W. & Hegerl, G. C. Human contribution to more-intense precipitation extremes. *Nature* **470**, 378–381 (2011).
28. England, M. R., Eisenman, I., Lutsko, N. J. & Wagner, T. J. The recent emergence of Arctic Amplification. *Geophys. Res. Lett.* **48**, e2021GL094086 (2021).
29. Fischer, E. M. & Knutti, R. Anthropogenic contribution to global occurrence of heavy-precipitation and high-temperature extremes. *Nat. Clim. Change* **5**, 560–564 (2015).
30. Pfahl, S., O'Gorman, P. A. & Fischer, E. M. Understanding the regional pattern of projected future changes in extreme precipitation. *Nat. Clim. Change* **7**, 423–427 (2017).
31. Callahan, C. W. & Mankin, J. S. Globally unequal effect of extreme heat on economic growth. *Sci. Adv.* **8**, eadd3726 (2022).
32. Diffenbaugh, N. S. & Burke, M. Global warming has increased global economic inequality. *Proc. Natl Acad. Sci.* **116**, 9808–9813 (2019).
33. Callahan, C. W. & Mankin, J. S. National attribution of historical climate damages. *Clim. Change* **172**, 40 (2022).
34. Burke, M. & Tanutama, V. Climatic constraints on aggregate economic output. National Bureau of Economic Research, Working Paper 25779. https://doi.org/10.3386/w25779 (2019).
35. Kahn, M. E. et al. Long-term macroeconomic effects of climate change: a cross-country analysis. *Energy Econ.* **104**, 105624 (2021).
36. Desmet, K. et al. Evaluating the economic cost of coastal flooding. National Bureau of Economic Research, Working Paper 24918. https://doi.org/10.3386/w24918 (2018).
37. Hsiang, S. M. & Jina, A. S. The causal effect of environmental catastrophe on long-run economic growth: evidence from 6,700 cyclones. National Bureau of Economic Research, Working Paper 20352. https://doi.org/10.3386/w2035 (2014).
38. Ritchie, P. D. et al. Shifts in national land use and food production in Great Britain after a climate tipping point. *Nat. Food* **1**, 76–83 (2020).
39. Dietz, S., Rising, J., Stoerk, T. & Wagner, G. Economic impacts of tipping points in the climate system. *Proc. Natl Acad. Sci.* **118**, e2103081118 (2021).
40. Bastien-Olvera, B. A. & Moore, F. C. Use and non-use value of nature and the social cost of carbon. *Nat. Sustain.* **4**, 101–108 (2021).
41. Carleton, T. et al. Valuing the global mortality consequences of climate change accounting for adaptation costs and benefits. *Q. J. Econ.* **137**, 2037–2105 (2022).
42. Bastien-Olvera, B. A. et al. Unequal climate impacts on global values of natural capital. *Nature* **625**, 722–727 (2024).
43. Malik, A. et al. Impacts of climate change and extreme weather on food supply chains cascade across sectors and regions in Australia. *Nat. Food* **3**, 631–643 (2022).
44. Kuhla, K., Willner, S. N., Otto, C., Geiger, T. & Levermann, A. Ripple resonance amplifies economic welfare loss from weather extremes. *Environ. Res. Lett.* **16**, 114010 (2021).
45. Schleypen, J. R., Mistry, M. N., Saeed, F. & Dasgupta, S. Sharing the burden: quantifying climate change spillovers in the European Union under the Paris Agreement. *Spat. Econ. Anal.* **17**, 67–82 (2022).
46. Dasgupta, S., Bosello, F., De Cian, E. & Mistry, M. Global temperature effects on economic activity and equity: a spatial analysis. European Institute on Economics and the Environment, Working Paper 22-1 (2022).
47. Neal, T. The importance of external weather effects in projecting the macroeconomic impacts of climate change. UNSW Economics Working Paper 2023-09 (2023).
48. Deryugina, T. & Hsiang, S. M. Does the environment still matter? Daily temperature and income in the United States. National Bureau of Economic Research, Working Paper 20750. https://doi.org/10.3386/w20750 (2014).

Methods

Historical climate data

Historical daily 2-m temperature and precipitation totals (in mm) are obtained for the period 1979–2019 from the W5E5 database. The W5E5 dataset comes from ERA-5, a state-of-the-art reanalysis of historical observations, but has been bias-adjusted by applying version 2.0 of the WATCH Forcing Data to ERA-5 reanalysis data and precipitation data from version 2.3 of the Global Precipitation Climatology Project to better reflect ground-based measurements[49–51]. We obtain these data on a 0.5° × 0.5° grid from the Inter-Sectoral Impact Model Intercomparison Project (ISIMIP) database. Notably, these historical data have been used to bias-adjust future climate projections from CMIP-6 (see the following section), ensuring consistency between the distribution of historical daily weather on which our empirical models were estimated and the climate projections used to estimate future damages. These data are publicly available from the ISIMIP database. See refs. 7,8 for robustness tests of the empirical models to the choice of climate data reanalysis products.

Future climate data

Daily 2-m temperature and precipitation totals (in mm) are taken from 21 climate models participating in CMIP-6 under a high (RCP8.5) and a low (RCP2.6) greenhouse gas emission scenario from 2015 to 2100. The data have been bias-adjusted and statistically downscaled to a common half-degree grid to reflect the historical distribution of daily temperature and precipitation of the W5E5 dataset using the trend-preserving method developed by the ISIMIP[50,52]. As such, the climate model data reproduce observed climatological patterns exceptionally well (Supplementary Table 5). Gridded data are publicly available from the ISIMIP database.

Historical economic data

Historical economic data come from the DOSE database of sub-national economic output[53]. We use a recent revision to the DOSE dataset that provides data across 83 countries, 1,660 sub-national regions with varying temporal coverage from 1960 to 2019. Sub-national units constitute the first administrative division below national, for example, states for the USA and provinces for China. Data come from measures of gross regional product per capita (GRPpc) or income per capita in local currencies, reflecting the values reported in national statistical agencies, yearbooks and, in some cases, academic literature. We follow previous literature[3,7,8,54] and assess real sub-national output per capita by first converting values from local currencies to US dollars to account for diverging national inflationary tendencies and then account for US inflation using a US deflator. Alternatively, one might first account for national inflation and then convert between currencies. Supplementary Fig. 12 demonstrates that our conclusions are consistent when accounting for price changes in the reversed order, although the magnitude of estimated damages varies. See the documentation of the DOSE dataset for further discussion of these choices. Conversions between currencies are conducted using exchange rates from the FRED database of the Federal Reserve Bank of St. Louis[55] and the national deflators from the World Bank[56].

Future socio-economic data

Baseline gridded gross domestic product (GDP) and population data for the period 2015–2100 are taken from the middle-of-the-road scenario SSP2 (ref. 15). Population data have been downscaled to a half-degree grid by the ISIMIP following the methodologies of refs. 57,58, which we then aggregate to the sub-national level of our economic data using the spatial aggregation procedure described below. Because current methodologies for downscaling the GDP of the SSPs use downscaled population to do so, per-capita estimates of GDP with a realistic distribution at the sub-national level are not readily available for the SSPs. We therefore use national-level GDP per capita (GDPpc) projections for all sub-national regions of a given country, assuming homogeneity within countries in terms of baseline GDPpc. Here we use projections that have been updated to account for the impact of the COVID-19 pandemic on the trajectory of future income, while remaining consistent with the long-term development of the SSPs[59]. The choice of baseline SSP alters the magnitude of projected climate damages in monetary terms, but when assessed in terms of percentage change from the baseline, the choice of socio-economic scenario is inconsequential. Gridded SSP population data and national-level GDPpc data are publicly available from the ISIMIP database. Sub-national estimates as used in this study are available in the code and data replication files.

Climate variables

Following recent literature[3,7,8], we calculate an array of climate variables for which substantial impacts on macroeconomic output have been identified empirically, supported by further evidence at the micro level for plausible underlying mechanisms. See refs. 7,8 for an extensive motivation for the use of these particular climate variables and for detailed empirical tests on the nature and robustness of their effects on economic output. To summarize, these studies have found evidence for independent impacts on economic growth rates from annual average temperature, daily temperature variability, total annual precipitation, the annual number of wet days and extreme daily rainfall. Assessments of daily temperature variability were motivated by evidence of impacts on agricultural output and human health, as well as macroeconomic literature on the impacts of volatility on growth when manifest in different dimensions, such as government spending, exchange rates and even output itself[7]. Assessments of precipitation impacts were motivated by evidence of impacts on agricultural productivity, metropolitan labour outcomes and conflict, as well as damages caused by flash flooding[8]. See Extended Data Table 1 for detailed references to empirical studies of these physical mechanisms. Marked impacts of daily temperature variability, total annual precipitation, the number of wet days and extreme daily rainfall on macroeconomic output were identified robustly across different climate datasets, spatial aggregation schemes, specifications of regional time trends and error-clustering approaches. They were also found to be robust to the consideration of temperature extremes[7,8]. Furthermore, these climate variables were identified as having independent effects on economic output[7,8], which we further explain here using Monte Carlo simulations to demonstrate the robustness of the results to concerns of imperfect multicollinearity between climate variables (Supplementary Methods Section 2), as well as by using information criteria (Supplementary Table 1) to demonstrate that including several lagged climate variables provides a preferable trade-off between optimally describing the data and limiting the possibility of overfitting.

We calculate these variables from the distribution of daily, d, temperature, $T_{x,d}$, and precipitation, $P_{x,d}$, at the grid-cell, x, level for both the historical and future climate data. As well as annual mean temperature, $\overline{T}_{x,y}$, and annual total precipitation, $P_{x,y}$, we calculate annual, y, measures of daily temperature variability, $\widetilde{T}_{x,y}$:

$$\widetilde{T}_{x,y} = \frac{1}{12}\sum_{m=1}^{12}\sqrt{\frac{1}{D_m}\sum_{d=1}^{D_m}(T_{x,d,m,y} - \overline{T}_{x,m})^2}, \quad (1)$$

the number of wet days, $\mathrm{Pwd}_{x,y}$:

$$\mathrm{Pwd}_{x,y} = \sum_{d=1}^{D_y} H(P_{x,d} - 1\,\mathrm{mm}) \quad (2)$$

and extreme daily rainfall:

$$\mathrm{Pext}_{x,y} = \sum_{d=1}^{D_y} H(P_{x,d} - P99.9_x) \times P_{x,d}, \quad (3)$$

in which $T_{x,d,m,y}$ is the grid-cell-specific daily temperature in month m and year y, $\overline{T}_{x,m,y}$ is the year and grid-cell-specific monthly, m, mean temperature, D_m and D_y the number of days in a given month m or year y, respectively, H the Heaviside step function, 1 mm the threshold used to define wet days and $P99.9_x$ is the 99.9th percentile of historical (1979–2019) daily precipitation at the grid-cell level. Units of the climate measures are degrees Celsius for annual mean temperature and daily temperature variability, millimetres for total annual precipitation and extreme daily precipitation, and simply the number of days for the annual number of wet days.

We also calculated weighted standard deviations of monthly rainfall totals as also used in ref. 8 but do not include them in our projections as we find that, when accounting for delayed effects, their effect becomes statistically indistinct and is better captured by changes in total annual rainfall.

Spatial aggregation

We aggregate grid-cell-level historical and future climate measures, as well as grid-cell-level future GDPpc and population, to the level of the first administrative unit below national level of the GADM database, using an area-weighting algorithm that estimates the portion of each grid cell falling within an administrative boundary. We use this as our baseline specification following previous findings that the effect of area or population weighting at the sub-national level is negligible[7,8].

Empirical model specification: fixed-effects distributed lag models

Following a wide range of climate econometric literature[16,60], we use panel regression models with a selection of fixed effects and time trends to isolate plausibly exogenous variation with which to maximize confidence in a causal interpretation of the effects of climate on economic growth rates. The use of region fixed effects, μ_r, accounts for unobserved time-invariant differences between regions, such as prevailing climatic norms and growth rates owing to historical and geopolitical factors. The use of yearly fixed effects, η_y, accounts for regionally invariant annual shocks to the global climate or economy such as the El Niño–Southern Oscillation or global recessions. In our baseline specification, we also include region-specific linear time trends, $k_r y$, to exclude the possibility of spurious correlations resulting from common slow-moving trends in climate and growth.

The persistence of climate impacts on economic growth rates is a key determinant of the long-term magnitude of damages. Methods for inferring the extent of persistence in impacts on growth rates have typically used lagged climate variables to evaluate the presence of delayed effects or catch-up dynamics[2,18]. For example, consider starting from a model in which a climate condition, $C_{r,y}$, (for example, annual mean temperature) affects the growth rate, $\Delta\mathrm{lgrp}_{r,y}$ (the first difference of the logarithm of gross regional product) of region r in year y:

$$\Delta\mathrm{lgrp}_{r,y} = \mu_r + \eta_y + k_r y + \alpha C_{r,y} + \varepsilon_{r,y}, \quad (4)$$

which we refer to as a 'pure growth effects' model in the main text. Typically, further lags are included,

$$\Delta\mathrm{lgrp}_{r,y} = \mu_r + \eta_y + k_r y + \sum_{L=0}^{\mathrm{NL}} \alpha_L C_{r,y-L} + \varepsilon_{r,y}, \quad (5)$$

and the cumulative effect of all lagged terms is evaluated to assess the extent to which climate impacts on growth rates persist. Following ref. 18, in the case that,

$$\sum_{L=0}^{\mathrm{NL}} \alpha_L < 0 \text{ for } \alpha_0 < 0 \text{ or } \sum_{L=0}^{\mathrm{NL}} \alpha_L > 0 \text{ for } \alpha_0 > 0, \quad (6)$$

the implication is that impacts on the growth rate persist up to NL years after the initial shock (possibly to a weaker or a stronger extent), whereas if

$$\sum_{L=0}^{\mathrm{NL}} \alpha_L = 0, \quad (7)$$

then the initial impact on the growth rate is recovered after NL years and the effect is only one on the level of output. However, we note that such approaches are limited by the fact that, when including an insufficient number of lags to detect a recovery of the growth rates, one may find equation (6) to be satisfied and incorrectly assume that a change in climatic conditions affects the growth rate indefinitely. In practice, given a limited record of historical data, including too few lags to confidently conclude in an infinitely persistent impact on the growth rate is likely, particularly over the long timescales over which future climate damages are often projected[2,24]. To avoid this issue, we instead begin our analysis with a model for which the level of output, $\mathrm{lgrp}_{r,y}$, depends on the level of a climate variable, $C_{r,y}$:

$$\mathrm{lgrp}_{r,y} = \mu_r + \eta_y + k_r y + \alpha C_{r,y} + \varepsilon_{r,y}. \quad (8)$$

Given the non-stationarity of the level of output, we follow the literature[19] and estimate such an equation in first-differenced form as,

$$\Delta\mathrm{lgrp}_{r,y} = \mu_r + \eta_y + k_r y + \alpha \Delta C_{r,y} + \varepsilon_{r,y}, \quad (8)$$

which we refer to as a model of 'pure level effects' in the main text. This model constitutes a baseline specification in which a permanent change in the climate variable produces an instantaneous impact on the growth rate and a permanent effect only on the level of output. By including lagged variables in this specification,

$$\Delta\mathrm{lgrp}_{r,y} = \mu_r + \eta_y + k_r y + \sum_{L=0}^{\mathrm{NL}} \alpha_L \Delta C_{r,y-L} + \varepsilon_{r,y}, \quad (9)$$

we are able to test whether the impacts on the growth rate persist any further than instantaneously by evaluating whether $\alpha_L > 0$ are statistically significantly different from zero. Even though this framework is also limited by the possibility of including too few lags, the choice of a baseline model specification in which impacts on the growth rate do not persist means that, in the case of including too few lags, the framework reverts to the baseline specification of level effects. As such, this framework is conservative with respect to the persistence of impacts and the magnitude of future damages. It naturally avoids assumptions of infinite persistence and we are able to interpret any persistence that we identify with equation (9) as a lower bound on the extent of climate impact persistence on growth rates. See the main text for further discussion of this specification choice, in particular about its conservative nature compared with previous literature estimates, such as refs. 2,18.

We allow the response to climatic changes to vary across regions, using interactions of the climate variables with historical average (1979–2019) climatic conditions reflecting heterogenous effects identified in previous work[7,8]. Following this previous work, the moderating variables of these interaction terms constitute the historical average of either the variable itself or of the seasonal temperature difference, $\hat{T}_r$, or annual mean temperature, $\overline{T}_r$, in the case of daily temperature variability[7] and extreme daily rainfall, respectively[8].

The resulting regression equation with N and M lagged variables, respectively, reads:

$$\begin{aligned}\Delta\text{lgrp}_{r,y} = {} & \mu_r + \eta_y + k_r y + \sum_{L=0}^{N} (\alpha_{1,L}\Delta\overline{T}_{r,y-L} + \alpha_{2,L}\Delta\overline{T}_{r,y-L} \times \overline{T}_r) \\ & + \sum_{L=0}^{N} (\alpha_{3,L}\Delta\widetilde{T}_{r,y-L} + \alpha_{4,L}\Delta\widetilde{T}_{r,y-L} \times \hat{T}_r) \\ & + \sum_{L=0}^{M} (\alpha_{5,L}\Delta P_{r,y-L} + \alpha_{6,L}\Delta P_{r,y-L} \times P_r) \\ & + \sum_{L=0}^{M} (\alpha_{7,L}\Delta\text{Pwd}_{r,y-L} + \alpha_{8,L}\Delta\text{Pwd}_{r,y-L} \times \text{Pwd}_r) \\ & + \sum_{L=0}^{M} (\alpha_{9,L}\Delta\text{Pext}_{r,y-L} + \alpha_{10,L}\Delta\text{Pext}_{r,y-L} \times \overline{T}_r) + \epsilon_{r,y}\end{aligned} \quad (10)$$

in which $\Delta\text{lgrp}_{r,y}$ is the annual, regional GRPpc growth rate, measured as the first difference of the logarithm of real GRPpc, following previous work[2,3,7,8,18,19]. Fixed-effects regressions were run using the fixest package in R (ref. 61).

Estimates of the coefficients of interest $\alpha_{i,L}$ are shown in Extended Data Fig. 1 for $N = M = 10$ lags and for our preferred choice of the number of lags in Supplementary Figs. 1–3. In Extended Data Fig. 1, errors are shown clustered at the regional level, but for the construction of damage projections, we block-bootstrap the regressions by region 1,000 times to provide a range of parameter estimates with which to sample the projection uncertainty (following refs. 2,31).

Spatial-lag model

In Supplementary Fig. 14, we present the results from a spatial-lag model that explores the potential for climate impacts to 'spill over' into spatially neighbouring regions. We measure the distance between centroids of each pair of sub-national regions and construct spatial lags that take the average of the first-differenced climate variables and their interaction terms over neighbouring regions that are at distances of 0–500, 500–1,000, 1,000–1,500 and 1,500–2000 km (spatial lags, 'SL', 1 to 4). For simplicity, we then assess a spatial-lag model without temporal lags to assess spatial spillovers of contemporaneous climate impacts. This model takes the form:

$$\begin{aligned}\Delta\text{lgrp}_{r,y} = {} & \mu_r + \eta_y + k_r y + \sum_{\text{SL}=0}^{N} (\alpha_{1,\text{SL}}\Delta\overline{T}_{r-\text{SL},y} + \alpha_{2,\text{SL}}\Delta\overline{T}_{r-\text{SL},y} \times \overline{T}_{r-\text{SL}}) \\ & + \sum_{\text{SL}=0}^{N} (\alpha_{3,\text{SL}}\Delta\widetilde{T}_{r-\text{SL},y} + \alpha_{4,\text{SL}}\Delta\widetilde{T}_{r-\text{SL},y} \times \hat{T}_{r-\text{SL}}) \\ & + \sum_{\text{SL}=0}^{N} (\alpha_{5,\text{SL}}\Delta P_{r-\text{SL},y} + \alpha_{6,\text{SL}}\Delta P_{r-\text{SL},y} \times P_{r-\text{SL}}) \\ & + \sum_{\text{SL}=0}^{N} (\alpha_{7,\text{SL}}\Delta\text{Pwd}_{r-\text{SL},y} + \alpha_{8,\text{SL}}\Delta\text{Pwd}_{r-\text{SL},y} \times \text{Pwd}_{r-\text{SL}}) \\ & + \sum_{\text{SL}=0}^{N} (\alpha_{9,\text{SL}}\Delta\text{Pext}_{r-\text{SL},y} + \alpha_{10,\text{SL}}\Delta\text{Pext}_{r-\text{SL},y} \times \overline{T}_{r-\text{SL}}) + \epsilon_{r,y},\end{aligned} \quad (11)$$

in which SL indicates the spatial lag of each climate variable and interaction term. In Supplementary Fig. 14, we plot the cumulative marginal effect of each climate variable at different baseline climate conditions by summing the coefficients for each climate variable and interaction term, for example, for average temperature impacts as:

$$\text{ME} = \sum_{\text{SL}=0}^{N} (\alpha_{1,\text{SL}} + \alpha_{2,\text{SL}}\overline{T}_{r-\text{SL}}). \quad (12)$$

These cumulative marginal effects can be regarded as the overall spatially dependent impact to an individual region given a one-unit shock to a climate variable in that region and all neighbouring regions at a given value of the moderating variable of the interaction term.

Constructing projections of economic damage from future climate change

We construct projections of future climate damages by applying the coefficients estimated in equation (10) and shown in Supplementary Tables 2–4 (when including only lags with statistically significant effects in specifications that limit overfitting; see Supplementary Methods Section 1) to projections of future climate change from the CMIP-6 models. Year-on-year changes in each primary climate variable of interest are calculated to reflect the year-to-year variations used in the empirical models. 30-year moving averages of the moderating variables of the interaction terms are calculated to reflect the long-term average of climatic conditions that were used for the moderating variables in the empirical models. By using moving averages in the projections, we account for the changing vulnerability to climate shocks based on the evolving long-term conditions (Supplementary Figs. 10 and 11 show that the results are robust to the precise choice of the window of this moving average). Although these climate variables are not differenced, the fact that the bias-adjusted climate models reproduce observed climatological patterns across regions for these moderating variables very accurately (Supplementary Table 6) with limited spread across models (<3%) precludes the possibility that any considerable bias or uncertainty is introduced by this methodological choice. However, we impose caps on these moderating variables at the 95th percentile at which they were observed in the historical data to prevent extrapolation of the marginal effects outside the range in which the regressions were estimated. This is a conservative choice that limits the magnitude of our damage projections.

Time series of primary climate variables and moderating climate variables are then combined with estimates of the empirical model parameters to evaluate the regression coefficients in equation (10), producing a time series of annual GRPpc growth-rate reductions for a given emission scenario, climate model and set of empirical model parameters. The resulting time series of growth-rate impacts reflects those occurring owing to future climate change. By contrast, a future scenario with no climate change would be one in which climate variables do not change (other than with random year-to-year fluctuations) and hence the time-averaged evaluation of equation (10) would be zero. Our approach therefore implicitly compares the future climate-change scenario to this no-climate-change baseline scenario.

The time series of growth-rate impacts owing to future climate change in region r and year y, $\delta_{r,y}$, are then added to the future baseline growth rates, $\pi_{r,y}$ (in log-diff form), obtained from the SSP2 scenario to yield trajectories of damaged GRPpc growth rates, $\rho_{r,y}$. These trajectories are aggregated over time to estimate the future trajectory of GRPpc with future climate impacts:

$$\begin{aligned}\text{GRPpc}_{r,Y} &= \text{GRPpc}_{r,2020} \sum_{y=2020}^{Y} \rho_{r,y} \\ &= \text{GRPpc}_{r,2020} \sum_{y=2020}^{Y} (1 + \pi_{r,y} + \delta_{r,y}),\end{aligned} \quad (13)$$

in which $\text{GRPpc}_{r,y=2020}$ is the initial log level of GRPpc. We begin damage estimates in 2020 to reflect the damages occurring since the end of the period for which we estimate the empirical models (1979–2019) and to match the timing of mitigation-cost estimates from most IAMs (see below).

For each emission scenario, this procedure is repeated 1,000 times while randomly sampling from the selection of climate models, the selection of empirical models with different numbers of lags (shown in Supplementary Figs. 1–3 and Supplementary Tables 2–4) and bootstrapped estimates of the regression parameters. The result is an ensemble of future GRPpc trajectories that reflect uncertainty from

both physical climate change and the structural and sampling uncertainty of the empirical models.

Estimates of mitigation costs

We obtain IPCC estimates of the aggregate costs of emission mitigation from the AR6 Scenario Explorer and Database hosted by IIASA[23]. Specifically, we search the AR6 Scenarios Database World v1.1 for IAMs that provided estimates of global GDP and population under both a SSP2 baseline and a SSP2-RCP2.6 scenario to maintain consistency with the socio-economic and emission scenarios of the climate damage projections. We find five IAMs that provide data for these scenarios, namely, MESSAGE-GLOBIOM 1.0, REMIND-MAgPIE 1.5, AIM/GCE 2.0, GCAM 4.2 and WITCH-GLOBIOM 3.1. Of these five IAMs, we use the results only from the first three that passed the IPCC vetting procedure for reproducing historical emission and climate trajectories. We then estimate global mitigation costs as the percentage difference in global per capita GDP between the SSP2 baseline and the SSP2-RCP2.6 emission scenario. In the case of one of these IAMs, estimates of mitigation costs begin in 2020, whereas in the case of two others, mitigation costs begin in 2010. The mitigation cost estimates before 2020 in these two IAMs are mostly negligible, and our choice to begin comparison with damage estimates in 2020 is conservative with respect to the relative weight of climate damages compared with mitigation costs for these two IAMs.

Data availability

Data on economic production and ERA-5 climate data are publicly available at https://doi.org/10.5281/zenodo.4681306 (ref. 62) and https://www.ecmwf.int/en/forecasts/datasets/reanalysis-datasets/era5, respectively. Data on mitigation costs are publicly available at https://data.ene.iiasa.ac.at/ar6/#/downloads. Processed climate and economic data, as well as all other necessary data for reproduction of the results, are available at the public repository https://doi.org/10.5281/zenodo.10562951 (ref. 63).

Code availability

All code necessary for reproduction of the results is available at the public repository https://doi.org/10.5281/zenodo.10562951 (ref. 63).

49. Hersbach, H. et al. The ERA5 global reanalysis. *Q. J. R. Meteorol. Soc.* **146**, 1999–2049 (2020).
50. Cucchi, M. et al. WFDE5: bias-adjusted ERA5 reanalysis data for impact studies. *Earth Syst. Sci. Data* **12**, 2097–2120 (2020).
51. Adler, R. et al. *The New Version 2.3 of the Global Precipitation Climatology Project (GPCP) Monthly Analysis Product* 1072–1084 (University of Maryland, 2016).
52. Lange, S. Trend-preserving bias adjustment and statistical downscaling with ISIMIP3BASD (v1.0). *Geosci. Model Dev.* **12**, 3055–3070 (2019).
53. Wenz, L., Carr, R. D., Kögel, N., Kotz, M. & Kalkuhl, M. DOSE – global data set of reported sub-national economic output. *Sci. Data* **10**, 425 (2023).
54. Gennaioli, N., La Porta, R., Lopez De Silanes, F. & Shleifer, A. Growth in regions. *J. Econ. Growth* **19**, 259–309 (2014).
55. Board of Governors of the Federal Reserve System (US). U.S. dollars to euro spot exchange rate. https://fred.stlouisfed.org/series/AEXUSEU (2022).
56. World Bank. GDP deflator. https://data.worldbank.org/indicator/NY.GDP.DEFL.ZS (2022).
57. Jones, B. & O'Neill, B. C. Spatially explicit global population scenarios consistent with the Shared Socioeconomic Pathways. *Environ. Res. Lett.* **11**, 084003 (2016).
58. Murakami, D. & Yamagata, Y. Estimation of gridded population and GDP scenarios with spatially explicit statistical downscaling. *Sustainability* **11**, 2106 (2019).
59. Koch, J. & Leimbach, M. Update of SSP GDP projections: capturing recent changes in national accounting, PPP conversion and Covid 19 impacts. *Ecol. Econ.* **206** (2023).
60. Carleton, T. A. & Hsiang, S. M. Social and economic impacts of climate. *Science* **353**, aad9837 (2016).
61. Bergé, L. Efficient estimation of maximum likelihood models with multiple fixed-effects: the R package FENmlm. DEM Discussion Paper Series 18-13 (2018).
62. Kalkuhl, M., Kotz, M. & Wenz, L. DOSE - The MCC-PIK Database Of Subnational Economic output. *Zenodo* https://zenodo.org/doi/10.5281/zenodo.4681305 (2021).
63. Kotz, M., Wenz, L. & Levermann, A. Data and code for "The economic commitment of climate change". *Zenodo* https://zenodo.org/doi/10.5281/zenodo.10562951 (2024).
64. Dasgupta, S. et al. Effects of climate change on combined labour productivity and supply: an empirical, multi-model study. *Lancet Planet. Health* **5**, e455–e465 (2021).
65. Lobell, D. B. et al. The critical role of extreme heat for maize production in the United States. *Nat. Clim. Change* **3**, 497–501 (2013).
66. Zhao, C. et al. Temperature increase reduces global yields of major crops in four independent estimates. *Proc. Natl Acad. Sci.* **114**, 9326–9331 (2017).
67. Wheeler, T. R., Craufurd, P. Q., Ellis, R. H., Porter, J. R. & Prasad, P. V. Temperature variability and the yield of annual crops. *Agric. Ecosyst. Environ.* **82**, 159–167 (2000).
68. Rowhani, P., Lobell, D. B., Linderman, M. & Ramankutty, N. Climate variability and crop production in Tanzania. *Agric. For. Meteorol.* **151**, 449–460 (2011).
69. Ceglar, A., Toreti, A., Lecerf, R., Van der Velde, M. & Dentener, F. Impact of meteorological drivers on regional inter-annual crop yield variability in France. *Agric. For. Meteorol.* **216**, 58–67 (2016).
70. Shi, L., Kloog, I., Zanobetti, A., Liu, P. & Schwartz, J. D. Impacts of temperature and its variability on mortality in New England. *Nat. Clim. Change* **5**, 988–991 (2015).
71. Xue, T., Zhu, T., Zheng, Y. & Zhang, Q. Declines in mental health associated with air pollution and temperature variability in China. *Nat. Commun.* **10**, 2165 (2019).
72. Liang, X.-Z. et al. Determining climate effects on US total agricultural productivity. *Proc. Natl Acad. Sci.* **114**, E2285–E2292 (2017).
73. Desbureaux, S. & Rodella, A.-S. Drought in the city: the economic impact of water scarcity in Latin American metropolitan areas. *World Dev.* **114**, 13–27 (2019).
74. Damania, R. The economics of water scarcity and variability. *Oxf. Rev. Econ. Policy* **36**, 24–44 (2020).
75. Davenport, F. V., Burke, M. & Diffenbaugh, N. S. Contribution of historical precipitation change to US flood damages. *Proc. Natl Acad. Sci.* **118**, e2017524118 (2021).
76. Dave, R., Subramanian, S. S. & Bhatia, U. Extreme precipitation induced concurrent events trigger prolonged disruptions in regional road networks. *Environ. Res. Lett.* **16**, 104050 (2021).

Acknowledgements We gratefully acknowledge financing from the Volkswagen Foundation and the Deutsche Gesellschaft für Internationale Zusammenarbeit (GIZ) GmbH on behalf of the Government of the Federal Republic of Germany and Federal Ministry for Economic Cooperation and Development (BMZ).

Author contributions All authors contributed to the design of the analysis. M.K. conducted the analysis and produced the figures. All authors contributed to the interpretation and presentation of the results. M.K. and L.W. wrote the manuscript.

Funding Open access funding provided by Potsdam-Institut für Klimafolgenforschung (PIK) e.V.

Competing interests The authors declare no competing interests.

Additional information

Supplementary information The online version contains supplementary material available at https://doi.org/10.1038/s41586-024-07219-0.

Correspondence and requests for materials should be addressed to Leonie Wenz.

Peer review information *Nature* thanks Xin-Zhong Liang, Chad Thackeray and the other, anonymous, reviewer(s) for their contribution to the peer review of this work. Peer reviewer reports are available.

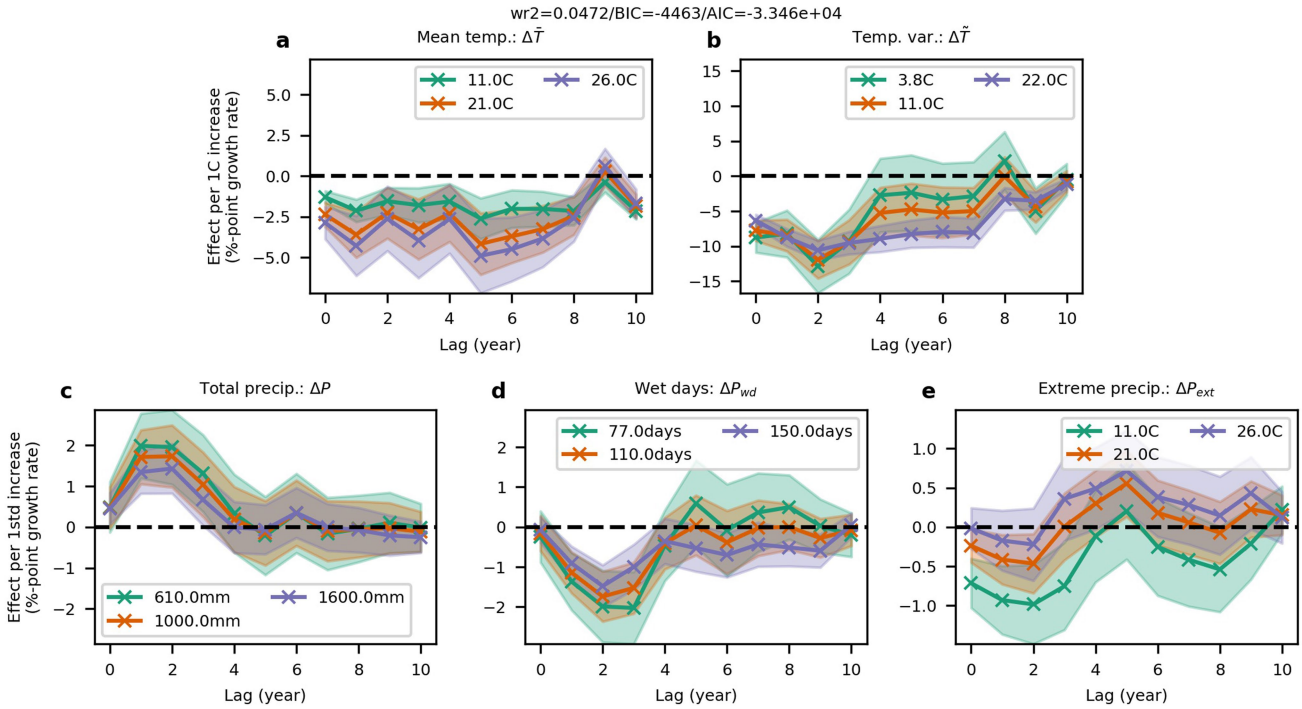

Extended Data Fig. 1 | Constraining the persistence of historical climate impacts on economic growth rates. The results of a panel-based fixed-effects distributed lag model for the effects of annual mean temperature (**a**), daily temperature variability (**b**), total annual precipitation (**c**), the number of wet days (**d**) and extreme daily precipitation (**e**) on sub-national economic growth rates. Point estimates show the effects of a 1 °C or one standard deviation increase (for temperature and precipitation variables, respectively) at the lower quartile, median and upper quartile of the relevant moderating variable (green, orange and purple, respectively) at different lagged periods after the initial shock (note that these are not cumulative effects). Climate variables are used in their first-differenced form (see main text for discussion) and the moderating climate variables are the annual mean temperature, seasonal temperature difference, total annual precipitation, number of wet days and annual mean temperature, respectively, in panels **a**–**e** (see Methods for further discussion). Error bars show the 95% confidence intervals having clustered standard errors by region. The within-region R^2, Bayesian and Akaike information criteria for the model are shown at the top of the figure. This figure shows results with ten lags for each variable to demonstrate the observed levels of persistence, but our preferred specifications remove later lags based on the statistical significance of terms shown above and the information criteria shown in Extended Data Fig. 2. The resulting models without later lags are shown in Supplementary Figs. 1–3.

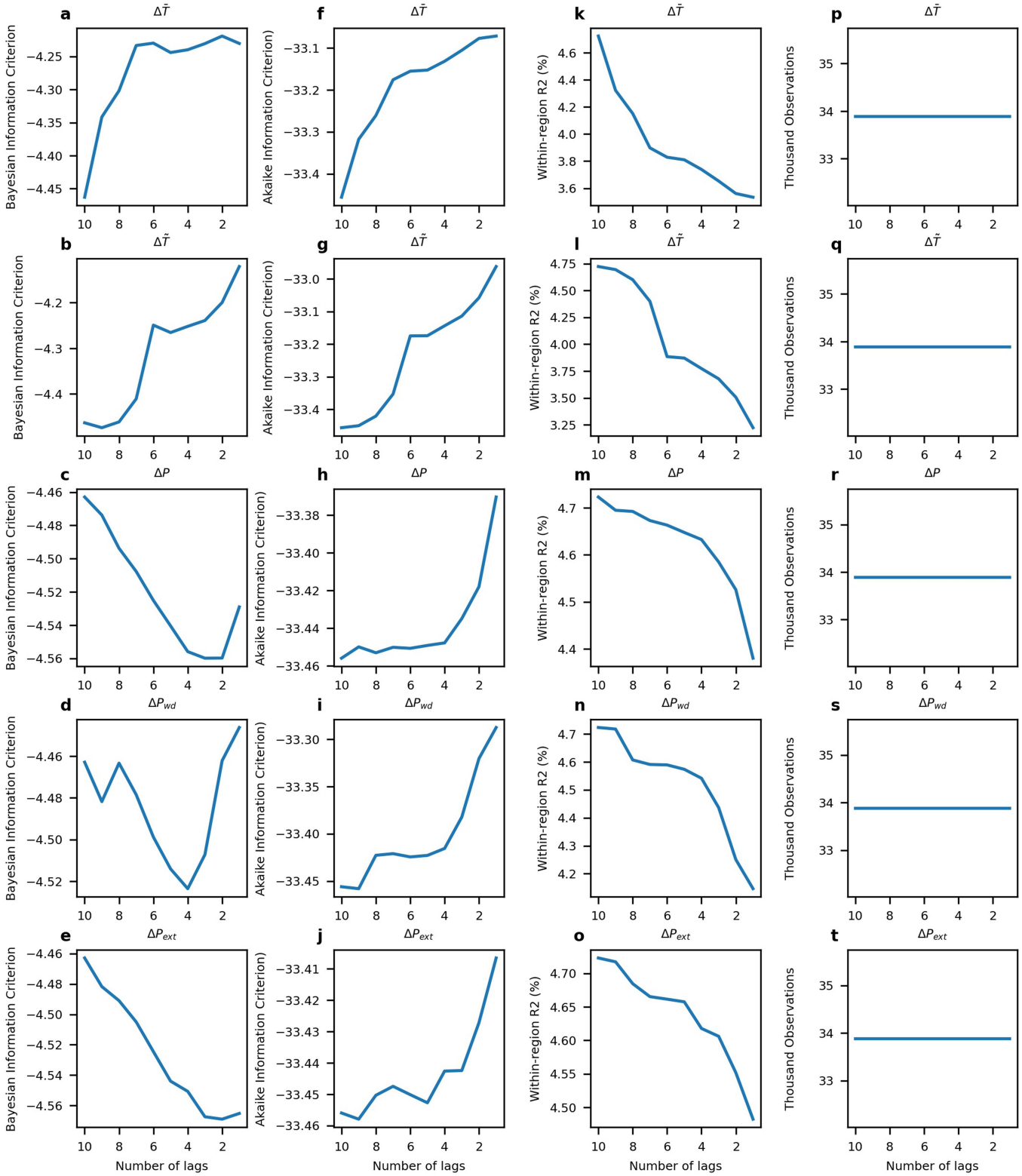

Extended Data Fig. 2 | Incremental lag-selection procedure using information criteria and within-region R^2. Starting from a panel-based fixed-effects distributed lag model estimating the effects of climate on economic growth using the real historical data (as in equation (4)) with ten lags for all climate variables (as shown in Extended Data Fig. 1), lags are incrementally removed for one climate variable at a time. The resulting Bayesian and Akaike information criteria are shown in **a**–**e** and **f**–**j**, respectively, and the within-region R^2 and number of observations in **k**–**o** and **p**–**t**, respectively. Different rows show the results when removing lags from different climate variables, ordered from top to bottom as annual mean temperature, daily temperature variability, total annual precipitation, the number of wet days and extreme annual precipitation. Information criteria show minima at approximately four lags for precipitation variables and ten to eight for temperature variables, indicating that including these numbers of lags does not lead to overfitting. See Supplementary Table 1 for an assessment using information criteria to determine whether including further climate variables causes overfitting.

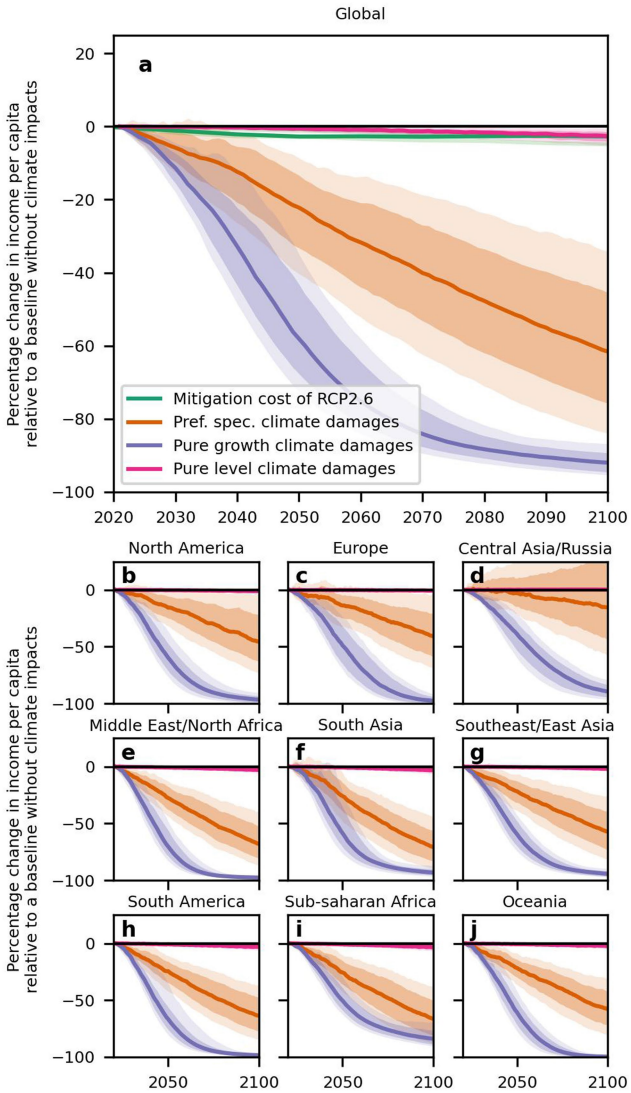

Extended Data Fig. 3 | Damages in our preferred specification that provides a robust lower bound on the persistence of climate impacts on economic growth versus damages in specifications of pure growth or pure level effects. Estimates of future damages as shown in Fig. 1 but under the emission scenario RCP8.5 for three separate empirical specifications: in orange our preferred specification, which provides an empirical lower bound on the persistence of climate impacts on economic growth rates while avoiding assumptions of infinite persistence (see main text for further discussion); in purple a specification of 'pure growth effects' in which the first difference of climate variables is not taken and no lagged climate variables are included (the baseline specification of ref. 2); and in pink a specification of 'pure level effects' in which the first difference of climate variables is taken but no lagged terms are included.

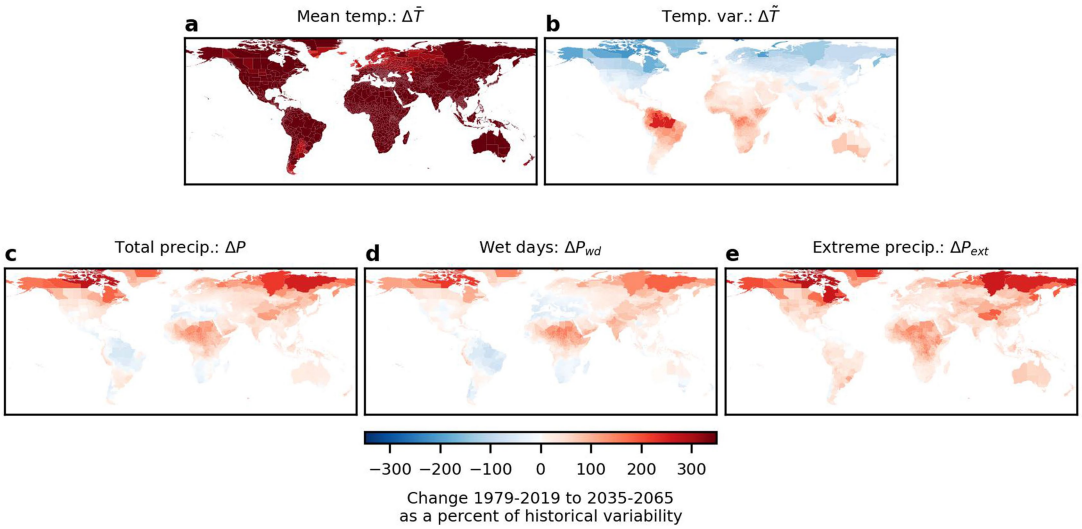

Extended Data Fig. 4 | Climate changes in different variables as a function of historical interannual variability. Changes in each climate variable of interest from 1979–2019 to 2035–2065 under the high-emission scenario SSP5-RCP8.5, expressed as a percentage of the historical variability of each measure. Historical variability is estimated as the standard deviation of each detrended climate variable over the period 1979–2019 during which the empirical models were identified (detrending is appropriate because of the inclusion of region-specific linear time trends in the empirical models). See Supplementary Fig. 13 for changes expressed in standard units. Data on national administrative boundaries are obtained from the GADM database version 3.6 and are freely available for academic use (https://gadm.org/).

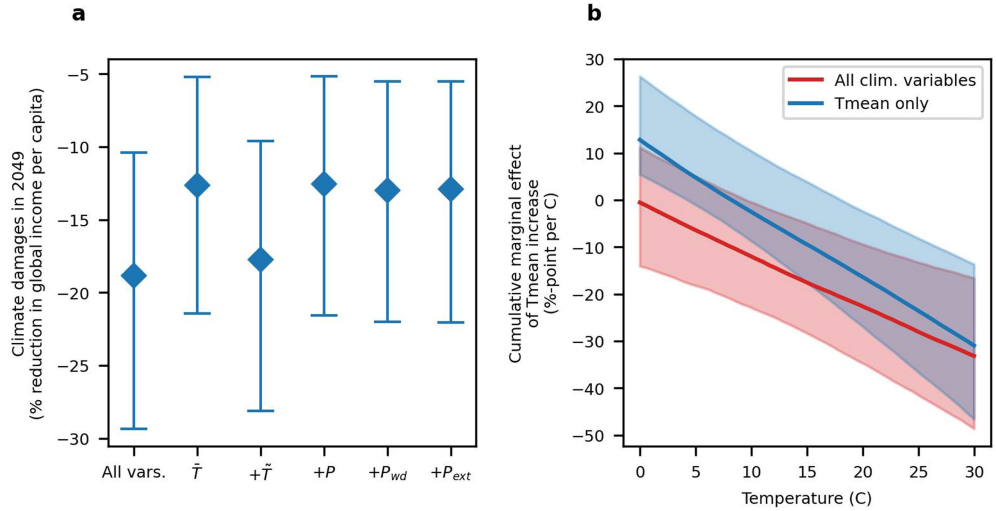

Extended Data Fig. 5 | Contribution of different climate variables to overall committed damages. a, Climate damages in 2049 when using empirical models that account for all climate variables, changes in annual mean temperature only or changes in both annual mean temperature and one other climate variable (daily temperature variability, total annual precipitation, the number of wet days and extreme daily precipitation, respectively). **b**, The cumulative marginal effects of an increase in annual mean temperature of 1 °C, at different baseline temperatures, estimated from empirical models including all climate variables or annual mean temperature only. Estimates and uncertainty bars represent the median and 95% confidence intervals obtained from 1,000 block-bootstrap resamples from each of three different empirical models using eight, nine or ten lags of temperature terms.

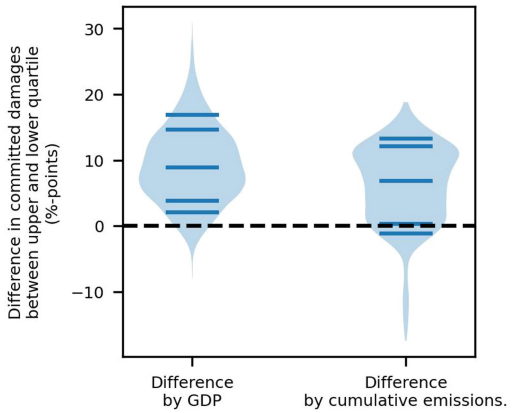

Extended Data Fig. 6 | The difference in committed damages between the upper and lower quartiles of countries when ranked by GDP and cumulative historical emissions. Quartiles are defined using a population weighting, as are the average committed damages across each quartile group. The violin plots indicate the distribution of differences between quartiles across the two extreme emission scenarios (RCP2.6 and RCP8.5) and the uncertainty sampling procedure outlined in Methods, which accounts for uncertainty arising from the choice of lags in the empirical models, uncertainty in the empirical model parameter estimates, as well as the climate model projections. Bars indicate the median, as well as the 10th and 90th percentiles and upper and lower sixths of the distribution reflecting the very likely and likely ranges following the likelihood classification adopted by the IPCC.

Extended Data Table 1 | A summary of several physical mechanisms that plausibly underlie the impact of the different climate variables on macroeconomic growth, with references to empirical evidence

Climate variable	Physical mechanisms	References
Average annual temperature	Labour productivity and supply; agricultural productivity	Dasgupta et al. (2021)[62];Lobell et al. (2013)[63], Zhao et al. (2017)[64]
Daily temperature variability	Agricultural productivity; physical health; mental health	Wheeler et al. (2000)[65], Rowhani et al. (2011)[66], Ceglar et al. (2016)[67]; Shi et al. (2015)[68]; Xue et al. (2019)[69]
Total annual precipitation	Agricultural productivity; metropolitan labour outcomes; conflict	Liang et al. (2017)[70]; Desbreaux et al. (2019)[71]; Damania et al. (2020)[72]
Number of wet days	Travel disruption	Lacking
Extreme daily precipitation	Flood damages; disruption	Davenport et al. (2021)[73], Dave et al. (2021)[74]

This summary is not intended to be an exhaustive list of all mechanisms or references. In the case of most climate variables, several plausible physical mechanisms supported by empirical evidence exist. The only exception here is the number of wet days, for which plausible mechanisms are listed but empirical evidence does not yet exist (as far as the authors are aware). The use of the number of wet days in the main empirical models is therefore guided primarily by the empirical evidence indicating robust impacts on economic growth[8]. References 64–76 in the table.

Extended Data Table 2 | Regression results for the historical effects of different climate variables on sub-national economic growth rates in the period 1979–2019

Variable	Formula	Lag 0	Lag 1	Lag 2	Lag 3	Lag 4	Lag 5	Lag 6	Lag 7	Lag 8	Lag 9	Lag 10
Annual mean temperature	$\Delta \bar{T}_{r,y}$	-0.17	-0.57	-0.78	-0.23	-0.79	-0.96	-0.23	-0.71	-1.8**	-1.1*	-2.5***
		(0.32)	(0.5)	(0.54)	(0.57)	(0.57)	(0.65)	(0.67)	(0.73)	(0.63)	(0.48)	(0.35)
	$\Delta \bar{T}_{r,y}.\bar{T}_r$	-0.0011***	-0.0014**	-0.00072	-0.0015**	-0.00072	-0.0015**	-0.0017***	-0.0012**	-0.00029	0.00065*	0.00029
		(0.00029)	(0.00049)	(0.00051)	(0.00055)	(0.00047)	(0.0005)	(0.00046)	(0.00047)	(0.0004)	(0.00032)	(0.00023)
Daily temp. variability	$\Delta \tilde{T}_{r,y}$	-9.3***	-8.1***	-13***	-9.3***	-1.5	-1.2	-2.4	-1.8	3.3	-5.3**	-0.34
		(1.3)	(2)	(2.3)	(2.7)	(3.1)	(3.2)	(3)	(2.9)	(2.5)	(1.9)	(1.3)
	$\Delta \tilde{T}_{r,y}.\hat{T}_r$	0.0013*	-0.0003	0.0013	-0.00011	-0.0034**	-0.0032*	-0.0025*	-0.0029*	-0.003**	0.00079	-0.00037
		(0.00054)	(0.00083)	(0.00087)	(0.0011)	(0.0012)	(0.0013)	(0.0012)	(0.0012)	(0.0011)	(0.00078)	(0.00057)
Total annual precipitation	$\Delta P_{r,y}$	0.002	0.0094***	0.009***	0.0068**	0.0021	-0.0012	0.0013	-0.001	-0.0001	0.0012	0.0005
		(0.0016)	(0.002)	(0.0023)	(0.0024)	(0.0024)	(0.0025)	(0.0025)	(0.0023)	(0.0021)	(0.0019)	(0.0015)
	$\Delta P_{r,y}.P_r$	-1.4e-09	-2.6e-08**	-2.1e-08*	-2.6e-08**	-1.4e-08	6.3e-09	4.6e-10	6.4e-09	-1.2e-09	-1.3e-08	-9.4e-09
		(6.9e-09)	(8.5e-09)	(9.7e-09)	(9.8e-09)	(1e-08)	(1e-08)	(1e-08)	(9.3e-09)	(8.6e-09)	(7.8e-09)	(6.1e-09)
Annual no. wet days	$\Delta Pwd_{r,y}$	-0.028	-0.12**	-0.17**	-0.2***	-0.038	0.12	0.037	0.079	0.1*	0.045	-0.03
		(0.038)	(0.043)	(0.055)	(0.055)	(0.052)	(0.065)	(0.068)	(0.058)	(0.048)	(0.04)	(0.032)
	$\Delta Pwd_{r,y}.Pwd_r$	1.5e-06	4.1e-06	4.5e-06	9.2e-06*	9.6e-07	-1e-05*	-5.5e-06	-7.1e-06	-9e-06**	-5.6e-06*	2.2e-06
		(2.3e-06)	(2.7e-06)	(3.6e-06)	(3.6e-06)	(3.4e-06)	(4.1e-06)	(4.1e-06)	(3.6e-06)	(3e-06)	(2.5e-06)	(1.9e-06)
Precipitation extremes	$\Delta Pext_{r,y}$	-0.023***	-0.028***	-0.029***	-0.029**	-0.01	-0.0032	-0.013	-0.017	-0.019*	-0.013	0.0054
		(0.0053)	(0.0073)	(0.0084)	(0.0094)	(0.0098)	(0.01)	(0.011)	(0.01)	(0.0093)	(0.0079)	(0.0052)
	$\Delta Pext_{r,y}.\bar{T}_r$	8.8e-06***	9.6e-06**	9.6e-06*	1.4e-05**	7.7e-06	6.5e-06	8e-06	8.8e-06	8.7e-06	8.1e-06*	-1.2e-06
		(2.5e-06)	(3.4e-06)	(4e-06)	(4.6e-06)	(4.7e-06)	(4.9e-06)	(4.9e-06)	(4.8e-06)	(4.5e-06)	(4e-06)	(2.7e-06)
R^2	0.291											
wR^2	0.0472											
BIC	-4.46e+03											
AIC	-3.35e+04											
N	34855											

Numbers show the point estimates for the effect of each climate variable and their interaction term on sub-national economic growth rates (in percentage points), having estimated equation (4) with ten lags for each climate variable (that is, each table entry denotes a specific regression coefficient $\alpha_{x,L}$ of the same model as indicated in equation (4)). Standard errors are shown in parentheses and *, ** and *** denote significance at the 5%, 1% and 0.1% levels, respectively, having clustered standard errors by region. Formulas for climate variables and their interaction terms are denoted as in equation (4). Note that an interpretation of the significance of the effects of a given climate variable requires an assessment of both the coefficient of the climate variable itself as well as its interaction term. Extended Data Fig. 1 provides the opportunity for such an interpretation by plotting the estimated marginal effects with confidence intervals. The R^2, within-region R^2 (the R^2 along the temporal dimension), Akaike information criterion (AIC), Bayesian information criterion (BIC) and number of observations are also shown.

Extended Data Table 3 | A comparison of the magnitude of estimated economic damage from future climate change across recent panel-based empirical studies

Study	Resolution	Number of climate variables	Baseline specification of growth- or level-effects	Number of lags	Damages by 2100 under RCP8.5
Burke et al. (2015)[2]	National	One	Growth	None	25%
Kahn et al. (2019)[35]	National	One	Level	Four	7.2%
Kalkuhl & Wenz (2020)[3]	Sub-national	One	Level	One	14.2%
This study	Sub-national	Five	Level	Eight-ten/four	61.6%

All studies use fixed-effects panel regressions. The first four columns describe differences in the underlying data and empirical specification. The third column shows the nature of the baseline specification without lags with regards to growth or level effects (see main text for further discussion). The last column compares projections of future economic damage under RCP8.5 by 2100 as reported by the respective study.

NBER WORKING PAPER SERIES

MORTALITY BURDEN FROM WILDFIRE SMOKE UNDER CLIMATE CHANGE

Minghao Qiu
Jessica Li
Carlos F. Gould
Renzhi Jing
Makoto Kelp
Marissa Childs
Mathew Kiang
Sam Heft-Neal
Noah Diffenbaugh
Marshall Burke

Working Paper 32307
http://www.nber.org/papers/w32307

NATIONAL BUREAU OF ECONOMIC RESEARCH
1050 Massachusetts Avenue
Cambridge, MA 02138
April 2024

We thank members of Stanford ECHOLab and Center on Food Security and the Environment, and seminar participants at Brookhaven National Lab and Harvard for helpful comments. MQ acknowledges the support from the planetary health fellowship at Stanford's Center for Innovation in Global Health. MLC was supported by an Environmental Fellowship at the Harvard University Center for the Environment. We also thank the Keck Foundation for support. Some of the computing for this project was performed on the Stanford Sherlock cluster, and we thank Stanford University and the Stanford Research Computing Center for providing these resources. The views expressed herein are those of the authors and do not necessarily reflect the views of the National Bureau of Economic Research.

Mortality Burden From Wildfire Smoke Under Climate Change
Minghao Qiu, Jessica Li, Carlos F. Gould, Renzhi Jing, Makoto Kelp, Marissa Childs, Mathew Kiang, Sam Heft-Neal, Noah Diffenbaugh, and Marshall Burke
NBER Working Paper No. 32307
April 2024
JEL No. Q51,Q53,Q54

ABSTRACT

Wildfire activity has increased in the US and is projected to accelerate under future climate change. However, our understanding of the impacts of climate change on wildfire smoke and health remains highly uncertain. We quantify the past and future mortality burden in the US due to wildfire smoke fine particulate matter (PM2.5). We construct an ensemble of statistical and machine learning models that link variation in climate to wildfire smoke PM2.5, and empirically estimate smoke PM2.5-mortality relationships using georeferenced data on all recorded deaths in the US from 2006 to 2019. We project that climate-driven increases in future smoke PM2.5 could result in 27,800 excess deaths per year by 2050 under a high warming scenario, a 76% increase relative to estimated 2011-2020 averages. Cumulative excess deaths from wildfire smoke PM2.5 could exceed 700,000 between 2025-2055. When monetized, climate-induced smoke deaths result in annual damages of $244 billion by mid-century, comparable to the estimated sum of all other damages in the US in prior analyses. Our research suggests that the health cost of climate-driven wildfire smoke could be among the most important and costly consequences of a warming climate in the US.

Minghao Qiu
Stanford University
mhqiu@stanford.edu

Jessica Li
Department of Economics
University of California, San Diego
9500 Gilman Dr. #0508
Mail Code: 0508
La Jolla, CA 92093
jel142@ucsd.edu

Carlos F. Gould
9515 Gilman Drive
School of Public Health University
of California San Diego La Jolla,
CA 92093
cagould@ucsd.edu

Renzhi Jing
Stanford University
jingrenzhi.go@gmail.com

Makoto Kelp
Stanford University
mkelp@stanford.edu

Marissa Childs
Center for the Environment
Harvard University
mchilds@fas.harvard.edu

Mathew Kiang
Stanford University
mkiang@stanford.edu

Sam Heft-Neal
Center on Food Security and the Environment
Stanford University
473 Via Ortega
Stanford, CA 94305
sheftneal@stanford.edu

Noah Diffenbaugh
Stanford University
diffenbaugh@stanford.edu

Marshall Burke
Doerr School of Sustainability
Stanford University
Stanford, CA 94305
and NBER
mburke@stanford.edu

1 Introduction

Wildfire activity has increased substantially over the US in the last two decades, with the largest increases observed in the western US (*1–5*). As a result, air pollution that is associated with wildfire smoke (specifically fine particulate matter, $PM_{2.5}$) has significantly increased (*6–9*). Given established relationships between ambient smoke $PM_{2.5}$ exposure and poor health (*10–13*), these increases have likely worsened several health outcomes. In many parts of the western US, smoke $PM_{2.5}$ accounted for over 50% of the annual concentration of $PM_{2.5}$ in extreme smoke years (*14*, *15*), and has led to stagnation or even reversal of the substantial improvements in ambient $PM_{2.5}$ concentrations over the last two decades – improvements brought about substantially by the Clean Air Act and its amendments (*16–18*). Importantly, and unlike most other sources of air pollutants, wildfire smoke is currently unregulated under the Clean Air Act, and thus quantifying drivers of past and future wildfire activity and smoke is central to understanding how this growing source of pollution will change in coming decades, how health might be impacted, and whether policy should respond.

Mounting evidence has suggested that human-induced climate change is a leading cause for the increased wildfire activity, especially in forested areas in the western US (*2–4*, *19–21*), alongside other important causes that include historical fire suppression and the expansion of human activities into forested areas (*22*). A warming climate can influence wildfire activities by altering the aridity of the fuel (*2*, *23*), conditions for fire spread (*24*, *25*), as well as lightning ignitions (*26*). For the western US, many studies have projected increasing wildfire risks under a warming climate primarily due to increasing fuel aridity under higher ambient temperature (*27–29*).

However, the relationship between a warming climate and the resulting increase in wildfire smoke and health impacts remains poorly quantified, and as a result, leading estimates of climate impacts in the US and globally do not consider health impacts from wildfire smoke (*30–32*). Several studies use regression models or land-vegetation-fire models to first project the wildfire activities under future climate and then utilize chemical transport models to estimate changes in smoke $PM_{2.5}$ concentrations (*33–37*) and associated health outcomes (*38–41*). However, prior projections of future mortality due to climate-driven fire smoke span a very wide range (*42*) – reflecting an important knowledge gap given the large potential impacts. Uncertainties in the prior projections come from three key sources. First, large uncertainties exist in how wildfire emissions respond to climate change (*43*). Second, modeling fire impacts on surface $PM_{2.5}$ often faces large uncer-

tainty in emission inventories (*44*, *45*), the vertical distribution of emission profiles (*46*), and fire-weather interactions (*47*), which results in modeled smoke concentrations that sometimes differ by an order of magnitude when compared to surface observations (*48*). Third, most prior studies quantify the health impacts of smoke $PM_{2.5}$ by applying existing concentration-response functions derived from total $PM_{2.5}$ exposures, which could fail to capture unique health impacts of smoke $PM_{2.5}$ exposure, such as from smoke-specific chemical composition and toxicity (*49*) or behavioral responses unique to smoke events (*13*).

Because of these challenges, very few studies to date have projected future smoke $PM_{2.5}$ concentrations using empirically grounded relationships between climate, wildfire, and $PM_{2.5}$ (*40*, *50*). To our knowledge, no studies have estimated the future smoke mortality burden accounting for the unique health impacts of smoke $PM_{2.5}$ using dose-response functions that are specific to smoke pollution exposure. Absent this quantification, leading estimates of the societal impact of climate change – many of which are directly used to guide policy – do not incorporate potential mortality impacts due to wildfire smoke $PM_{2.5}$ (*31*, *32*, *51*). Detailed projections of future smoke $PM_{2.5}$ exposure and health burden are crucial to inform policies to mitigate and adapt to the negative impacts of smoke $PM_{2.5}$ on humans.

In this paper, we develop a comprehensive, data-driven approach that directly address all three of the above challenges. First, to improve understanding of the climate-fire emissions relationship, we construct an ensemble of statistical and machine learning models that predict fire emissions as a function of climate and land-use variables over North America (including Mexico and Canada), using observational data from 2001-2021. By using historical data that includes recent years with extreme weather conditions (e.g., drought in the western US in 2020), which is projected to increase under future climate change, our ensemble of models can better characterize how climate influences wildfire emissions in future scenarios. By modeling changes in wildfire emissions in Canada and Mexico, our approach can also capture important transboundary influences on US smoke $PM_{2.5}$ and health effects, such as those that occurred in the summer of 2023 (*52*).

Second, we use surface wildfire smoke $PM_{2.5}$ estimates from (*8*) to establish an empirical relationship between wildfire emissions and smoke $PM_{2.5}$ concentration across the contiguous US at 10 km resolution, accounting for variation in wind directions and spatial transport. Our approach fits the observed surface $PM_{2.5}$ data well and allows us to efficiently predict smoke concentration in one location from changes in wildfire emissions in another

(Methods). Third, to address the challenge of accurately estimating the health impacts of ambient smoke exposure, we empirically estimate the effects of annual smoke $PM_{2.5}$ concentration on annual mortality rates using county-level data from 2006 to 2019 on all recorded deaths in the US. We estimate dose-response functions using a Poisson model in which mortality rates are allowed to respond non-linearly to variation in smoke $PM_{2.5}$, consistent with prior papers that suggest responses could be non-linear (*13*, *53*), while flexibly controlling for temperature, precipitation, and a broad range of possible spatial and temporal confounds (Methods).

Finally, we combine the empirical relationships between climate, wildfire emissions, smoke $PM_{2.5}$, and mortality rates derived above with projected climate variables derived from CMIP6 global climate model ensembles to generate future projections of smoke $PM_{2.5}$ and mortality burden. We project the annual average smoke $PM_{2.5}$ concentration in each 10 km location across the contiguous US (48 states and the District of Columbia) between 2046 and 2055 under different climate scenarios. We then quantify changes in mortality rates in each county in the contiguous US between 2050 and the historical period, and the difference across three future emissions scenarios representing ambitious emissions reductions, moderate emissions, and a high-emissions scenario (SSP1-2.6, SSP2-4.5, and SSP3-7.0) to quantify the potential health benefits from climate mitigation and adaptation. We value future excess deaths using standard VSL-based methods and quantify the uncertainty in the final projected mortality burden across the different components of our modeling framework. Finally, we compare our mortality estimates with estimates of direct temperature-related mortality burden and aggregate climate costs from prior work (*51*, *54*, *55*) to contextualize the importance of climate-smoke channels relative to other known climate impacts.

We report four main findings. First, using an ensemble of statistical and machine learning models, we find that wildfire smoke is likely to substantially increase under future climate change, with average exposure across the US population increasing 2-3 fold in 2050 relative to 2011-2020. This large increase is a result of the tight coupling between fuel aridity and wildfire activity, and the large projected changes in fuel aridity under a warming climate. Second, using historical data, we show that increases in annual exposure to smoke $PM_{2.5}$ are associated with higher county-level annual mortality rates across the contiguous US, with increases detectable at even very low levels of wildfire smoke exposure. Our findings are consistent with a host of recent work suggesting that there is no safe level of air pollution exposure (e.g. (*56*)). Third, using our empirically-derived dose response functions, we estimate that smoke $PM_{2.5}$ will cause 23,800 to 27,800 annual

excess deaths by mid-century across the three climate scenarios – an increase of 51-76% relative to 2011-2020 estimates. Even under a low warming scenario (SSP1-2.6), we estimate that climate-induced smoke $PM_{2.5}$ will lead to 8,000 more annual excess deaths in the US than were observed in the last decade, suggesting that even aggressive mitigation will not substantially limit this source of climate damages through mid-century. Fourth, when monetized, climate-induced smoke deaths result in annual damages of $244 billion by mid-century, comparable to prior *aggregate* estimates of all other economic damage due to climate change in the US (*51*, *55*). We also estimate that increasing deaths from smoke offset about two-thirds of one of the largest (and frequently under-recognized) benefits of climate change in the US: the substantial decline in cold-related deaths that is expected in the US in coming decades (*54*). Our research suggests that the health cost of climate-driven wildfire smoke could be among the most important and costly consequences of a warming climate in the US.

2 Data and empirical approach

2.1 Wildfire and smoke $PM_{2.5}$ datasets

We use annual fire emissions from the fourth version of the Global Fire Emissions Database with small fires (GFED4s) from 2001-2021 (*57*). The native spatial resolution of GFED4s is 0.25×0.25 degrees. We use the estimated dry matter (DM) emissions as our primary variable for the emissions. DM emissions capture the amount of biomass being consumed in the burning process. We choose DM emissions as the proxy for overall fire emissions (rather than individual emissions species such as black carbon or NO_x) due to uncertainty in the emission factors used in GFED4s. GFED4s include fire emissions from agriculture fires and land-use change as well. However, as wildland fire emissions dominate in most study regions (especially in western US and Canada where we see the largest effects), we refer to our estimates as "wildfire emissions" and "wildfire smoke" for simplicity and consistency (Table S1).

For smoke $PM_{2.5}$, we use gridded daily wildfire smoke $PM_{2.5}$ predictions for the contiguous US at 10 km resolution from January 1, 2006 to December 31, 2020 derived from (*8*). This dataset specifically estimates the ambient $PM_{2.5}$ concentration due to wildfire smoke influence by constructing a machine learning model that uses smoke plume data, remotely-sensed variables, and meteorological variables to predict the anomalous increases in surface $PM_{2.5}$ measured by surface air quality monitors during wildfire. To estimate contributions of smoke $PM_{2.5}$ to total $PM_{2.5}$, we use the total $PM_{2.5}$ estimates from (*58*), which com-

bines satellite retrievals of aerosol optical depth, chemical transport modeling, and ground-based measurements to estimate monthly total ambient $PM_{2.5}$ concentrations.

2.2 Climate and meteorological datasets

We use climate and land use variables to predict wildfire DM emissions. The climate variables include 2m air temperature, precipitation, relative humidity, soil moisture (of the top soil layer), vapor pressure deficit (VPD), wind speed (at 10m level), and runoff (sum of surface and subsurface). We include these climate variables because they are available in both the historical data and the climate projections from CMIP6 climate model ensembles. Our models do not include other potentially important variables such as fire weather index and fuel moisture (as used in (*59*)) because they are unavailable in future projections. These climate variables are derived from the North American Regional Reanalysis (NARR) (*60*), with the exception of soil moisture. Soil moisture is derived from the VIC land-surface model of phase 2 of the North American Land Data Assimilation System (NLDAS-2) (*61*) and only available in the contiguous US. The native spatial resolution is 32 km for NARR variables and 0.125 degree for NLDAS-2 variables. Land use variables are derived from the North American Land Change Monitoring System (NALCMS) for the year 2015 (*62*). More specifically, we use three land use variables which each represents the percentage of area in three categories: cropland, forest, and grassland. The native resolution of land use variables is 30m. Because high-resolution projections of future land use change are not available, the land use variables are held constant across time in both the historical and future periods.

For future climate change scenarios, we use the projected climate variables from the Coupled Model Intercomparison Project Phase 6 (CMIP6). We examine three primary climate-forcing scenarios featured by the IPCC, which are constructed as pairs between the Shared Socio-economic Pathways (SSPs) and the Representative Concentration Pathways (RCPs) (*63*). We use SSP1-2.6 (which the IPCC refers to as the "Low" scenario), SSP2-4.5 (which the IPCC refers to as the "Intermediate" scenario), and SSP3-7.0 (which the IPCC refers to as the "High" scenario). We use projections from 28 global climate models that include the selected variables that cover the study region (Table S6). Following practice of IPCC, we select only one ensemble realization for each model – we use the first ensemble variant of each model ("r1i1p1f1") when possible.

When modeling the relationship between wildfire emissions and smoke $PM_{2.5}$, we also include meteorological variables in the regression model. The daily gridded meteorological

variables are derived from gridMET (*64*). In our main specification, we aggregate the meteorological variable to the monthly and smoke grid cell level. We include the splines of daily surface temperature, precipitation, dewpoint temperature, boundary layer height, air pressure, 10m wind direction (U and V components) and wind speed.

2.3 Predicting wildfire emissions

We construct an ensemble of statistical and machine learning models to predict wildfire emissions using climate and land use variables. Our models predict the annual dry matter (DM) emissions derived from GFED4s emission inventory using climate and land-use variables from 2001 to 2021. We build separate models for each of the five regions (western US, southeastern US, northeastern US, Canada-Alaska, and Mexico) to capture the regionally heterogeneous relationships between climate, land type and wildfire emissions. For each region, we construct six different models as potential model candidates: linear regression model, linear regression model with log outcomes, Least Absolute Shrinkage and Selection Operator (LASSO) models, LASSO models with log outcomes, 2-layer Neural Network (NN) model, and NN models with log outcomes. These six algorithms are selected to cover a possible range of model candidates with varying desired characteristics – including simple models that are commonly used in prior studies (e.g., the linear and log-linear regression models), models that are easy to interpret (e.g., the linear regression and LASSO models), and more flexible machine learning models that are used in prior studies (e.g., the NN model).

One key challenge for this prediction problem is that the fire occurrence, spread, and resulting emissions at local scales are often fairly stochastic due to varying and hard-to-predict non-climate factors, including where and when human and natural ignitions occur and how much suppression effort is applied. Therefore, to better capture the predictable components of the climate-wildfire relationship, we create models to predict annual emissions aggregated at different spatial scales for each of the six model types mentioned above. We aggregate the outcome variables and model features at four spatial scales: the grid scale (0.25 deg, 26956 cells in total), the North America Level-3 Ecoregion scale (177 regions in total), the North America Level-2 Ecoregion scale (51 regions in total), and the regional scale (5 regions in total). We then select the spatial resolution that optimizes model performance for each model type (as described below), allowing the optimal spatial resolution to differ across different model types and regions (see Figure S3 for model performances across spatial scales).

To evaluate the model performance, we use nested leave-one-out cross-validations (LOOCV) at the temporal scale. We divide our data into 21 temporal folds, each including one year of data. For each holdout fold, we train the model using the remaining 20 folds of data with hyper-parameters selected using an inner-loop 5-fold CV within the training data. We then obtain out-of-sample predictions for the holdout fold and repeat this process to obtain out-of-sample predictions for the entire time period. As we focus on projecting the future wildfire emissions over a 10-year period (i.e. decadal averages) under future climate scenarios, we thus evaluate the performance of our models on similar 10-year intervals. We compute the moving averages of predicted and observed emissions over 10-year moving windows. We compute two metrics and use them as the basis for evaluating the performance of each model: 1) the root mean square error between predictions and observations, and 2) the prediction biases of the highest-emitting 10-year period. The first metric allows us to assess the model performance across years with different climate conditions to detect differences between current and future climate for different climate scenarios. The second metric allows us to assess the model performance under the extreme smoke conditions which are more likely to occur under future climate. To obtain the final model that can be used for future projections, we create an "ensemble model" which combines the predictions from the selected base models with the corresponding optimal spatial resolution. The selected models and their performances can be found in Table S2.

2.4 Quantifying fire impacts on smoke $PM_{2.5}$

To estimate smoke $PM_{2.5}$ concentrations associated with future wildfire emissions, we design a statistical approach to establish an empirical relationship between ambient smoke $PM_{2.5}$ from (*8*) and wildfire emissions derived from GFED4s. We estimate the relationship between wildfire emissions and smoke $PM_{2.5}$ concentration across the contiguous US (48 states and the District of Columbia) at 10 km resolution, accounting for variation in wind directions and atmospheric transport. This approach allows us to efficiently predict smoke concentration in one location from changes in wildfire emissions in another. Despite using estimated DM emissions from GFED4s as an input, our estimates of smoke $PM_{2.5}$ concentrations strongly predict the variations in the empirical estimates of surface smoke $PM_{2.5}$ concentrations, and are thus directly constrained by surface $PM_{2.5}$ measurement during wildfire episodes.

Specifically, we use the following regression equation to empirically quantify the impacts of

the wildfire DM emissions on smoke $PM_{2.5}$ in the US in our historical data:

$$Smoke_{iym} = \sum_{d,w} \beta_{dw} \Delta Emis_{dw,iym} + \gamma \boldsymbol{W_{iym}} + \eta y + \psi_m + \theta_i + \epsilon_{iym} \quad (1)$$

where $Smoke_{iym}$ denotes the smoke $PM_{2.5}$ at grid cell i (resolution: 10 km), year y and month-of-year m. $Emis_{dw,iym}$ denotes the wildfire DM emissions that in the distance bin d and wind direction w ($w \in \{upwind, other, downwind\}$) of the smoke location i on month-of-year m and year y. In our main specification, we estimate the impacts of wildfire DM emissions at different distances from the smoke location: *<50 km, 50-100 km, 100-200 km, 200-350 km, 350-500 km, 500-750 km, 750-1000 km, 1000-1500 km, 1500-2000 km, >2000 km.* $\boldsymbol{W_{iym}}$ are the meteorological variables at the grid cell i (as described in the dataset section). We include these meteorological variables to capture potential meteorological variability that could influence ambient $PM_{2.5}$ concentrations. Our main specification includes linear year trend (ηy) and month-of-year fixed effects (ψ_m) to capture the long-term trend and seasonality of smoke $PM_{2.5}$ concentration, and grid cell-level fixed effects (θ_i) to control for the time-invariant unobserved factors at the grid cell location. ϵ_{iym} represents the error term.

To better capture the atmospheric transport of smoke $PM_{2.5}$, we divide the wildfire emissions (from a given distance bin) into three categories depending on wind direction and the location of fire. Following methods in (*65*), wildfire emissions are classified into "upwind" or "downwind", depending on whether the wildfire location is at the upwind or downwind direction of the smoke grid cell. We combine daily emissions with daily wind direction (10m wind) to calculate the daily emission from each wind direction and further aggregate to the monthly level.

Many previous studies have demonstrated that wildfire emission factors (e.g., mass of organic carbon particles emitted from burning one kg fuel) strongly depend on the combustion conditions (e.g., the combustion completeness) and the underlying fuel type among many other factors (*66–69*). As many of these characteristics (e.g., the combustion efficiency of different fires) are not available at the national scale, we use a data-driven approach and estimate different models/equations for the nine US climate regions determined by National Centers for Environmental Information (see Figure 2 for region definitions), which allows the relationship between emissions and surface smoke $PM_{2.5}$ to differ by region. The resulting regional estimates therefore implicitly account for some heterogeneity in the vegetation fuel types, fire intensities (as characterized in historical fires), and topographies for different locations. For example, prior studies have shown that smol-

dering fires often have higher $PM_{2.5}$ emission factors compared to flaming fires due to incomplete combustion (*68*), which might partly explain the relatively high emissions factors in the Southeast as smoldering fires are more common there due to high humidity (*70*).

2.5 Projecting wildfire emissions and smoke $PM_{2.5}$ under future climate

We combine our ensemble of statistical and machine learning models with climate projections from ensembles of global climate models to project the wildfire emissions and smoke $PM_{2.5}$ under future climate scenarios. Consistent with the optimal spatial resolutions selected for each region, we predict the annual wildfire DM emissions at different spatial resolutions, from 2001-2055. We then statistically downscale the predicted regional emissions to the native grid cell level (0.25 degree) by distributing predicted DM emissions using average historical spatial distribution of emissions at the grid cell level (2001-2021).

We combine the downscaled predicted DM emissions at GFED4s grid cell level (0.25 degree) with the empirical relationship we established between smoke $PM_{2.5}$ and GFED4s DM emissions to calculate predicted smoke $PM_{2.5}$ in each smoke grid cell (resolution of 10 km). When calculating the smoke $PM_{2.5}$ in future scenarios, the wind direction and meteorological conditions are held constant at the average conditions in the historical period. We further calculate the difference between the estimated smoke in any future year and the average *estimated* smoke between 2011-2020. The delta difference is then added to the average *observed* smoke $PM_{2.5}$ concentration between 2011-2020 to obtain the final smoke predictions for each grid cell in the future years.

2.6 Impacts of smoke $PM_{2.5}$ on mortality

We calculate all-cause mortality associated with wildfire smoke exposure historically and under future climate scenarios using a dose-response function empirically derived from 2006-2019 county-level data. We combine county-level population-weighted annual smoke $PM_{2.5}$, derived from (*8*), with county-level all-cause mortality rates by different age groups. We obtain individual-level multiple cause of death mortality data from the National Center for Health Statistics to calculate age-standardized mortality rates for all ages, those under 65 years of age, and those 65 years and older (*71*). County-level mortality rates were age-standardized using the direct method and 5-year bins (0-4, 5-9, ..., 85 and over) based on the 2000 US Census Standard Population. Monthly mortality rates were standardized per 100,000 population. To fully capture damages from ambient wildfire smoke

concentrations, our preferred outcome is age-standardized, all-cause, all-age mortality rates at the county-year level. We also separately estimate impacts among those 65 years and older and those under 65 years of age (Figure S6).

In our main analysis, we estimate a Poisson model in which we allow non-linear impacts of annual smoke $PM_{2.5}$ on mortality rates at the county-year level:

$$D_{csy} = \exp\left(\sum_i \beta_i smokeBIN^i_{csy} + \gamma W_{csy} + \eta_{sy} + \theta_c + \varepsilon_{csy}\right) \quad (2)$$

where D_{csy} denotes the age-adjusted all-cause mortality rates in county c, state s, and year y. $smokeBIN^i_{csy}$ is a dummy variable for whether annual population-weighted smoke $PM_{2.5}$ in county c, state s, and year y falls into the range of bin i (0-0.1, 0.1-0.25, 0.25-0.5, 0.5-0.75, 0.75-1, 1-2, 2-3, 3-4, 4-5, 5-6, >6 $\mu g/m^3$; 0-0.1 is the reference category). The main coefficients of interest are the β_i's, which estimate the effects of a year with annual smoke concentration of bin i on mortality rates, relative to a year with annual mean smoke $PM_{2.5}$ concentration below 0.1 $\mu g/m^3$. The reference category included <0.1 because only 4 county-year observations had exactly zero ambient wildfire smoke. W_{csy} denotes a flexible control of temperature (the number of days that fall in different temperature bins) and linear and quadratic terms of annual population-weighted precipitation. η_{sy} denotes a vector of state-year fixed effects (i.e. separate intercepts for each year in each state) that accounts for all factors that differ across states in a given year (e.g. California 2018 versus Oregon 2018) as well as all factors that differ within states across years (e.g. California 2017 versus California 2018). θ_c denotes a set of county-level fixed effects that accounts for any county-specific time-invariant factors that could be correlated with both smoke exposure and mortality (e.g., high income communities in the mountainous areas on the west coast could have higher smoke exposure but lower mortality rates due to non-smoke reasons). In essence, we identify the effect of wildfire smoke on mortality using within-county variation over time, after accounting for any factors that trend over time within that county's state, and for any correlation between smoke variation and variation in temperature and precipitation. Because temporal variation in wildfire smoke exposure is largely a function of idiosyncratic factors such as where a given fire starts and which way the wind blows, our estimates have a plausibly causal interpretation. The coefficients are estimated using weighted Poisson regression models, with function "fepois" from R package "fixest". The estimations are weighted by county-level population counts to enable estimates of population-averaged effects, as well as to reduce statistical uncertainty. The uncertainty of the coefficients are estimated using bootstrap of 500 runs. ϵ_{csy} represents the

error terms.

While we observe historical data on daily smoke $PM_{2.5}$ concentrations and monthly cause-specific mortality rates, we estimate the dose-response functions at the annual level to be consistent with our smoke concentration projections, which are only feasible at the annual level. This approach deviates from previous studies estimating health impacts from wildfire smoke which focus primarily on sub-annual exposures, but it allows for a direct application of the estimated response functions to annual smoke projections. It also has the advantage of allowing us to capture the net effect of either behavioral dynamics in response to short-term variation, as has been observed in related settings (*13*), or "displacement" of mortality that would of otherwise occurred but was hastened as a result of short-term exposure – a common concern in climate impact studies (*30*).

To evaluate the influence of functional forms of the dose-response function, we estimate alternative response functions using a Poisson model, a least-squares linear regression, and a quadratic model where wildfire smoke concentrations were treated as a continuous exposure, and calculate how different functional forms influence the estimates of projected annual excess deaths (Figure S9). We find that non-binned models generally fail to capture meaningful impacts of both low-level and high-level smoke exposure (Figure S12).

Further, to assess the sensitivity of our results to multiple assumptions, we estimate several alternative specifications of the Poisson model. Specifically, we estimate a model which uses alternative bin definitions, a model which includes year 2020, a model which calculates the number of months or the number of days in a year that fall in different smoke bins to represent different temporal aggregations, and a model which is estimated at county-month level. While we cannot calculate the impact on projected mortality under scenarios using these sub-annual measures of wildfire smoke $PM_{2.5}$ given the resolution of the wildfire smoke projections, we instead compare between estimated historical excess deaths during 2011-2020, calculated as the difference between predicted deaths at observed smoke levels relative to what would have occurred absent any smoke. We find that the largest differences occur when using monthly bins, likely due to the lagged effects of smoke on mortality at the monthly level (Figure S10).

To calculate smoke attributable deaths in the historical scenario, we use the county-level population data for the year 2019. We use the county-level average death rate between 2006 to 2019 as the baseline mortality rate for calculations with the Poisson model. For projections of future mortality burden, we scale the population according to the future

population projections from the US Census (*72*).

2.7 Monetizing health impacts

The mortality impacts are monetized using a value of statistical life (VSL) of $10.95 million (year 2019 dollars), as recommended by the US EPA (*73*) and used in previous studies (*54*). For future scenarios, we adjust VSL values using the projected economic growth of 2% and income elasticity of one, following a similar method from Carleton et al. (*54*). We compare the monetized health impacts from climate-induced smoke with two prior estimates of aggregate monetized/economic damage due to climate change. Hsiang et al. estimated an annual damage of 0.4%-0.8% of US GDP or $166-332 billion (in year 2019 dollars, using annual projected GDP of $38.5 trillion from (*55*)). Their approach empirically calculated the effects of climate change on a variety of economic damages from temperature-related mortality, agriculture, crime, coastal storms, energy, and labor channels (*51*). The Framework for Evaluating Damages and Impacts (FrEDI), developed by US EPA (*55*), estimated an annual damage of $292 billion in the 2050s. FrEDI considered 21 sectors (including estimated wildfire damages from western US (*40*)). The wildfire health damages considered in FrEDI only accounted for effects of wildfire in the western US and used an empirical climate-fire relationship derived from historical data before 2013 which did not include recent extreme wildfire years (*40*). We use the default parameters and results from FrEDI in the year of 2050.

3 Results

3.1 Empirical relationship between climate and smoke $PM_{2.5}$

We considered three different statistical and machine learning frameworks for modeling the climate-fire relationship (Methods). To account for geographical heterogeneity, we estimated each of our frameworks separately by region, resulting in five ensembles of climate-fire models. Our models can capture the variability of wildfire dry matter emissions at 10-year intervals (to account for fire stochasticity at the annual level, see Methods), highlighting their ability to quantify changes in wildfire emissions under different climate conditions (Figure 1A). When evaluating through cross-validation of temporal blocks (i.e. randomly splitting a time series of observations into disjoint sets of training and testing years), our models achieve high prediction performance, especially in the western US, Canada, and Mexico, with correlation coefficients of 0.87-0.95 in the out-of-sample evaluations (Table S2). Under these evaluation criteria, our model achieves higher performance relative to

other commonly-used regression methods such as a log-linear model to model climate impacts on burned area (*2*), as well as more flexible machine learning methods (*43*) (Figure S1). However, the model performance indicates that climate conditions are not the only factors influencing the variability of wildfire emissions over time. For example, we find that the model performs less well in the southeastern US and northeastern US, where many fires are agricultural or prescribed fires, which are less directly influenced by climate factors (*74*). Furthermore, while our models can predict spatially- and temporally-aggregated emissions effectively, the predictive performance deteriorates when the same model is evaluated at finer temporal and spatial resolutions (Figures S3 and S4). Such evaluation results are consistent with prior literature on global fire modeling (*75*). Our findings suggest that, although climate conditions such as low soil moisture and high ambient temperatures are related to enhanced fire activity in aggregate, whether a fire occurs in a specific location depends on more stochastic factors such as lightning and human ignitions that are very hard to predict (*76*).

Combining our statistical and machine learning models with future climate projections from CMIP6 global climate models, we project that wildfire emissions will increase by 2050 in all study regions except for the eastern US (Figure 1B). The largest increases in wildfire emissions are projected in the western US, where the model estimates that the annual wildfire emissions will increase by between 248% (SSP1-2.6) and 470% (SSP3-7.0) in the 2050s relative to average emissions during 2011-2020. When compared to 2020, the largest wildfire year for the western US in our historical data, projected annual wildfire emissions during the 2050s will either reach (as in the case of SSP1-2.6) or exceed (by 34% under SSP2-4.5 or 62% under SSP3-7.0) emissions observed in 2020. This magnitude of increases is largely consistent with prior estimates of the western US derived from statistical models and process-based models (*28*, *29*, *36*). Consistent with prior literature, we find that decreased soil moisture and increased ambient temperature, especially in the forest areas in the western US, are the leading contributors to increased wildfire emissions (Figure S5, Table S3, Table S4). In the eastern US, we estimate a decrease of wildfire emissions by 15% under SSP1-2.6 and an increase of wildfire emissions by 10% under SSP3-7.0. These opposing predictions are driven by a combination of two conflicting factors: projected increases in ambient temperature, which increase emissions, and projected increases in precipitation, which decrease projected emissions (Figure S5). Our projected patterns in the eastern US are consistent with a prior study that used a process-based fire-climate model (*36*). By the 2050s, we project an increase in emissions of 33-43% in Mexico, and of 30-49% in Canada, relative to average emissions during 2011-2020, in large part due to

projected increases in Vapor Pressure Deficit (VPD).

To link wildfire emissions to smoke $PM_{2.5}$ concentrations, we develop an empirical relationship that accounts for wind direction, distance from fire, and geographical region (Figure 2). As shown in Figure 2A, we find that wildfire emissions increase smoke $PM_{2.5}$ concentrations near an active fire, with the effects gradually decaying as the distance from the fire increases. Consistent with previous evidence of long-range transport of smoke (*77*, *78*), we find a statistically significant effect ($p<0.05$) of wildfire emissions on downwind locations up to 1000 km away. We find substantial regional heterogeneity in the impacts of dry matter emissions on wildfire $PM_{2.5}$ (Figure 2B). For example, we find that one ton of dry matter emissions (as estimated in GFED4s fire emissions database) can generate as much as 3x surface smoke $PM_{2.5}$ in the Northwest compared to the Southwest and South. Such regional heterogeneity likely reflects a multitude of factors, such as vegetation type, vegetation density, and fire intensity (Methods).

3.2 Projected smoke $PM_{2.5}$ concentration under future climate

As a result of projected rising wildfire emissions, we find increases in annual smoke $PM_{2.5}$ concentrations throughout the US in 2050 under all future climate scenarios (Figure 3A). Under our highest warming scenario (SSP3-7.0), we estimate that annual average smoke $PM_{2.5}$ concentration could reach 10 $\mu g/m^3$ in some regions on the west coast, a level that has only been observed in extreme smoke years such as 2020 (*8*). While the most substantial changes in smoke $PM_{2.5}$ happen across the western US, smoke $PM_{2.5}$ concentrations are also projected to increase in the northeast US, largely due to projected increases in wildfire emissions in the western US and Canada and subsequent increases in cross-boundary transport of wildfire smoke from these fires.

We find that the relative contribution of wildfire smoke to total population-weighted $PM_{2.5}$ increases by 240-320% in 2050. This finding holds even if non-smoke $PM_{2.5}$ remains constant – a conservative assumption given recent and ongoing declines in non-smoke $PM_{2.5}$ concentrations (*18*). We estimate that smoke $PM_{2.5}$ will account for 13-17% of total population-weighted $PM_{2.5}$ in the US in 2050, which is 2-3x its contribution of 5.4% during 2011-2020. Wildfire smoke will account for at least 15% of total population-weighted $PM_{2.5}$ in 17 states, including states both in the West such as Oregon (with 61% smoke contribution), Washington (56%), and California (30%), as well as states in the South and Midwest such as Oklahoma (19%) and Minnesota (16%). Figure 3B shows the smoke contribution in the top 10 states (see Table S5 for more states).

Under the SSP3-7.0 scenario, average population-weighted smoke $PM_{2.5}$ exposure is projected to reach 1.47 $\mu g/m^3$, an increase of over 200% relative to the average level between 2011-2020 (Figure 3C), and 1.6x the population-weighted smoke $PM_{2.5}$ concentration in the historically extreme year of 2020 (0.90 $\mu g/m^3$). The differences across the three climate scenarios are negligible in 2030 and 2040 due to little difference in projections of the climate variables (Figure S5). However, by the 2050s, population-weighted smoke $PM_{2.5}$ is meaningfully smaller in the low warming scenarios, at 1.05 $\mu g/m^3$ under SSP1-2.6 or 1.27 $\mu g/m^3$ under SSP2-4.5, averaged across GCMs. Some individual GCMs project much larger or smaller increases (Figure 3D). Also, these estimates represent decadal averages of annual smoke $PM_{2.5}$ concentrations, in this case averaged 2046 to 2055. Given interannual climate variability, projections suggest that average smoke $PM_{2.5}$ concentrations in individual years could differ substantially, with the highest projected smoke year having roughly 5-10x the concentration of the lowest year (Figure 3E). Our method likely underestimates the interannual variability as it does not capture variability in non-climate factors.

3.3 Mortality burden due to smoke $PM_{2.5}$ exposure

We find that exposure to annual smoke $PM_{2.5}$ increases all-age mortality rates (Figure 4A), even at low smoke concentrations (<1 $\mu g/m^3$), consistent with recent evidence from studies of low levels of all-source $PM_{2.5}$ (*56*). Compared to a year of zero or minimal smoke $PM_{2.5}$ (annual mean concentration <0.1 $\mu g/m^3$), we find that a year with annual average smoke $PM_{2.5}$ of 0.75-1 $\mu g/m^3$ increases county-level mortality rate by 1.3% (95%CI: 0.6%, 2.0%). Years with extreme ambient wildfire smoke concentrations (>6 $\mu g/m^3$) increase annual mortality rates by 5.8% (95%CI: 2.2%, 8.9%). Wildfire smoke increases mortality rates among both the elderly and the general population (Figure S6). Our estimated smoke-mortality relationship is similar in shape to the results estimated by (*53*) at the county-month level. For a given increase in $PM_{2.5}$ concentration by 1 $\mu g/m^3$, our observed effects for smoke $PM_{2.5}$ exceed a recent meta-analysis estimate for all-source $PM_{2.5}$ (0.8% increase in mortality rates per 1 $\mu g/m^3$ (*79*)), although our confidence interval contains this lower estimate.

Combining our empirically-derived dose-response function and historical smoke $PM_{2.5}$ concentrations, we estimate that smoke $PM_{2.5}$ caused 15,800 excess deaths (95% CI: 6900, 25300) per year during 2011-2020 (Figure 4B), relative to a counterfactual of no smoke $PM_{2.5}$. This number of smoke-related deaths would account for 9.2% of total estimated deaths due to total (smoke and non-smoke) $PM_{2.5}$ exposure during the same period (estimated using the response function from (*79*) and total $PM_{2.5}$ estimates from (*58*)). As

shown in Figures 4B and S7, roughly 90% of estimated excess deaths from wildfire smoke exposure come from relatively low but frequent exposures to annual concentrations below 1 $\mu g/m^3$.

We estimate that smoke $PM_{2.5}$ will cause 23,800 to 27,800 annual excess deaths by mid-century across the three climate scenarios – an increase of 51-76% in mortality burden from smoke relative to 2011-2020. Even under the low warming scenario (SSP1-2.6), we estimate that smoke $PM_{2.5}$ will lead to 8,000 more annual excess deaths in the 2050s relative to today. Over the period of 2025-2055, we estimate that wildfire smoke$PM_{2.5}$ could lead to cumulative excess deaths of 690,000 (SSP1-2.6) to 720,000 (SSP3-7.0). Although in the historical period, annual mean wildfire smoke concentrations above 5 $\mu g/m^3$ were rare and represented only 3% of the total mortality burden (Figure 4A), we estimate that these more extreme years will account for between 20-26% of the total excess deaths from smoke in the 2050s (Figure S7). The climate-induced smoke deaths are distributed across populous counties in the western US as well as in the Midwest, Northeast, and South (Figure 4C). The top five states that are predicted to experience the largest increases in annual smoke $PM_{2.5}$ deaths in 2050s under SSP3-7.0 are California (3300 excess deaths per year), Washington (900), Texas (680), Oregon (610), and Florida (380). While projected smoke concentrations are highest in the western US, almost half of the smoke mortality come from eastern states (east of 95° W) due to higher population densities and damages from low wildfire smoke concentrations (Figure S8 and Table S7). Estimated mortality effects are largely robust across alternative specifications of the smoke-mortality models including alternative functional forms, temporal aggregations, and bin definitions (Figure S9 and S10).

We contextualize the magnitude of these mortality impacts in two ways. First, we compare our estimates of excess deaths from climate-driven smoke $PM_{2.5}$ to the direct effects of extreme temperatures on mortality – an impact which has been the primary focus of climate change impacts on mortality and is projected to be one of the leading economic costs of global climate change (*31*, *32*, *54*, *80*). Recent studies find that, by mid-century in the US, increasing mortality from more frequent extreme heat is likely to be more than offset by declining mortality due to cold weather with a projected decrease in annual excess deaths of 15,800 by mid-century (under the SSP2-4.5 scenario) compared to 2001-2010 (*54*). Our projected increase in smoke mortality over the same period represents 62% of this reduction in direct temperature-related deaths (Figure 4D), significantly offsetting a potential benefit of future warming in the US. However, as shown in Figure 4E, the size of this offset differs across the US, with certain states likely to suffer compounded conse-

quences from increases in both smoke-related and heat-related deaths (e.g., CA, TX, FL), and other states likely to see minimal smoke-related mortality and a substantial decline in heat-related deaths (e.g., IL).

As a second comparison, we compare our estimates of climate-induced smoke damages with two prior estimates of aggregated monetized damage due to climate change. Using a Value of Statistical Life (VSL) of $10.95 million dollars (year 2019 dollars, as suggested by EPA (*73*)), we find that the projected 12k increase in annual excess deaths due to climate-driven wildfire smoke would result in annual damages of $244 billion in 2050 (not discounted, in year 2019 dollars, see Methods). Under a similar projected warming level of SSP3-7.0 scenario, Hsiang et al. (*51*) estimated annual damage of 0.4%-0.8% of US GDP or $166-332 billion (in year 2019 dollars, using annual projected GDP of $38.5 trillion from (*55*)), which included damages from temperature-related mortality, agriculture, crime, coastal storms, energy, and labor channels. The Framework for Evaluating Damages and Impacts (FrEDI), developed by US EPA (*55*), considered more sectors (including estimated wildfire damages from the western US (*40*)) and estimated annual damage of $292 billion in 2050s. Our estimates suggest that damages from increase smoke-related mortality could roughly equal damages from all other estimated causes by mid-century in the US.

4 Discussion

While the effects of climate change on wildfire smoke and human health have become an emerging research topic, these effects are rarely incorporated into estimates of climate impacts. In this study, we estimate that climate-induced smoke $PM_{2.5}$ could lead to 12k additional excess deaths per year under the SSP3-7.0 scenario in the US, substantially offsetting the reduction in direct temperature-related deaths expected due to climate change. These estimated deaths lead to an amount of monetized damage on par with quantified damages from all other sectors combined. Our results suggest that increasing wildfire smoke pollution due to climate change could be one of the most important and costly consequences of a warming climate in the US.

We find that aggressive mitigation of global greenhouse gas emissions would limit increases in smoke-related deaths, but that such deaths are likely to increase substantially even under low-emission scenarios. This finding points to the need to develop adaptation strategies if damages are to be avoided. Adaptation could occur at many points along the wildfire-smoke-mortality chain. Increased fuel management, such as prescribed burning, could reduce the likelihood of extreme wildfire activity during adverse climate conditions, but will

create smoke of its own; while the reduction in smoke from high-intensity fire is likely to substantially outweigh the increase from purposeful low-intensity fire, quantifying such tradeoffs is another critical area for work (*81–83*). Adaptation could also target the relationship between smoke and adverse health outcomes. This could include better informing individuals of, and protecting them from, smoke that does occur as current reliance on individuals to self-protect appears highly inadequate and inequitable (*84*, *85*). Improved indoor filtration, including low-cost portable filters, appears a particularly promising and scalable solution, and ensuring that such filtration is affordable, accessible, and used is a potential policy priority (*86*).

Using georeferenced data on deaths and ambient wildfire smoke concentrations, we show that increasing annual exposures to smoke $PM_{2.5}$ are associated with higher county-level annual mortality rates across the contiguous US. Our work contributes to a large literature documenting the impacts of annual exposures to total $PM_{2.5}$ on mortality, which has shaped decades of policy to improve ambient air quality in the US. Due to our annual level projections of wildfire smoke, impacts of wildfire smoke on mortality were necessarily conducted at the annual level. However, wildfires are episodic and typically generate short-term spikes in ambient air pollution, which our measure of exposure may partly obscure (*87*). As such, our results are a complement to other studies on the health effects of short-term (e.g., daily) wildfire smoke exposures (*12*).

We find that elevated long-term average smoke $PM_{2.5}$ concentrations increase mortality rates at both low and high concentrations. These increases lead to two important implications. First, we project large mortality burden not only in regions where large fires occur but also in populous regions with low smoke concentrations (e.g., the eastern US) that have historically received less focus in wildfire studies. We find that 67% of the estimated historical smoke mortality and 42% of the projected future mortality come from the eastern US, as a result of increases in low-level smoke concentrations, consistent with previous historical estimates from (*77*). Second, despite larger differences in projected smoke $PM_{2.5}$ concentration across the three climate scenarios, we estimate substantial mortality increases even in the low warming scenario (SSP1-2.6), again because this scenario generates low-level annual concentration increases that we estimate can have substantial mortality impacts. Our projected mortality impacts are in the uncertainty band of one prior study that applied a range of dose-response functions of total $PM_{2.5}$ exposure (*39*), while substantially higher than the other estimate which only focuses on the western US (*40*), in part due to the mortality impacts we find at low exposure levels.

Our approach can isolate the "direct" impacts of climate change on wildfire air pollution, but does not account for potential "indirect" effects of climate on wildfire through channels such as climate's influence on vegetation growth or lightning-related ignitions. Existing evidence has suggested that vegetation overall would increase under higher warming levels, which could lead to higher wildfire emissions and smoke (*29*). Furthermore, we did not attempt to model the many non-climate factors that contribute to wildfire activity, including the location of energy infrastructure, distance to road, housing development, and fire suppression efforts. Instead, we sought a model that could isolate the influence of climate while holding these other factors fixed. If these factors change dramatically in the future, then our estimates could understate or overstate future emissions, smoke, and mortality. For example, if expansions of houses near wildland vegetation continue (*22*), the effects of a warming climate on wildfire emissions could be larger given more human ignitions, particularly as population growth in the wildland-urban interface has been most rapid in areas where the vegetation is most vulnerable to wildfire (*88*). Alternatively, large increases in wildfire activity could be self-limiting as fires regulate the amount and availability of fuel load for future combustion. Existing studies suggest that this feedback is likely modest (*28*), but constraining this feedback empirically is a critical area for future work.

Our projection analysis quantifies the key uncertainties in climate-wildfire-smoke-mortality estimations (Figure S11). Addressing these uncertainties could further improve understanding of the climate influences on wildfire pollution and health, and thus inform relevant policies. One of the largest uncertainties is how climate change will influence wildfire emissions and smoke $PM_{2.5}$. The statistical models we train can predict the emissions well given observational data, but we know little about their ability to predict wildfire levels under unprecedented climate conditions. Also, we could only robustly establish the climate-wildfire relationship when evaluated at aggregated spatial and temporal scales; predicting wildfire ignitions and growth at local scales remains very challenging. In the future, combining statistical models that can leverage the observational constraints with process-based climate-vegetation-fire models could likely generate a useful framework for understanding climate impacts on wildfire pollution. Another critical uncertainty is the health effects of smoke $PM_{2.5}$ exposure. Quantifying health impacts of smoke $PM_{2.5}$ at both low and high concentrations in the context of the unique chemical composition of smoke $PM_{2.5}$ and fire influence on human behaviors remains an important area of future research. Furthermore, our estimated health cost is likely only a subset of the overall health burden due to possible morbidity effects of smoke, or health costs from other wildfire-driven pollutants.

Our projections of smoke $PM_{2.5}$ and mortality effects can support climate science, health, and policy research to better understand drivers and consequences of smoke $PM_{2.5}$ under climate change, and help inform policy priorities to address their negative impacts. Our estimates suggest that health costs due to climate-induced smoke $PM_{2.5}$ could be among the most damaging consequences of climate change in the US. Based on our results, designing and implementing policies to reduce wildfire smoke and protect vulnerable communities has the potential to deliver substantial health benefits now and in the coming decades.

References

1. V. Iglesias, J. K. Balch, W. R. Travis, US fires became larger, more frequent, and more widespread in the 2000s. *Science advances* **8**, eabc0020 (2022).
2. J. T. Abatzoglou, A. P. Williams, Impact of anthropogenic climate change on wildfire across western US forests. *Proceedings of the National Academy of Sciences* **113**, 11770–11775 (2016).
3. Y. Zhuang, R. Fu, B. D. Santer, R. E. Dickinson, A. Hall, Quantifying contributions of natural variability and anthropogenic forcings on increased fire weather risk over the western United States. *Proceedings of the National Academy of Sciences* **118**, e2111875118 (2021).
4. M. W. Jones *et al.*, Global and regional trends and drivers of fire under climate change. *Reviews of Geophysics* **60**, e2020RG000726 (2022).
5. V. M. Donovan, R. Crandall, J. Fill, C. L. Wonkka, Increasing large wildfire in the eastern United States. *Geophysical Research Letters* **50**, e2023GL107051 (2023).
6. C. D. McClure, D. A. Jaffe, US particulate matter air quality improves except in wildfire-prone areas. *Proceedings of the National Academy of Sciences* **115**, 7901–7906 (2018).
7. K. O'Dell, B. Ford, E. V. Fischer, J. R. Pierce, Contribution of wildland-fire smoke to US PM2. 5 and its influence on recent trends. *Environmental science & technology* **53**, 1797–1804 (2019).
8. M. L. Childs *et al.*, Daily Local-Level Estimates of Ambient Wildfire Smoke PM2. 5 for the Contiguous US. *Environmental Science & Technology* **56**, 13607–13621 (2022).
9. D. Zhang *et al.*, Wildland Fires Worsened Population Exposure to PM2. 5 Pollution in the Contiguous United States. *Environmental Science & Technology* **57**, 19990–19998 (2023).

10. C. E. Reid *et al.*, Critical review of health impacts of wildfire smoke exposure. *Environmental health perspectives* **124**, 1334–1343 (2016).

11. G. Chen *et al.*, Mortality risk attributable to wildfire-related PM2· 5 pollution: a global time series study in 749 locations. *The Lancet Planetary Health* **5**, e579–e587 (2021).

12. C. F. Gould *et al.*, Health effects of wildfire smoke exposure. *Annual Review of Medicine* **75** (2023).

13. S. Heft-Neal *et al.*, Emergency department visits respond nonlinearly to wildfire smoke. *Proceedings of the National Academy of Sciences* **120**, e2302409120 (2023).

14. Y. Li *et al.*, Dominance of wildfires impact on air quality exceedances during the 2020 record-breaking wildfire season in the United States. *Geophysical Research Letters* **48**, e2021GL094908 (2021).

15. M. Burke *et al.*, The changing risk and burden of wildfire in the United States. *Proceedings of the National Academy of Sciences* **118**, e2011048118 (2021).

16. J. Currie, R. Walker, What do economists have to say about the Clean Air Act 50 years after the establishment of the Environmental Protection Agency? *Journal of Economic Perspectives* **33**, 3–26 (2019).

17. J. E. Aldy, M. Auffhammer, M. Cropper, A. Fraas, R. Morgenstern, Looking back at 50 years of the Clean Air Act. *Journal of Economic Literature* **60**, 179–232 (2022).

18. M. Burke *et al.*, The contribution of wildfire to PM2. 5 trends in the USA. *Nature* **622**, 761–766 (2023).

19. N. S. Diffenbaugh, A. G. Konings, C. B. Field, Atmospheric variability contributes to increasing wildfire weather but not as much as global warming. *Proceedings of the National Academy of Sciences* **118**, e2117876118 (2021).

20. A. L. Westerling, Increasing western US forest wildfire activity: sensitivity to changes in the timing of spring. *Philosophical Transactions of the Royal Society B: Biological Sciences* **371**, 20150178 (2016).

21. Z. A. Holden *et al.*, Decreasing fire season precipitation increased recent western US forest wildfire activity. *Proceedings of the National Academy of Sciences* **115**, E8349–E8357 (2018).

22. V. C. Radeloff *et al.*, Rapid growth of the US wildland-urban interface raises wildfire risk. *Proceedings of the National Academy of Sciences* **115**, 3314–3319 (2018).

23. T. M. Ellis, D. M. Bowman, P. Jain, M. D. Flannigan, G. J. Williamson, Global increase in wildfire risk due to climate-driven declines in fuel moisture. *Global change biology* **28**, 1544–1559 (2022).

24. J. K. Balch *et al.*, Warming weakens the night-time barrier to global fire. *Nature* **602**, 442–448 (2022).

25. P. T. Brown *et al.*, Climate warming increases extreme daily wildfire growth risk in California. *Nature* **621**, 760–766 (2023).

26. T. D. Hessilt *et al.*, Future increases in lightning ignition efficiency and wildfire occurrence expected from drier fuels in boreal forest ecosystems of western North America. *Environmental Research Letters* **17**, 054008 (2022).

27. A. A. Gutierrez *et al.*, Wildfire response to changing daily temperature extremes in California's Sierra Nevada. *Science advances* **7**, eabe6417 (2021).

28. J. T. Abatzoglou *et al.*, Projected increases in western US forest fire despite growing fuel constraints. *Communications Earth & Environment* **2**, 227 (2021).

29. S. S.-C. Wang, L. R. Leung, Y. Qian, Projection of future fire emissions over the contiguous US using explainable artificial intelligence and CMIP6 models. *Journal of Geophysical Research: Atmospheres* **128**, e2023JD039154 (2023).

30. S. Hsiang, Climate econometrics. *Annual Review of Resource Economics* **8**, 43–75 (2016).

31. K. Rennert *et al.*, Comprehensive evidence implies a higher social cost of CO2. *Nature* **610**, 687–692 (2022).

32. U.S. Environmental Protection Agency, *Report on the social cost of greenhouse gases: Estimates incorporating recent scientific advances*, 2022.

33. Y. Lam, J. Fu, S Wu, L. Mickley, Impacts of future climate change and effects of biogenic emissions on surface ozone and particulate matter concentrations in the United States. *Atmospheric Chemistry and Physics* **11**, 4789–4806 (2011).

34. X. Yue, L. J. Mickley, J. A. Logan, J. O. Kaplan, Ensemble projections of wildfire activity and carbonaceous aerosol concentrations over the western United States in the mid-21st century. *Atmospheric Environment* **77**, 767–780 (2013).

35. Y. Li, L. J. Mickley, P. Liu, J. O. Kaplan, Trends and spatial shifts in lightning fires and smoke concentrations in response to 21st century climate over the national forests and parks of the western United States. *Atmospheric Chemistry and Physics* **20**, 8827–8838 (2020).

36. C. Sarangi *et al.*, Projected increases in wildfires may challenge regulatory curtailment of PM 2.5 over the eastern US by 2050. *Atmospheric Chemistry and Physics Discussions*, 1–30 (2022).

37. J. C. Liu *et al.*, Particulate air pollution from wildfires in the Western US under climate change. *Climatic change* **138**, 655–666 (2016).

38. J. C. Liu *et al.*, Future respiratory hospital admissions from wildfire smoke under climate change in the Western US. *Environmental Research Letters* **11**, 124018 (2016).

39. B. Ford *et al.*, Future fire impacts on smoke concentrations, visibility, and health in the contiguous United States. *GeoHealth* **2**, 229–247 (2018).

40. J. E. Neumann *et al.*, Estimating PM2. 5-related premature mortality and morbidity associated with future wildfire emissions in the western US. *Environmental Research Letters* **16**, 035019 (2021).

41. J. D. Stowell *et al.*, Asthma exacerbation due to climate change-induced wildfire smoke in the Western US. *Environmental Research Letters* **17**, 014023 (2021).

42. E. Grant, J. D. Runkle, Long-term health effects of wildfire exposure: a scoping review. *The Journal of Climate Change and Health* **6**, 100110 (2022).

43. S. S.-C. Wang, Y. Qian, L. R. Leung, Y. Zhang, Interpreting machine learning prediction of fire emissions and comparison with FireMIP process-based models. *Atmospheric Chemistry and Physics* **22**, 3445–3468 (2022).

44. X. Pan *et al.*, Six global biomass burning emission datasets: intercomparison and application in one global aerosol model. *Atmospheric Chemistry and Physics* **20**, 969–994 (2020).

45. T. S. Carter *et al.*, How emissions uncertainty influences the distribution and radiative impacts of smoke from fires in North America. *Atmospheric Chemistry and Physics* **20**, 2073–2097 (2020).

46. X. Ye *et al.*, Evaluation and intercomparison of wildfire smoke forecasts from multiple modeling systems for the 2019 Williams Flats fire. *Atmospheric Chemistry and Physics* **21**, 14427–14469 (2021).

47. X. Huang *et al.*, Smoke-weather interaction affects extreme wildfires in diverse coastal regions. *Science* **379**, 457–461 (2023).

48. Y. Xie, M. Lin, L. W. Horowitz, Summer PM2. 5 pollution extremes caused by wildfires over the western United States during 2017–2018. *Geophysical Research Letters* **47**, e2020GL089429 (2020).

49. R. B. Rice *et al.*, Wildfires Increase Concentrations of Hazardous Air Pollutants in Downwind Communities. *Environmental Science & Technology* **57**, 21235–21248 (2023).

50. Y. Xie *et al.*, Tripling of western US particulate pollution from wildfires in a warming climate. *Proceedings of the National Academy of Sciences* **119**, e2111372119 (2022).

51. S. Hsiang *et al.*, Estimating economic damage from climate change in the United States. *Science* **356**, 1362–1369 (2017).

52. K. Chen, Y. Ma, M. L. Bell, W. Yang, Canadian wildfire smoke and asthma syndrome emergency department visits in New York City. *JAMA* **330**, 1385–1387 (2023).

53. Y. Ma *et al.*, Wildfire smoke PM2. 5 and mortality in the contiguous United States. *medRxiv* (2023).

54. T. Carleton *et al.*, Valuing the global mortality consequences of climate change accounting for adaptation costs and benefits. *The Quarterly Journal of Economics* **137**, 2037–2105 (2022).

55. U.S. Environmental Protection Agency, *Technical Documentation on the Framework for Evaluating Damages and Impacts (FrEDI)*, 2021.

56. J. Chen *et al.*, Long-Term Exposure to Low-Level PM 2.5 and Mortality: Investigation of Heterogeneity by Harmonizing Analyses in Large Cohort Studies in Canada, United States, and Europe. *Environmental Health Perspectives* **131**, 127003 (2023).

57. G. R. Van Der Werf *et al.*, Global fire emissions estimates during 1997–2016. *Earth System Science Data* **9**, 697–720 (2017).

58. A. Van Donkelaar *et al.*, Monthly global estimates of fine particulate matter and their uncertainty. *Environmental Science & Technology* **55**, 15287–15300 (2021).

59. J. Buch, A. P. Williams, C. S. Juang, W. D. Hansen, P. Gentine, SMLFire1. 0: a stochastic machine learning (SML) model for wildfire activity in the western United States. *Geoscientific Model Development* **16**, 3407–3433 (2023).

60. F. Mesinger *et al.*, North American regional reanalysis. *Bulletin of the American Meteorological Society* **87**, 343–360 (2006).

61. Y. Xia *et al.*, Continental-scale water and energy flux analysis and validation for the North American Land Data Assimilation System project phase 2 (NLDAS-2): 1. Intercomparison and application of model products. *Journal of Geophysical Research: Atmospheres* **117** (2012).

62. Produced by Natural Resources Canada/ The Canada Centre for Mapping and Earth Observation (NRCan/CCMEO), United States Geological Survey (USGS); Instituto Nacional de Estadística y Geografía (INEGI), Comisión Nacional para el Conocimiento y Uso de la Biodiversidad (CONABIO) and Comisión Nacional Forestal (CONAFOR), *2015 North American Land Cover at 30 m spatial resolution.*

63. IPCC, in *Climate Change 2021: The Physical Science Basis. Contribution of Working Group I to the Sixth Assessment Report of the Intergovernmental Panel on Climate Change*, ed. by V. Masson-Delmotte *et al.* (Cambridge University Press, Cambridge, United Kingdom and New York, NY, USA, 2021), 332.

64. J. T. Abatzoglou, Development of gridded surface meteorological data for ecological applications and modelling. *International Journal of Climatology* **33**, 121–131 (2013).

65. M. Qiu, N. Ratledge, I. M. Azevedo, N. S. Diffenbaugh, M. Burke, Drought impacts on the electricity system, emissions, and air quality in the western United States. *Proceedings of the National Academy of Sciences* **120**, e2300395120 (2023).

66. S. Urbanski, Wildland fire emissions, carbon, and climate: Emission factors. *Forest Ecology and Management* **317**, 51–60 (2014).

67. C. N. Jen *et al.*, Speciated and total emission factors of particulate organics from burning western US wildland fuels and their dependence on combustion efficiency. *Atmospheric Chemistry and Physics* **19**, 1013–1026 (2019).

68. Y. Liang *et al.*, Emissions of Organic Compounds from Western US Wildfires and Their Near Fire Transformations. *Atmospheric Chemistry and Physics Discussions*, 1–32 (2022).

69. D. A. Jaffe *et al.*, Wildfire and prescribed burning impacts on air quality in the United States. *Journal of the Air & Waste Management Association* **70**, 583–615 (2020).

70. G. L. Achtemeier, Measurements of moisture in smoldering smoke and implications for fog. *International Journal of Wildland Fire* **15**, 517–525 (2006).

71. National Center for Health Statistics Division of Vital Statistics, *NVSS Restricted-use Mortality Files, 1999-2021. Hyattsville, Maryland.*

72. U.S. Census Bureau, *2023 National Population Projections Tables: Main Series*, 2023.

73. U.S. Environmental Protection Agency, *Regulatory Impact Analysis for the Clean Power Plan Final Rule*, 2015.

74. J. A. Kupfer, A. J. Terando, P. Gao, C. Teske, J. K. Hiers, Climate change projected to reduce prescribed burning opportunities in the south-eastern United States. *International Journal of Wildland Fire* **29**, 764–778 (2020).

75. M. Grillakis *et al.*, Climate drivers of global wildfire burned area. *Environmental Research Letters* **17**, 045021 (2022).

76. K. Rao *et al.*, Dry live fuels increase the likelihood of lightning-caused fires. *Geophysical Research Letters* **50**, e2022GL100975 (2023).

77. K. O'Dell *et al.*, Estimated mortality and morbidity attributable to smoke plumes in the United States: not just a western US problem. *GeoHealth* **5**, e2021GH000457 (2021).

78. B. Shrestha, J. A. Brotzge, J. Wang, Observations and Impacts of Long-Range Transported Wildfire Smoke on Air Quality Across New York State During July 2021. *Geophysical Research Letters* **49**, e2022GL100216 (2022).

79. C. A. Pope III, N. Coleman, Z. A. Pond, R. T. Burnett, Fine particulate air pollution and human mortality: 25+ years of cohort studies. *Environmental research* **183**, 108924 (2020).

80. A. Gasparrini *et al.*, Projections of temperature-related excess mortality under climate change scenarios. *The Lancet Planetary Health* **1**, e360–e367 (2017).

81. M. M. Kelp *et al.*, Prescribed burns as a tool to mitigate future wildfire smoke exposure: Lessons for states and rural environmental justice communities. *Earth's Future* **11**, e2022EF003468 (2023).

82. X. Wu, E. Sverdrup, M. D. Mastrandrea, M. W. Wara, S. Wager, Low-intensity fires mitigate the risk of high-intensity wildfires in California's forests. *Science advances* **9**, eadi4123 (2023).

83. C. L. Schollaert *et al.*, Quantifying the smoke-related public health trade-offs of forest management. *Nature Sustainability*, 1–10 (2023).

84. M. Burke *et al.*, Exposures and behavioural responses to wildfire smoke. *Nature human behaviour* **6**, 1351–1361 (2022).

85. B. Krebs, M. Neidell, Wildfires exacerbate inequalities in indoor pollution exposure. *Environmental Research Letters* (2024).

86. N. W. May, C. Dixon, D. A. Jaffe, *et al.*, Impact of wildfire smoke events on indoor air quality and evaluation of a low-cost filtration method. *Aerosol and Air Quality Research* **21**, 210046 (2021).

87. J. A. Casey *et al.*, Measuring long-term exposure to wildfire PM2. 5 in California: Time-varying inequities in environmental burden. *Proceedings of the National Academy of Sciences* **121**, e2306729121 (2024).

88. K. Rao, A. P. Williams, N. S. Diffenbaugh, M. Yebra, A. G. Konings, Plant-water sensitivity regulates wildfire vulnerability. *Nature ecology & evolution* **6**, 332–339 (2022).

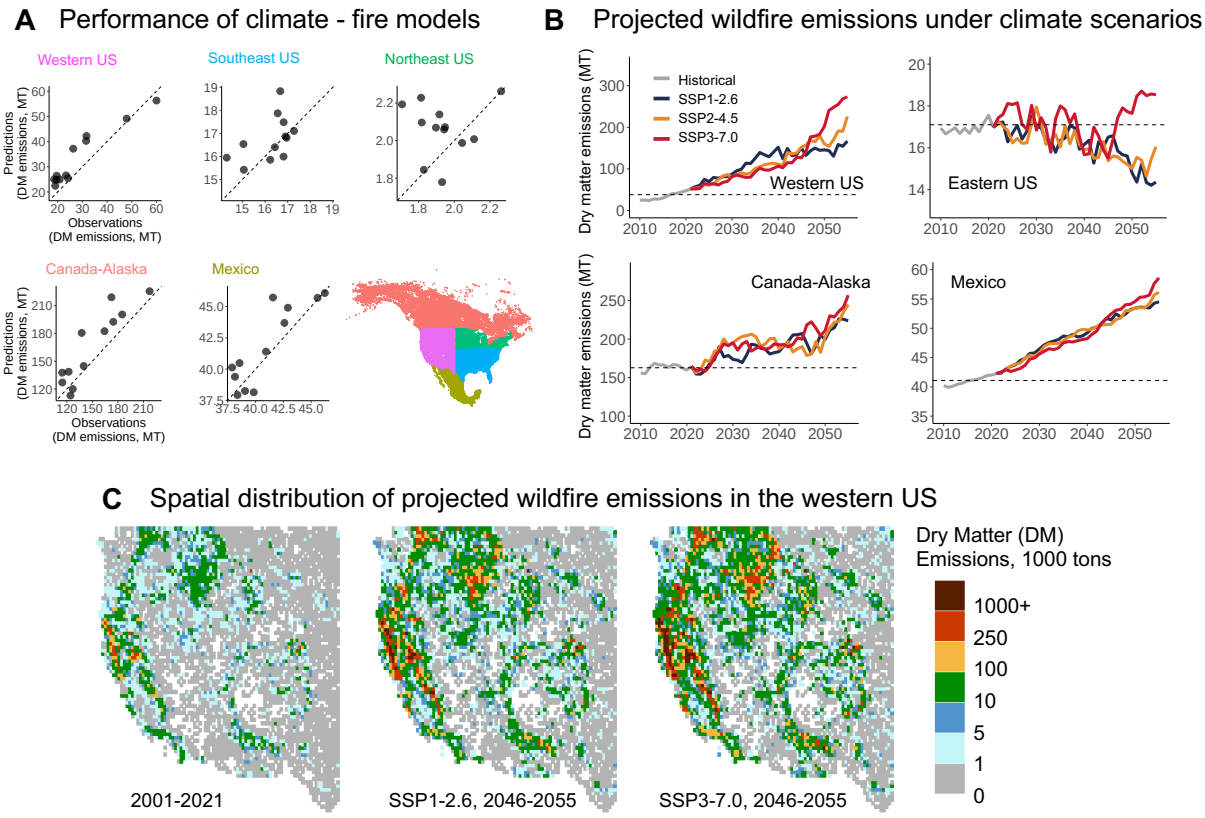

Figure 1: **Projected wildfire emissions under future climate change scenarios.** Panel A: Performance of the statistical and machine learning ensemble models. We build separate models to predict wildfire Dry Matter (DM) emissions for five regions respectively: Western US, Southeast US, Northeast US, Canada-Alaska, and Mexico. The plot shows the 10-year moving average of predicted emissions (y-axis) against the observed emissions (x-axis), aggregated at the regional level. Panel B: Projected wildfire emissions (unit: Million Tons, MT) under the historical scenarios and three future climate scenarios (SSP1-2.6, SSP2-4.5, and SSP3-7.0). The plot shows the 10-year moving average of the wildfire emission projections. The dashed line represents the average observed emissions over 2001-2021 for each region. For presentation purpose, we aggregate predictions from northeast US and southeast US to calculate the total for eastern US. Panel C: Observed DM emissions at the native resolution (0.25 degree) in 2001-2021 from GFED4s, and projected annual emissions averaged between 2046-2055 under SSP1-2.6 and SSP3-7.0 scenarios (down-scaled from aggregated projections).

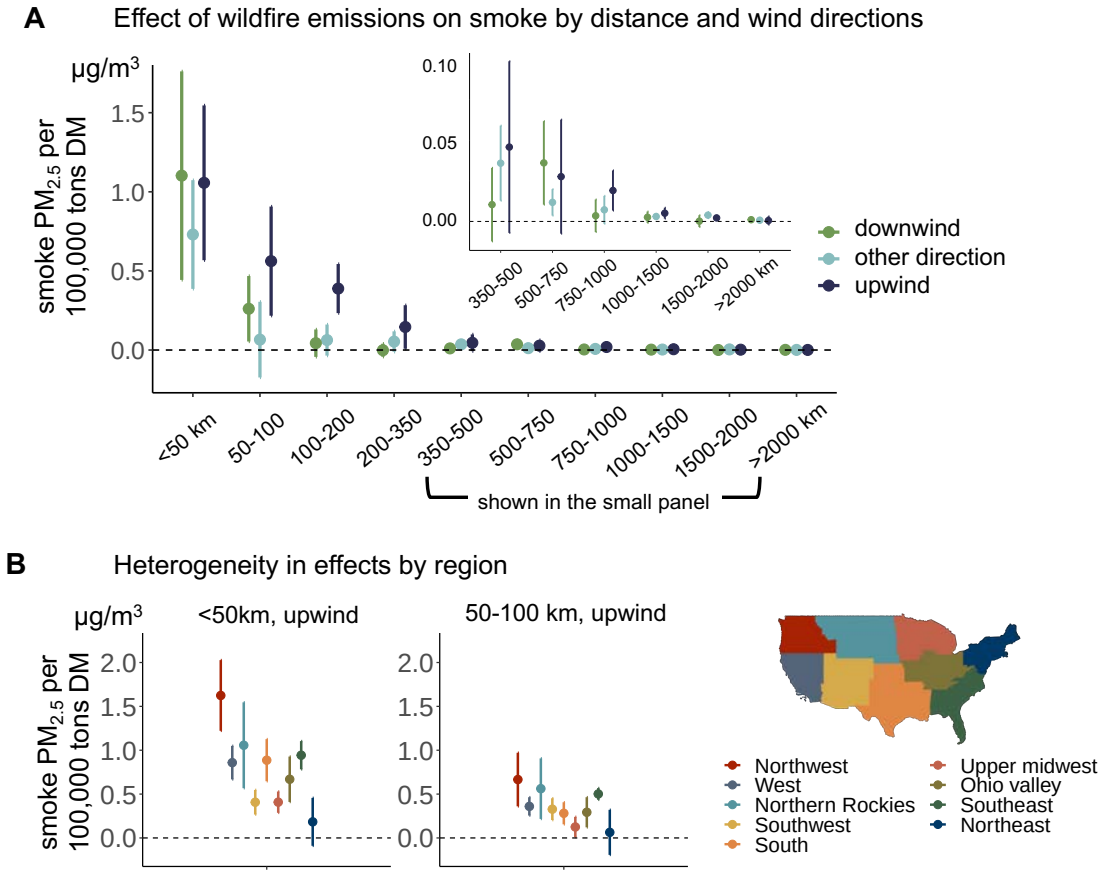

Figure 2: **Wildfire emissions increase the observed smoke $PM_{2.5}$ concentration in the neighboring and downwind areas.** Panel A: The empirically estimated effects of wildfire emissions on smoke $PM_{2.5}$ by distance from emissions and wind directions. "Upwind" means the fire is upwind of the location at which $PM_{2.5}$ is measured. Wildfire emissions are estimated to have larger impacts on smoke $PM_{2.5}$ when smoke location is closer to fire (distance to emissions is shown on the x-axis), and when wildfire emissions happen upwind of the smoke locations (wind patterns shown in colors). Separate models are estimated for the 9 climatic regions in the US determined by National Centers for Environmental Information (as shown in Panel B). Panel A shows the results in the *Northern Rockies* region. Panel B: Regional heterogeneity in emission impacts on smoke $PM_{2.5}$. Panel B shows the estimated effects of *upwind* emissions in the <50 km and 500-100 km bins, across the nine regions in the US.

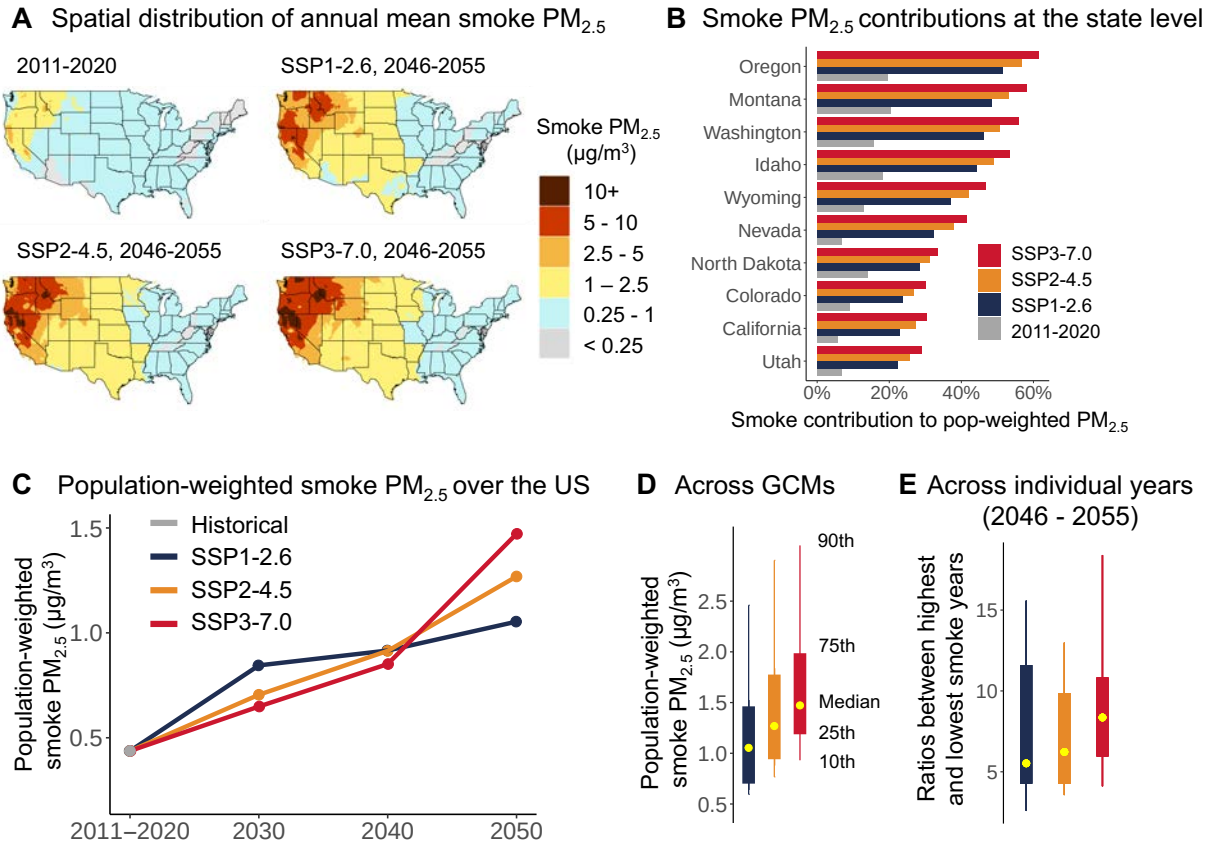

Figure 3: **Population exposure to wildfire smoke $PM_{2.5}$ increases by 2- to 3-fold under future climate change scenarios.** Panel A: The annual mean smoke $PM_{2.5}$ concentration in the historical data (2011-2020), and projected annual mean smoke $PM_{2.5}$ concentration under the three climate scenarios in 2046-2055. Panel B: the contribution of smoke $PM_{2.5}$ to total population-weighted $PM_{2.5}$ at the state level. Non-smoke $PM_{2.5}$ is calculated as the difference between total $PM_{2.5}$ (derived from (*58*)) and smoke $PM_{2.5}$ in 2016-2020, and is assumed to be constant in future. The panel only lists the top ten states with the highest smoke contribution under SSP3-7.0 scenario in 2050. Panel C: population-weighted smoke $PM_{2.5}$ over the US in different decades. Panel D: uncertainty in the population-weighted smoke $PM_{2.5}$ across the 28 GCMs used in the projection. Panel E: for each GCM, we calculate the ratio between the highest and lowest projected population-weighted smoke $PM_{2.5}$ during 2046-2055. The panel shows the quantiles of these ratios across the 28 GCMs.

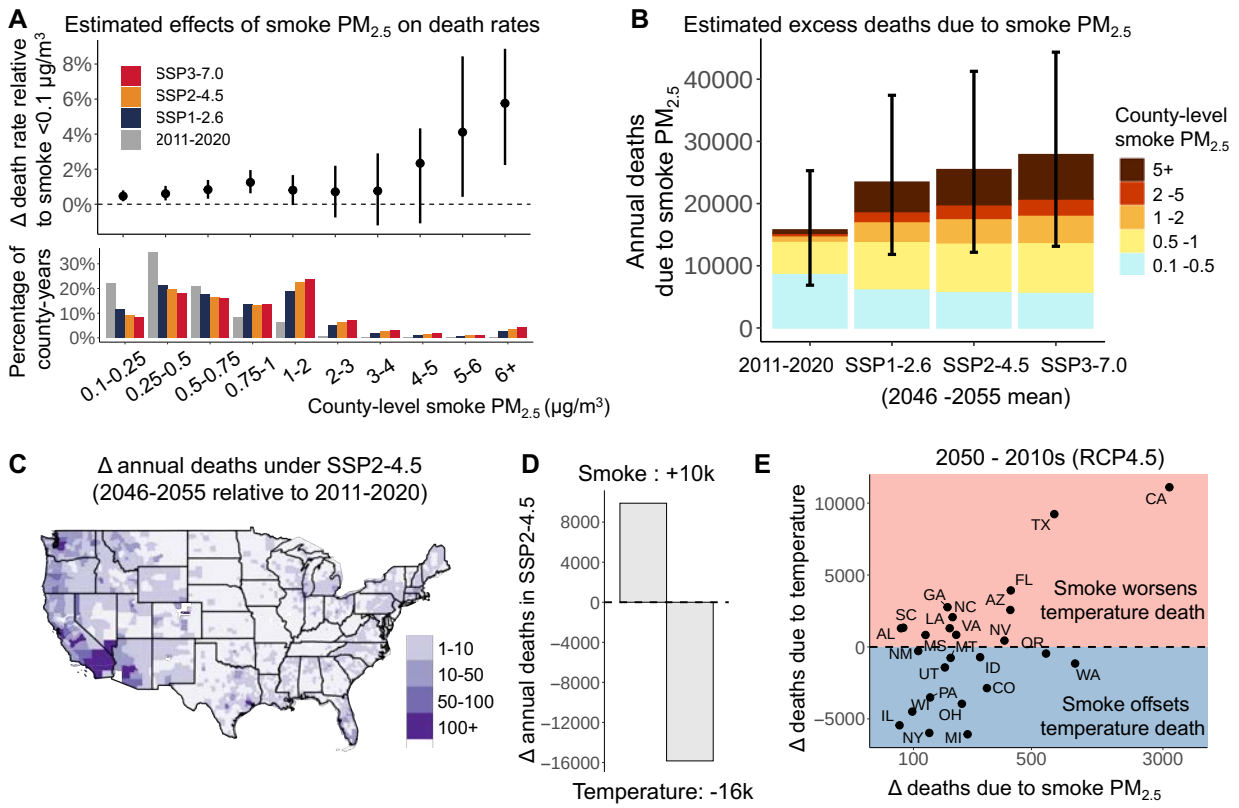

Figure 4: **Mortality impacts of wildfire smoke $PM_{2.5}$ and estimated mortality due to smoke $PM_{2.5}$ under future climate scenarios.** Panel A: empirically estimated effects of annual smoke $PM_{2.5}$ concentration on county-level all-age annual mortality rates. The figure shows the effects of exposure to different annual mean concentration of smoke $PM_{2.5}$ (shown in the x-axis) relative to a year with smoke concentration <0.1 $\mu g/m^3$, estimated using a Poisson model at the county and annual level and data from 2006-2019. The error bars show the 95% confidence interval estimated using bootstrap. The bottom part of panel A shows the percentage of county-years in each smoke concentration bin over the historical period (2011-2020) as well as future climate scenarios (2046-2055). Panel B: estimated annual excess deaths due to smoke $PM_{2.5}$, and contribution to total smoke excess deaths from different smoke concentration bins. The error bars show the 95% bootstrapped confidence intervals. Panel C: county-level projected increases in annual excess deaths due to smoke $PM_{2.5}$ in 2050; increases are calculated as the differences between the average deaths under SSP2-4.5 scenario over 2046-2055 and the 2011-2020 average. Panel D shows US-wide total estimated annual smoke deaths and direct temperature-related deaths in 2050, with increasing smoke deaths offsetting 62% of the reduction in temperature deaths. Panel E: projected increase in smoke deaths offsets projected reductions in direct temperature-related deaths by 2050s, the latter as estimated in a recent study (*54*). The x-axis shows the changes in deaths due to smoke $PM_{2.5}$ in 2050s (note the log-scale), and the y-axis shows the changes in deaths due to temperature change, where only the 25 states with $>$ 75 smoke related deaths per year are visualized.

5 Supplementary tables and figures

Table S1: Estimated dry matter (DM) emissions by land-use type in historical period and future scenarios. For the historical period, the table shows the annual mean DM emissions from each land-use type in each region from 2001-2021, directly derived from GFED4s. For the future scenario, the table shows the annual mean DM emissions from each land-use type in each region under SSP3-7.0 from 2046-2055. Landuse types are derived from GFED4s inventory. "Forest" includes emissions from both temperate forests and boreal forests.

Region	Type	2001 - 2021		2050 SSP3-7.0
		emissions (MT)	percent	emissions (MT)
Western US	forest	25.8	68%	184.7
	savanna	10.7	28%	76.5
	agriculture	1.7	4%	12.3
	landuse change	0.0	0%	0.0
	peatland	0.0	0%	0.0
Southeastern US	forest	4.2	28%	4.4
	savanna	5.3	35%	5.8
	agriculture	5.6	37%	5.6
	landuse change	0.0	0%	0.0
	peatland	0.0	0%	0.0
Northeastern US	forest	0.6	29%	0.6
	savanna	0.2	11%	0.2
	agriculture	1.2	60%	1.1
	landuse change	0.0	0%	0.0
	peatland	0.0	0%	0.0
Canada-Alaska	forest	152.6	94%	240.8
	savanna	0.2	0%	0.4
	agriculture	1.7	1%	2.7
	landuse change	0.0	0%	0.0
	peatland	8.2	5%	13.0
Mexico	forest	1.2	3%	1.7
	savanna	19.4	47%	29.0
	agriculture	6.4	16%	9.5
	landuse change	14.1	34%	17.1
	peatland	0.0	0%	0.0

Table S2: Performance of the individual statistical and machine learning models. For each region, we train six algorithms {Linear, LASSO, Neural Net} × {level, log of the outcome}. The table shows the optimal spatial resolution and three evaluation metrics for each algorithm. The three evaluation metrics are correlation coefficient (R), bias in predicting the highest-emitting 10-year (Bias), and Root Mean Square Error over the mean of the outcome (RMSE/Mean). Bias is calculated as *(Prediction - Observation) / Observation* for the 10-year period with the highest emissions. Models selected in the final model ensembles are bolded and labeled "Y" in the "Selected" column. The selection is based on RMSE + |Bias| to consider both metrics. In our main analysis, for each region, only the algorithms with "RMSE + |Bias|" within 5% of the best algorithm are selected.

Region	Algorithm	Optimal resolution	R	Bias	RMSE/ Mean	RMSE + |Bias|	Diff	Selected
Western US	**Linear, level**	**regional**	**0.98**	**-10%**	**20%**	**29%**	**0%**	**Y**
Western US	Linear, log	eco2	0.91	-16%	22%	37%	8%	N
Western US	LASSO, level	regional	0.99	-14%	28%	43%	13%	N
Western US	**LASSO, log**	**regional**	**0.89**	**-3%**	**31%**	**33%**	**4%**	**Y**
Western US	Neural Net, level	eco2	0.73	0%	90%	91%	61%	N
Western US	Neural Net, log	eco3	0.98	-20%	19%	39%	9%	N
Southeastern US	**Linear, level**	**eco3**	**0.51**	**-1%**	**6%**	**7%**	**0%**	**Y**
Southeastern US	Linear, log	eco2	0.36	-18%	14%	32%	25%	N
Southeastern US	LASSO, level	eco2	0.58	-12%	9%	21%	14%	N
Southeastern US	LASSO, log	eco2	0.02	-16%	14%	30%	23%	N
Southeastern US	Neural Net, level	grid	0.11	5%	11%	16%	9%	N
Southeastern US	Neural Net, log	eco2	0.30	-12%	12%	24%	17%	N
Northeastern US	**Linear, level**	**grid**	**0.05**	**-2%**	**11%**	**13%**	**0%**	**Y**
Northeastern US	Linear, log	regional	0.06	-11%	9%	20%	7%	N
Northeastern US	LASSO, log	eco2	0.19	-26%	19%	45%	32%	N
Northeastern US	**Neural Net, level**	**eco2**	**0.07**	**2%**	**14%**	**15%**	**2%**	**Y**
Northeastern US	Neural Net, log	eco3	0.29	-20%	12%	32%	20%	N
Canada-Alaska	**Linear, level**	**regional**	**0.91**	**4%**	**15%**	**19%**	**0%**	**Y**
Canada-Alaska	Linear, log	eco2	0.70	43%	35%	78%	59%	N
Canada-Alaska	LASSO, level	eco2	0.94	-15%	19%	34%	15%	N
Canada-Alaska	LASSO, log	regional	0.73	-13%	16%	29%	10%	N
Canada-Alaska	Neural Net, level	eco3	0.20	-9%	27%	36%	17%	N
Canada-Alaska	Neural Net, log	regional	0.71	-30%	15%	45%	26%	N
Mexico	**Linear, level**	**eco2**	**0.88**	**0%**	**4%**	**4%**	**0%**	**Y**
Mexico	Linear, log	eco2	0.85	-2%	14%	16%	12%	N
Mexico	**LASSO, level**	**eco3**	**0.86**	**0%**	**5%**	**5%**	**1%**	**Y**
Mexico	LASSO, log	eco2	0.71	-13%	14%	27%	23%	N
Mexico	Neural Net, level	eco2	0.72	0%	10%	10%	6%	N
Mexico	Neural Net, log	regional	0.82	-7%	7%	14%	9%	N

Table S3: Estimated coefficients from the selected linear regression models that use climate features to predict wildfire emissions. The table only shows the coefficients from the final selected models in each region with the corresponding optimal spatial resolution. Statistically significant coefficients ($p < 0.1$) are bolded.

	Western US		Southeastern US		Northeastern US		Canada-Alaska		Mexico	
	coef	p-value	coef	p-value	coef	p-value	coef	p-value	coef	p-value
temperature	2.0E-02	0.25	-9.9E-04	0.15	2.1E-04	0.30	-3.0E-02	0.08	**-1.2E-02**	**0.00**
precipitation	-3.3E-02	0.27	**-4.9E-03**	**0.00**	-2.5E-04	0.63	-3.6E-02	0.43	**8.8E-03**	**0.00**
RH	5.6E-03	0.26	2.4E-04	0.55	-1.2E-04	0.36	2.3E-02	0.23	**4.8E-03**	**0.00**
wind speed	7.3E-02	0.12	**9.6E-03**	**0.00**	**-1.6E-03**	**0.09**	4.6E-02	0.79	-1.1E-03	0.92
VPD	-2.3E-02	0.94	3.3E-03	0.74	-2.5E-03	0.55	**2.4E+00**	**0.02**	**2.6E-01**	**0.00**
runoff	1.2E-02	0.24	5.5E-04	0.83	5.1E-04	0.49	1.2E-01	0.13	-9.1E-03	0.26
soil moisture	**-2.6E-02**	**0.01**	**-3.8E-03**	**0.00**	-2.8E-04	0.51				

Table S4: Estimated coefficients from the selected LASSO models that use climate features to predict wildfire emissions. As LASSO models are only selected in the western US and Mexico, the table shows the coefficients from these two final selected models with the corresponding optimal spatial resolution.

Western US		Mexico	
Selected variables	coef	Selected variables	coef
soil moisture	-1.2E+00	VPD*grass	4.1E-01
temperature	1.1E+00	VPD*precipitation	9.0E-03
VPD*precipitation	-2.8E+00	VPD*RH	1.3E-03
VPD*runoff	2.5E+00		
RH^2	-1.5E-04		
runoff^2	-1.6E-01		
runoff*wind speed	1.3E-02		
temperature^2	4.6E-05		
wind speed^2	4.1E-01		

Table S5: Estimated population-weighted average smoke $PM_{2.5}$, total $PM_{2.5}$, and smoke $PM_{2.5}$ contribution at the state level. Total $PM_{2.5}$ are calculated as the sum of smoke and non-smoke $PM_{2.5}$ concentrations. Non-smoke $PM_{2.5}$ are assumed to be the same as the average non-smoke $PM_{2.5}$ between 2016-2020, calculated as the difference between total $PM_{2.5}$ from (*58*) and smoke $PM_{2.5}$ from (*8*). Only states with >10% smoke contributions under SSP3-7.0 scenario are listed.

State	Smoke $PM_{2.5}$ $\mu g/m^3$	Total $PM_{2.5}$ $\mu g/m^3$	Smoke percent	State	Smoke $PM_{2.5}$ $\mu g/m^3$	Total $PM_{2.5}$ $\mu g/m^3$	Smoke percent	Scenario
Oregon	1.3	6.6	20%	Kansas	0.7	7.3	9%	2011-2020
	5.0	9.7	51%		1.5	7.7	19%	SSP1-2.6
	6.2	11.0	57%		1.7	7.9	21%	SSP2-4.5
	7.5	12.3	61%		1.8	8.1	22%	SSP3-7.0
Montana	1.3	6.4	20%	Nebraska	0.7	7.4	9%	2011-2020
	4.7	9.7	48%		1.2	7.4	16%	SSP1-2.6
	5.7	10.7	53%		1.3	7.5	18%	SSP2-4.5
	6.9	11.9	58%		1.5	7.6	19%	SSP3-7.0
Washington	0.9	6.0	16%	Oklahoma	0.6	7.8	8%	2011-2020
	3.8	8.3	46%		1.2	8.0	15%	SSP1-2.6
	4.6	9.0	51%		1.4	8.2	17%	SSP2-4.5
	5.6	10.0	56%		1.5	8.3	19%	SSP3-7.0
Idaho	1.3	7.1	18%	Minnesota	0.6	6.6	9%	2011-2020
	4.4	10.0	44%		0.9	6.5	14%	SSP1-2.6
	5.4	11.0	49%		1.0	6.7	15%	SSP2-4.5
	6.4	12.0	54%		1.1	6.8	16%	SSP3-7.0
Wyoming	0.7	5.4	13%	Arkansas	0.6	8.2	7%	2011-2020
	2.6	7.1	37%		1.1	8.0	14%	SSP1-2.6
	3.2	7.7	42%		1.2	8.2	15%	SSP2-4.5
	3.9	8.4	47%		1.3	8.2	16%	SSP3-7.0
Nevada	0.5	7.0	7%	Texas	0.5	8.3	6%	2011-2020
	3.1	9.6	32%		1.1	8.5	12%	SSP1-2.6
	3.9	10.4	38%		1.2	8.6	14%	SSP2-4.5
	4.6	11.1	42%		1.3	8.7	15%	SSP3-7.0
North Dakota	0.7	5.3	14%	Arizona	0.2	8.2	2%	2011-2020
	1.7	6.1	28%		0.9	8.7	11%	SSP1-2.6
	2.0	6.3	31%		1.1	8.9	13%	SSP2-4.5
	2.2	6.5	33%		1.3	9.1	14%	SSP3-7.0
California	0.6	10.5	6%	Iowa	0.6	7.8	8%	2011-2020
	2.8	12.2	23%		0.8	7.5	11%	SSP1-2.6
	3.5	12.9	27%		0.9	7.6	12%	SSP2-4.5
	4.1	13.5	30%		1.0	7.7	13%	SSP3-7.0
Colorado	0.5	6.1	9%	Wisconsin	0.5	7.4	7%	2011-2020
	1.7	7.2	24%		0.8	7.1	11%	SSP1-2.6
	2.0	7.5	27%		0.9	7.3	12%	SSP2-4.5
	2.3	7.8	30%		1.0	7.3	13%	SSP3-7.0
Utah	0.5	6.9	7%	Louisiana	0.4	8.5	5%	2011-2020
	1.7	7.7	22%		0.8	8.5	10%	SSP1-2.6
	2.0	8.0	26%		1.0	8.6	11%	SSP2-4.5
	2.4	8.4	29%		1.0	8.6	12%	SSP3-7.0
South Dakota	0.7	6.1	11%	Mississippi	0.4	8.3	5%	2011-2020
	1.4	6.3	22%		0.7	8.0	9%	SSP1-2.6
	1.5	6.5	24%		0.9	8.1	11%	SSP2-4.5
	1.7	6.7	26%		0.9	8.2	11%	SSP3-7.0
New Mexico	0.3	5.4	6%	Michigan	0.4	8.0	5%	2011-2020
	1.2	6.0	20%		0.6	7.6	8%	SSP1-2.6
	1.4	6.2	23%		0.7	7.7	9%	SSP2-4.5
	1.6	6.4	25%		0.8	7.7	10%	SSP3-7.0

Table S6: Climate models used in this study for future projections. We use projections from 28 global climate models with available output under the historical and three climate scenarios from the CMIP6 model ensembles. The spatial resolution of each model is shown in latitude × longitude (unit: degree). Resolutions are approximated for models with varying latitudes. Data is downloaded in February, 2023.

Model	**Ensemble variant**	**Resolution**
ACCESS-CM2	r1i1p1f1	1.25 x 1.88
ACCESS-ESM1-5	r1i1p1f1	1.25 x 1.88
BCC-CSM2-MR	r1i1p1f1	1.12 x 1.12
CanESM5	r1i1p1f1	2.79 x 2.81
CAS-ESM2-0	r1i1p1f1	1.42 x 1.41
CESM2-WACCM	r1i1p1f1	0.94 x 1.25
CMCC-CM2-SR5	r1i1p1f1	0.94 x 1.25
CMCC-ESM2	r1i1p1f1	0.94 x 1.25
CNRM-CM6-1	r1i1p1f2	1.4 x 1.41
CNRM-CM6-1-HR	r1i1p1f2	0.5 x 0.5
CNRM-ESM2-1	r1i1p1f2	1.4 x 1.41
EC-Earth3	r1i1p1f1	0.7 x 0.7
EC-Earth3-Veg	r1i1p1f1	0.7 x 0.7
EC-Earth3-Veg-LR	r1i1p1f1	1.12 x 1.12
FGOALS-f3-L	r1i1p1f1	0.94 x 1.25
FGOALS-g3	r1i1p1f1	2.03 x 2
GFDL-ESM4	r1i1p1f1	1 x 1.25
GISS-E2-1-G	r1i1p1f2	2 x 2.5
GISS-E2-1-H	r1i1p1f2	2 x 2.5
IPSL-CM6A-LR	r1i1p1f1	1.27 x 2.5
KACE-1-0-G	r1i1p1f1	1.25 x 1.88
MIROC-ES2L	r1i1p1f2	2.79 x 2.81
MIROC6	r1i1p1f1	1.4 x 1.41
MRI-ESM2-0	r1i1p1f1	1.12 x 1.12
NorESM2-LM	r1i1p1f1	1.89 x 2.5
NorESM2-MM	r1i1p1f1	0.94 x 1.25
TaiESM1	r1i1p1f1	0.94 x 1.25
UKESM1-0-LL	r1i1p1f2	1.25 x 1.88

Table S7: Estimated annual excess deaths due to wildfire smoke at the state level. For historical period, the table shows average annual excess deaths due to smoke $PM_{2.5}$ exposure during 2011-2020. For future climate scenarios, the table shows average annual excess deaths due to smoke $PM_{2.5}$ exposure during 2046-2055 (median across 28 GCMs).

State	Historical	SSP1-2.6	SSP2-4.5	SSP3-7.0	State	Historical	SSP1-2.6	SSP2-4.5	SSP3-7.0
California	1381	4164	4657	5700	South Carolina	266	327	353	380
Texas	1276	1974	1958	1999	Tennessee	360	283	358	373
Washington	360	1108	1266	1530	Massachusetts	283	257	330	359
Florida	821	1119	1198	1295	Montana	87	219	253	318
Oregon	411	858	1020	1245	Mississippi	184	295	302	306
New York	800	749	924	979	Arkansas	244	323	305	302
Michigan	610	807	819	825	Kentucky	256	238	285	291
Ohio	651	701	845	821	Iowa	243	277	283	286
Pennsylvania	633	617	759	820	Kansas	224	265	260	269
Illinois	779	746	862	817	Utah	92	186	245	259
North Carolina	442	575	612	667	Maryland	236	168	213	232
Georgia	447	567	606	643	New Mexico	82	175	188	212
Arizona	184	511	558	574	Connecticut	162	150	193	201
Nevada	117	421	463	560	Nebraska	147	168	167	180
Colorado	225	398	497	540	West Virginia	94	69	101	109
Virginia	288	431	467	497	Wyoming	31	72	81	99
Wisconsin	366	461	464	471	South Dakota	63	81	85	91
Missouri	476	406	453	462	Maine	62	59	79	87
Indiana	392	394	464	452	New Hampshire	54	59	74	79
Louisiana	274	440	438	441	North Dakota	53	63	67	77
New Jersey	394	328	406	437	Rhode Island	49	43	55	61
Idaho	100	296	348	431	Delaware	44	24	33	37
Minnesota	340	399	405	418	Vermont	26	25	32	35
Alabama	306	358	391	409	D.C.	29	25	32	33
Oklahoma	320	415	394	404					

A

Model	Evaluation	R	RMSE/mean	Bias
Our model	LOOCV	0.95	22%	-6%
log(fire) ~ VPD	LOOCV	0.34	42%	-44%
XGBOOST grid	LOOCV	0.48	82%	-1%
XGBOOST grid	Random CV	1.00	23%	6%

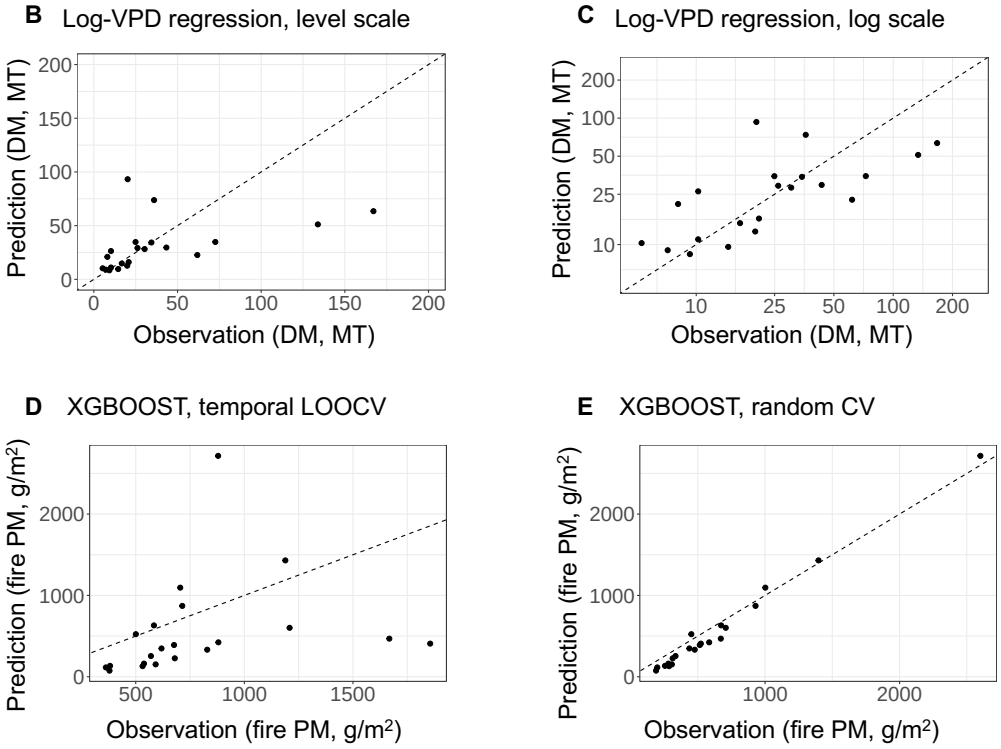

Figure S1: Predictive performance of our model and two other approaches used in previous research to predict wildfire emissions using climate variables. For comparison purposes, this figure only shows the results in western US. Panel A compares the predictive performance between our ensemble statistical and machine learning model ("Our model"), a regression method that uses fire-season VPD to predict the logged fire emissions ("log(fire)-VPD") as used in (*2*), and a XGBOOST model that predicts the fire emissions at the grid cell level as used in (*43*). The table shows the correlation coefficient (R), RMSE/mean, and bias of the highest-emitting 10-year period. Panels B and C show the out-of-sample prediction from the log(fire)-VPD regressions, with the same underlying data shown in level scale (B) and log scale (C). This demonstrates that while log(fire)-VPD regression achieves reasonable performance in the log scale (as reported by previous papers), its performance is inferior to our models in predicting the absolute levels of fire emissions. Panels D and E show the out-of-sample predictions from XGBOOST model under temporal LOOCV (D) and random CV (E) using the underlying dataset from (*43*). Random CV randomly partitions data to training and test sets with the same grid cell from different years possibly existing in both training and test sets. Panels D and E suggest the XGBOOST model trained at the grid cell has an inflated performance under random CV which grid cells can contribute data to both training and test sets.

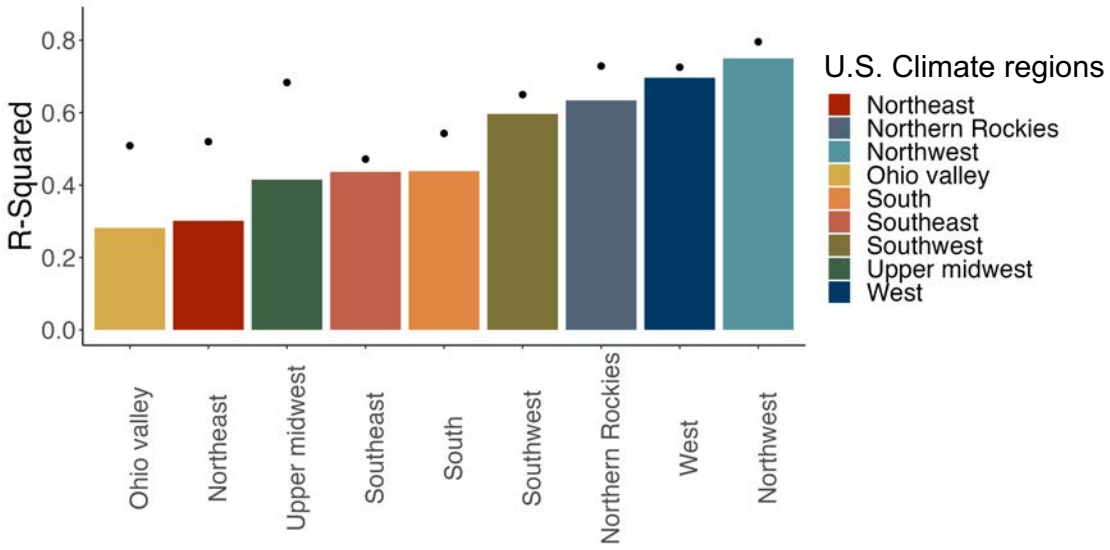

Figure S2: Performance of the fire-smoke regression models. The black dots show the full adjusted R^2 of the regression model. The color bars show the within R^2 after partialing out the month-of-year and grid cell fixed effects. The within R^2 thus quantify the model predictive performance within each grid cell and month-of-year. Each bar shows the performance of a fire-smoke model in one of the nine US climate regions.

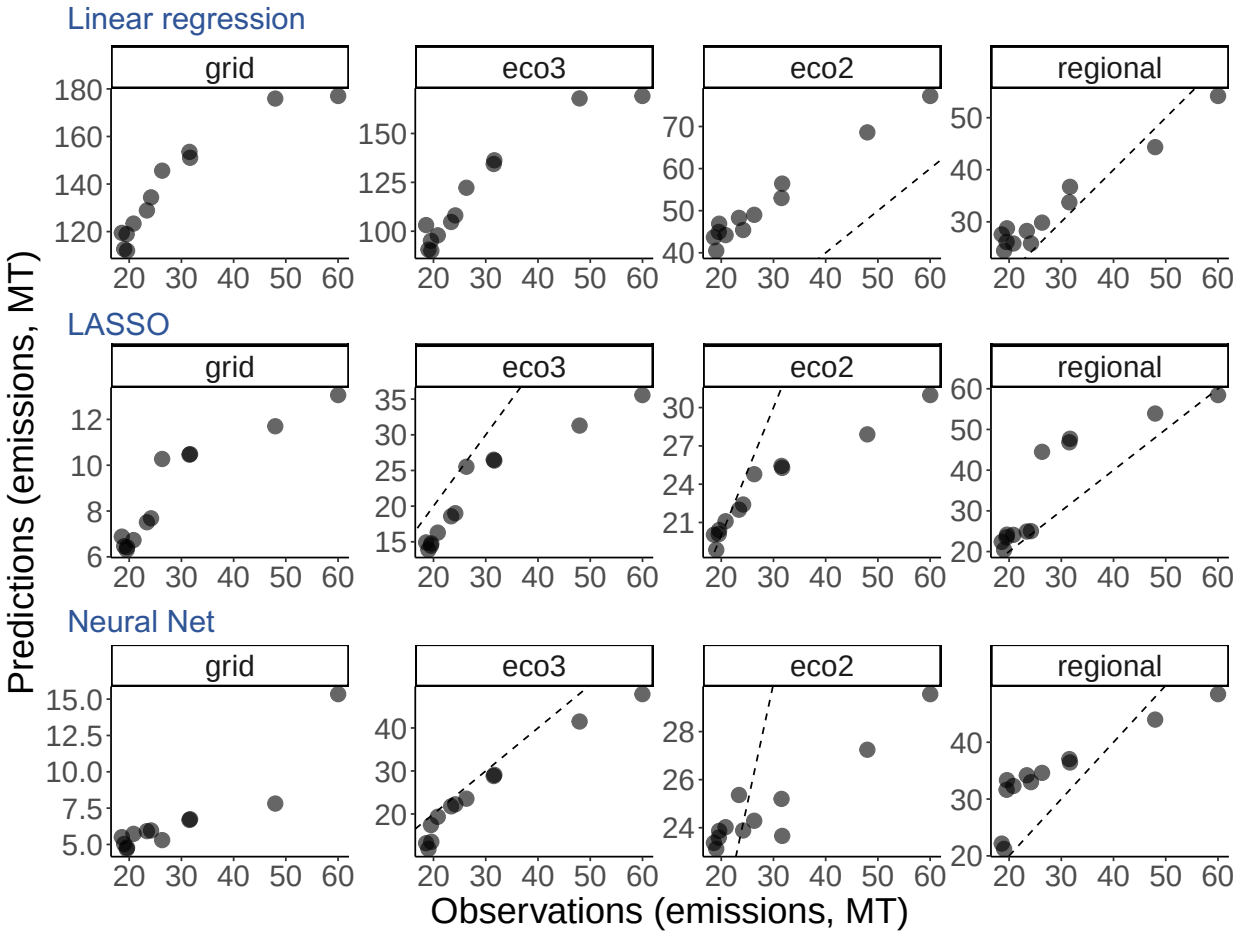

Figure S3: Predictive performance of models trained at different spatial resolutions (Western US). The plot shows the 10-year moving average of predicted emissions (y-axis) against the observed emissions (x-axis) from models trained at different spatial resolutions. For each algorithm (row), results are presented for models trained using grid cell data ("grid"), data aggregated at the level-3 ecoregion ("eco3"), data aggregated at the level-2 ecoregion ("eco2"), and data aggregated at the regional level ("regional"). Despite the different spatial resolutions of training data, the evaluation is at the regional level: we first aggregate the out-of-sample prediction to the regional level and compare the aggregated predictions against the aggregated observations. Dashed lines are 1-1 lines.

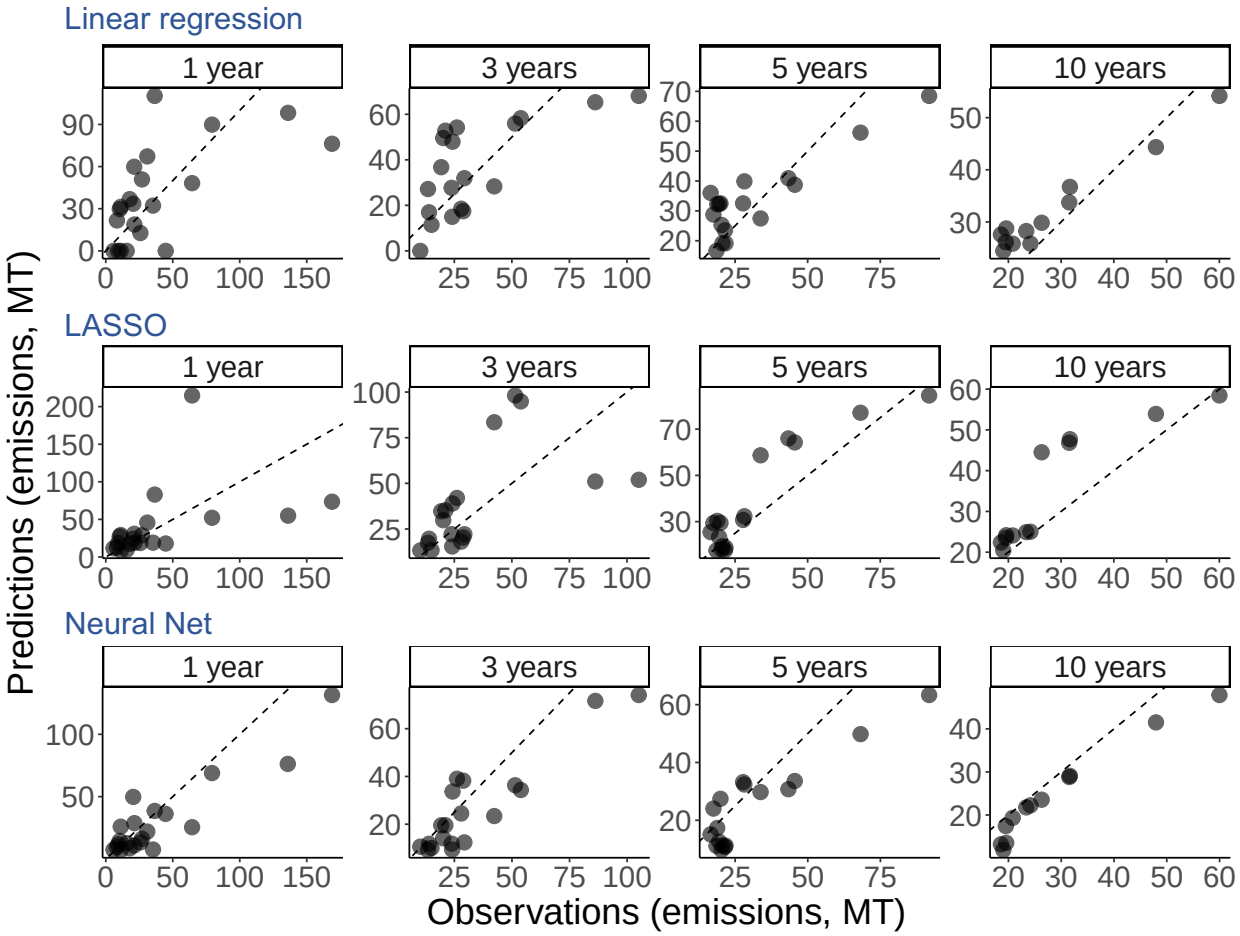

Figure S4: Predictive performance of models evaluated at different temporal scales (Western US). The plot shows the 10-year moving average of predicted emissions (y-axis) against the observed emissions (x-axis) from the same set of model but evaluated at different temporal scales. For each algorithm (row), the results show the out-of-sample prediction aggregated at different temporal scales ranging from no-aggregation (i.e. 1 year), to aggregation at the 10-year intervals. Dashed lines are 1-1 lines.

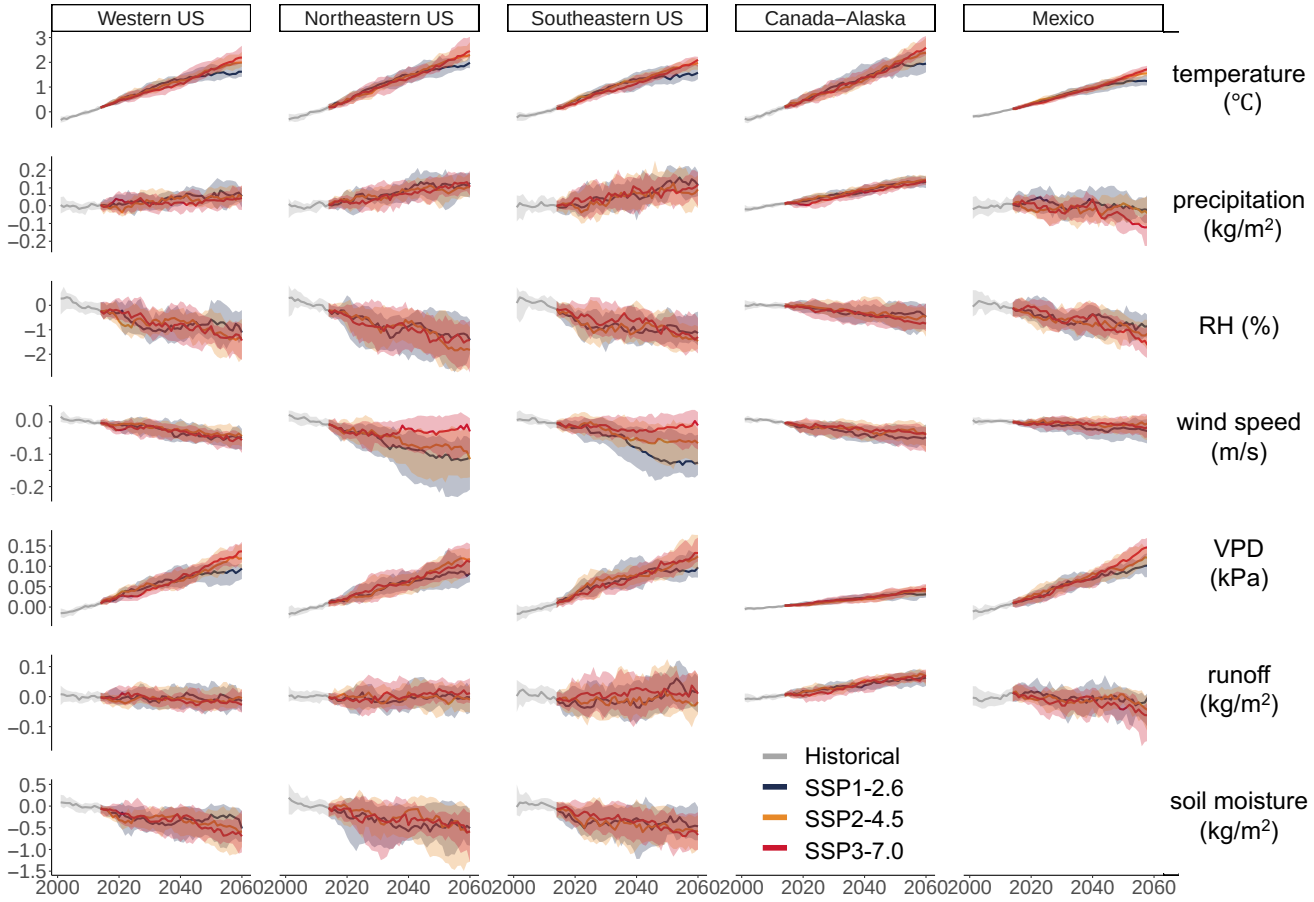

Figure S5: Projections of the climatic variables used in our statistical and machine learning models. Colour line indicates the median across 28 GCMs, and the shade area shows the 25th and 75th percentile across GCMs. The plot shows the 10-year moving average of the anomalies of each variable relative to the average values under historical scenario during 2001-2014. Soil moisture is not shown in Canada-Alaska and Mexico, as historical observations of soil moisture from NLDAS-2 are not available for these two regions.

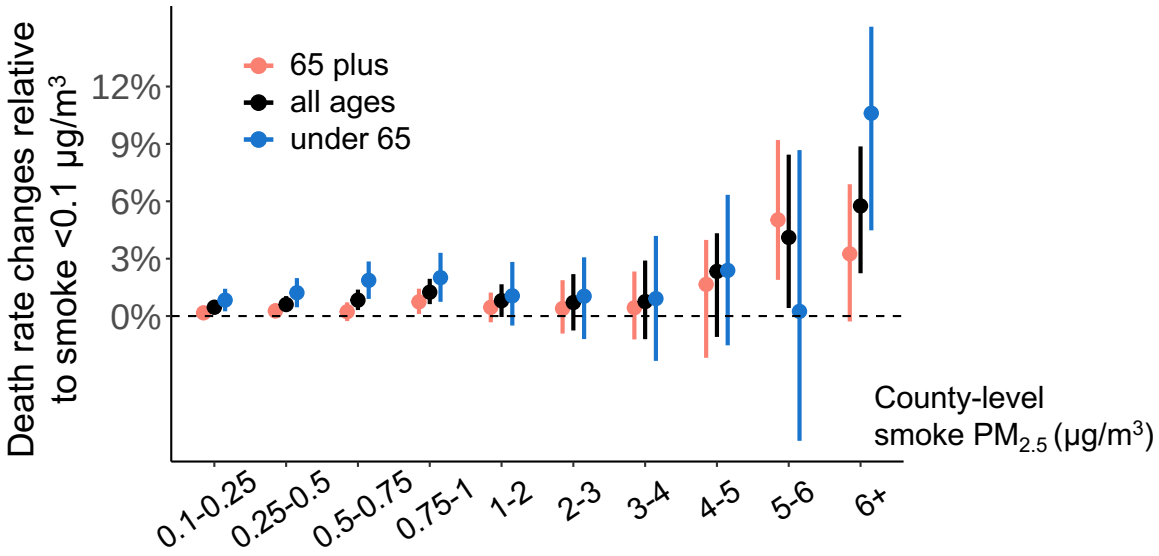

Figure S6: Impacts of smoke $PM_{2.5}$ concentration on mortality rates estimated by age group. The figure shows the effects of exposure to different annual mean concentration of smoke $PM_{2.5}$ (x-axis) relative to a no-smoke year (defined as a year with smoke $PM_{2.5}$ concentration less than 0.1 $\mu g/m^3$), estimated using a Poisson model at the county and annual level. The error bars show the 95% confidence interval estimated using bootstrap.

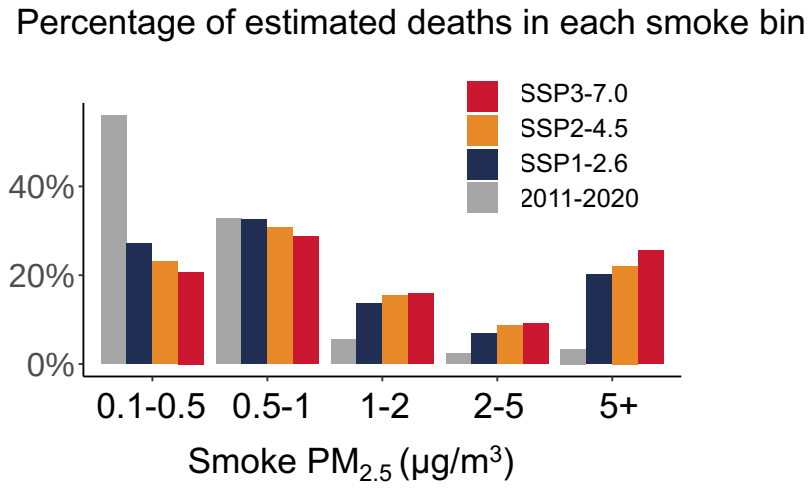

Figure S7: Percentage of estimated death contributions from each smoke concentration bin. The plot shows the contribution to total smoke-related deaths from county-years with annual mean smoke concentrations that fall in different smoke concentration bins under each scenario.

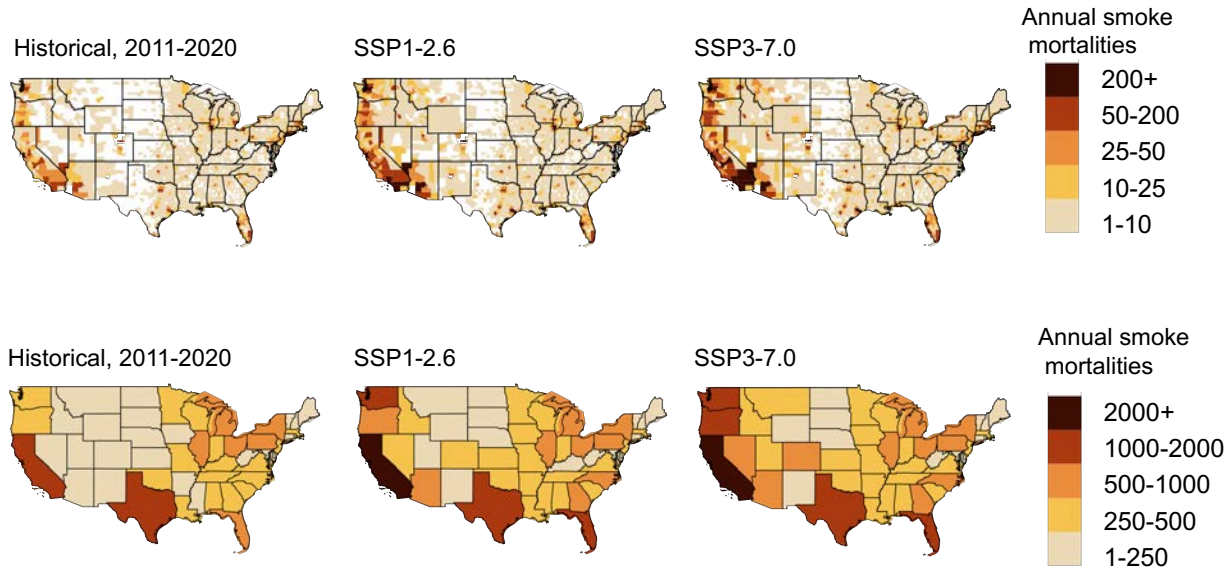

Figure S8: Estimated annual excess deaths due to smoke $PM_{2.5}$ under the historical, SSP1-2.6, and SSP3-7.0 scenarios. The top panels show estimates at the county level. The bottom panels show estimates at the state level.

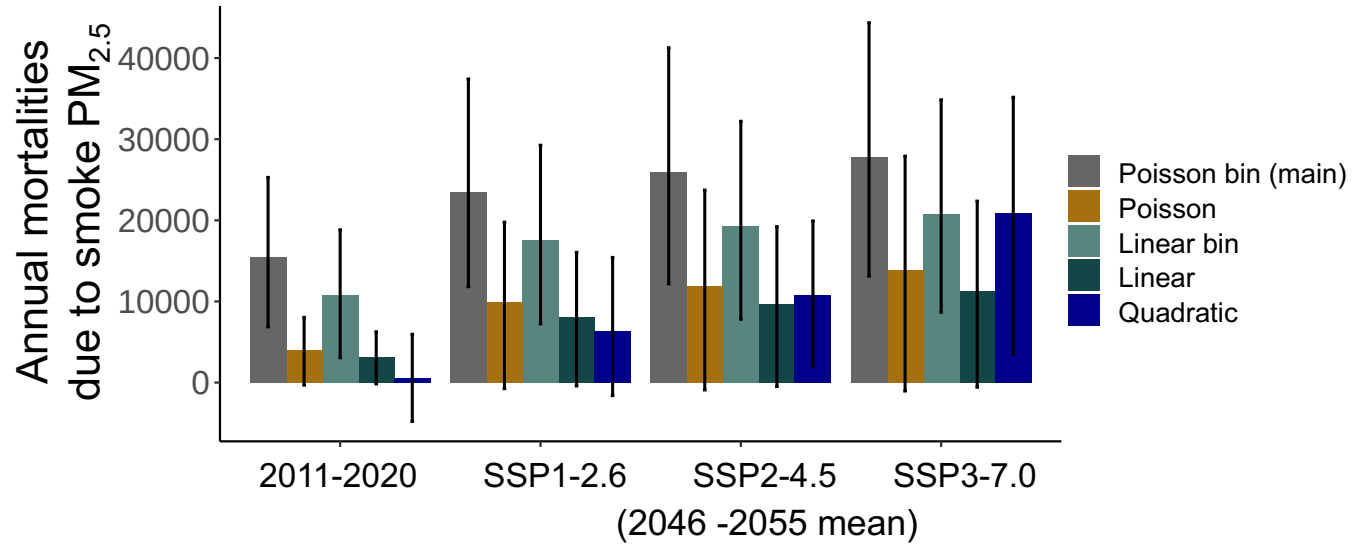

Figure S9: Estimated annual excess deaths due to smoke $PM_{2.5}$ across alternative dose-response functions. Our main analysis uses the "Poisson bin" specification. The error bars show the 95% confidence interval estimated using bootstrap.

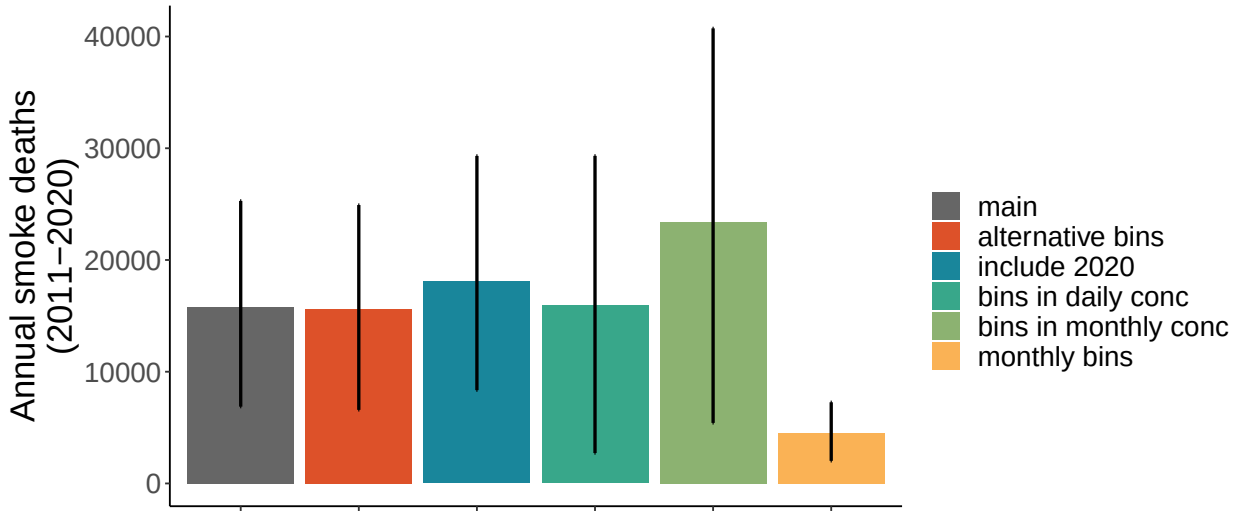

Figure S10: Estimated annual excess deaths due to smoke $PM_{2.5}$ (2011-2020) across alternative specifications of the Poisson model. In addition to our main model (grey bar), we estimate a model which uses alternative bin definitions, a model which includes year 2020, a model which calculates the number of months or the number of days in a year that fall in different smoke bins to represent different temporal aggregations, and a model which is estimated at the county-month level. The error bars show the 95% confidence interval estimated using bootstrap.

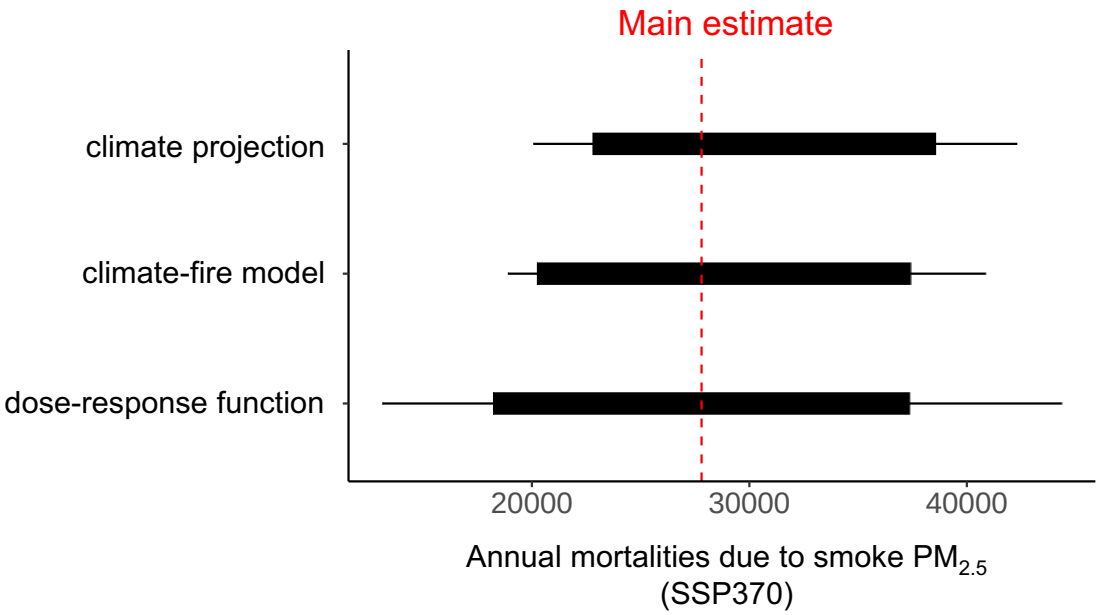

Figure S11: Uncertainty in estimated annual excess deaths due to wildfire smoke $PM_{2.5}$ under SSP3-7.0 scenario. The figure shows the uncertainty of the mortality estimates due to climate projections, climate-fire model, and the dose-response function between smoke and mortality. The red dashed line shows the main estimate reported in the paper (i.e. 27,800 excess deaths per year). The solid bar shows the 10th and 90th percentile, and the black line shows the 2.5th and 97.5th percentile. Uncertainty from "climate projection" is calculated using the percentiles of the estimated mortality from the 28 GCMs. Uncertainty from "climate-fire model" is calculated using bootstrap procedures performed on the individual fire-climate models from each region. More specifically, we first construct bootstrapped samples of the fire-climate panel dataset (sample with replacement) and then fit fire-climate model from each bootstrapped sample, and use these models to project smoke deaths. Uncertainty from "dose-response function" is calculated using bootstrap procedures performed on the health response functions. More specifically, we construct bootstrapped samples of the smoke-death dataset and estimate one dose-response function from each sample.

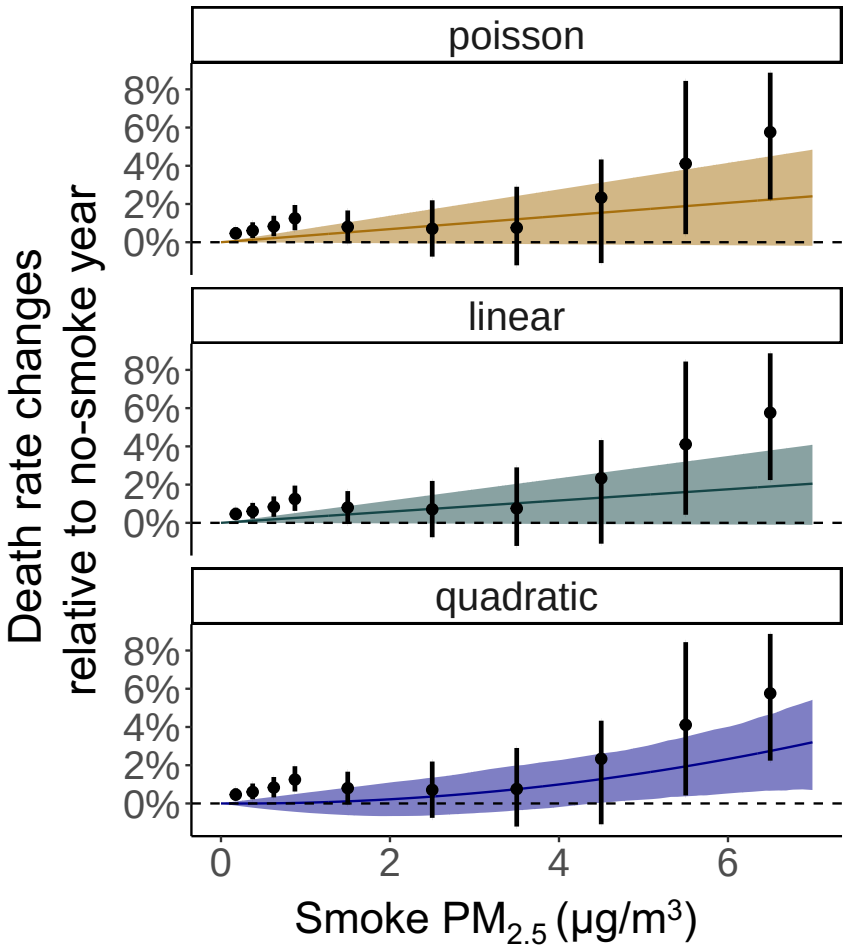

Figure S12: Impacts of smoke $PM_{2.5}$ concentration on mortality rates estimated using three alternative dose-response functions. The three colour lines show the estimated results from three non-binned models with poisson, linear, and quadratic specifications. For comparison, the black dots show the estimated coefficients from our main model (Poisson bin model). The shaded areas and the error bars represent the 95% confidence interval estimated using bootstrap procedure.